DEVELOPMENT OF THE RESPONSE COEFFICIENT-ROOT FUNCTION METHOD FOR THE TRANSIENT VIBRATION SERVICEABLITY DESIGN OF FLAT CONCRETE FLOORS

(*In Partial Fulfilment of the Requirements for the Degree of Doctor of Philosophy*)

presented to

The Research Degrees Committee

by

Charles A. Jetann, B.Eng, M.Eng, RPEQ

under the supervision of

Professor David Thambiratnam, PhD
Professor Stephen Kajewski, PhD

Queensland University of Technology

(Faculty of Built Environment and Engineering, School of Urban Development)

ABSTRACT

The vibration serviceability limit state is an important design consideration for two-way, suspended concrete floors that is not always well understood by many practicing structural engineers. Although the field of floor vibration has been extensively developed, at present there are no convenient design tools that deal with this problem. Results from this research have enabled the development of a much-needed, new method for assessing the vibration serviceability of flat, suspended concrete floors in buildings. This new method has been named, the Response Coefficient-Root Function (RCRF) method.

Full-scale, laboratory tests have been conducted on a post-tensioned floor specimen at Queensland University of Technology's structural laboratory. Special support brackets were fabricated to perform as frictionless, pinned connections at the corners of the specimen. A series of static and dynamic tests were performed in the laboratory to obtain basic material and dynamic properties of the specimen. Finite-element-models have been calibrated against data collected from laboratory experiments. Computational finite-element-analysis has been extended to investigate a variety of floor configurations. Field measurements of floors in existing buildings are in good agreement with computational studies. Results from this parametric investigation have led to the development of new approach for predicting the design frequencies and accelerations of flat, concrete floor structures. The RCRF method is convenient tool to assist structural engineers in the design for the vibration serviceability limit-state of in-situ concrete floor systems.

For your support, encouragement and patience....
thank you, Jodie and Tasman...
my wife, my daughter...

with love,
your husband, your dad...

Contents

List of Figures

Selected Variable Definitions

a (mm/s^2) = acceleration;

$a_p(\alpha, \lambda)$ = Acceleration Coefficient-Root Function, (ACRF);

c (N-s/mm) = viscous damping coefficient;

C_{cr} = critical viscous damping coefficient;

$C_{a,p}(\alpha)$ = floor panel acceleration-coefficient-function, (ACF);

$C_{f,p}(\alpha)$ = floor panel frequency-coefficient function, (FCF);

C_i = modal coefficient of vibration;

d (mm) = depth of the slab;

$d_{adjusted}$ (mm) = adjusted depth of the slab with drop-panels;

d_{drop} (mm) = depth of the drop-panel;

E_{dyn} (MPa) = dynamic elastic modulus of the concrete;

E_{stat} (MPa) = static elastic modulus of the concrete;

f (Hz) = natural frequency;

f_d (Hz) = damped natural frequency;

f_i (Hz) = modal frequency;

$f_p(\alpha, \lambda)$ = floor panel Frequency Coefficient-Root Function, (FCRF);

I (mm^3) = second moment of area per unit width of the floor panel;

k (N/mm^3) = floor panel stiffness;

k_i (N/mm^3) = floor panel modal stiffness;

L_x (mm) = floor panel short span dimension;

L_y (mm) = floor panel long span dimension;

$L_{x,drop}$ (mm) = span of the drop panel in the direction of L_x;

$L_{y,drop}$ (mm) = span of the drop panel in the direction of L_y;

(L_y/d) = floor panel span-to-depth ratio;

m $(tonne/mm^2)$ = floor panel mass per unit area;

'p ' = subscript representing the panel number;

$R_{f,p}(\alpha)$ = floor panel frequency-root function, (FRF);

$R_{a,p}(\alpha)$ = floor panel acceleration-root function, (ARF);

y (mm) = displacement as a function of time;

$[M]$ = mass matrix;

$[C]$ = damping matrix;

$[K]$ = stiffness matrices;

$\{y\}$ = displacement vector as a function of time;

$\{y'\}$ = velocity vector as a function of time;

$\{y''\}$ = acceleration vector as a function of time;

$\alpha = L_y/L_x$ = panel aspect ratio;

λ $(rad/s^2) = (E_{dyn}I) / (L_y^4 m)$ = dynamic stiffness-to-mass ratio;

$\zeta = {}^{c}/C_{cr}$ = damping ratio

CHAPTER 1

INTRODUCTION

1.1. **Objective**

Vibration is a serviceability limit state for the design of suspended concrete floor systems in buildings that is not always well understood by many structural engineers. Design codes do not cover this adequately while practice guides are not very practical. Without convenient design guidance for general practitioners of structural engineering, vibration problems are often dealt with by specialist consultants. In other cases, vibration serviceability may be incorrectly assessed or even ignored in the design phase.

The objective of this research was to develop a new method for the design of the vibration serviceability limit state of two-way concrete floors in buildings. In doing so, the aim was that this new method should be a convenient tool that any structural engineer can use without the need for advanced background knowledge of transient dynamic analysis. This research has led to the formulation of a set of empirically derived expressions for accurately predicting the frequency and acceleration response of flat, concrete floor structures subjected to human-induced transient loads for the purpose of assessing vibration serviceability in the design phase of a project. This new method has been called, the Response Coefficient-Root Function (RCRF) method.

1.2. **Research Methodology**

This research has been conducted through a complete parametric investigation, which involved: an ongoing literature review; laboratory testing of a full-scale floor specimen; computational finite-element analysis; and validation of results through field testing. Each of these phases forms the chapters of this dissertation as follows:

Chapter 2 will discuss the first phase of this research which was a literature review that was an ongoing throughout the duration of the program. The scope of the literature review was focused on the primary factors that influence vibration in buildings as set forth by the International Standards Organisation: the receiver, the source and the transmission path. The literature review also served to expose the knowledge gap regarding the lack of guidance for the transient vibration serviceability design of flat concrete floors.

Chapter 3 will describe the second phase of this research program which involved full-scale, laboratory tests conducted on a post-tensioned floor specimen constructed in the structural laboratory of the Queensland University of Technology. Special support brackets were fabricated to simulate frictionless pinned connections at the corners of the specimen which served to isolate the specimen for the convenience of subsequent finite-element modelling. A series tests were performed in the laboratory to obtain static and dynamic properties of

the specimen for the purpose of developing a material model for subsequent computational studies.

Chapter 4 will explain the third phase of this study which involved extensive computer modelling and analysis using the finite-element method. A finite-element model of the laboratory specimen was calibrated against data collected from laboratory experiments. Computational finite-element-analysis was extended to investigate the transient vibration serviceability behaviour of a variety of floor configurations. The results obtained from this phase of the program were used to develop an innovative set of expressions for the design frequency and acceleration of flat concrete slabs for various geometries.

Chapter 5 will present the fourth and final phase of this research program which involved field instrumentation and testing of floors in three real buildings. Measurements of response frequencies and accelerations from field tests have shown good agreement with the expressions developed in the previous of analysis. Field instrumentation and testing was a valuable experimental exercise that served to validate the results of computational studies.

Results from this complete parametric investigation have led to the development of new approach for predicting the response frequency and acceleration of flat, two-way concrete floor structures. This new method has been named, the Response Coefficient-Root Function (RCRF) method. The RCRF method is

convenient tool structural engineers can use in design for the vibration serviceability limit-state of in-situ concrete floor systems.

1.3. **Significance of Research**

Floor structures will vibrate in response to dynamic loads. The acceptability criterion for human exposure to vibration in buildings is a function of frequency of vibration and the acceleration response. Predictive determination of the frequency of vibration and the acceleration response of a floor structure is crucial for assessing its dynamic serviceability during the design phase of a project. Without the ability to predict the dynamic performance of a floor, vibration assessment becomes retrospective. If vibration is determined to be a serviceability problem after the floor has been constructed, costly structural

Figure 1.1: Retrofit - structural steel struts installed to reduce vibration

retrofit could be required that may disrupt or alter the originally intended function of the tenancy. To illustrate the importance of predictive determination of vibration serviceability in the design phase of any project, Figure 1.1 is a photo of the basement carpark of a building that has been retrofitted with structural steel struts in an attempt to minimise the vibration response of the suspended, post-tensioned floor above, which happens to be a government office. The struts can

be seen extending diagonally from the base of the columns to the underside of the ceiling. The function of the tenancy in this case was disrupted by the altered architectural aesthetics and the reduced turning radius for parking vehicles.

This research aims to develop expressions engineers can use to assist with the prediction of vibration serviceability in the design phase of projects, therefore avoiding expensive and inconvenient retrofits as described above.

1.4.**Floor Vibration**

Typically, floor vibration is regarded as a serviceability issue because of the negative psychological effects it has on. In addition, vibration may also adversely impact the performance of sensitive equipment. Rarely do such vibrations compromise structural capacity; however, there is the potential for floor vibration to cause overload and fatigue (Allen, 1990a). The International Standards Organisation, ISO 10137, has distinguished three primary components of vibration serviceability assessment (ISO10137, 2007):

- The Receiver - A receiver may be a person or an object that is experiencing the vibration disturbance. Objects may range from components of the structure itself to items placed on or fastened to the structure. The level of vibration that the receiver is subjected to must meet the appropriate acceptability criteria. This research is concerned with the human receiver, which is always located on the floor.
- The Source - The source of floor vibration in buildings is usually the result of occupant-imposed, dynamic loading. These occupant imposed

dynamic loads may originate from people walking, running, jumping and group activities such as exercise or dancing on floors. In the case of multi-story parking garages, vehicular traffic can also produce undesirable and excessive vibration. In addition to internal dynamic actions, external sources of vibration due to human activities may come from traffic or heavy construction.

- The Transmission Path - The transmission path is the route by which vibration waves travel through the structure, from the source to the receiver. For internal sources of occupant-induced vibration, the floor itself is the transmission path. The most general transmission path for vibration from an external ground source would be through foundations, into the columns and then through the floor system.

The ISO 2631 provides a comprehensive set of criteria for gauging the acceptability of human exposure to vibration in buildings for which the probability

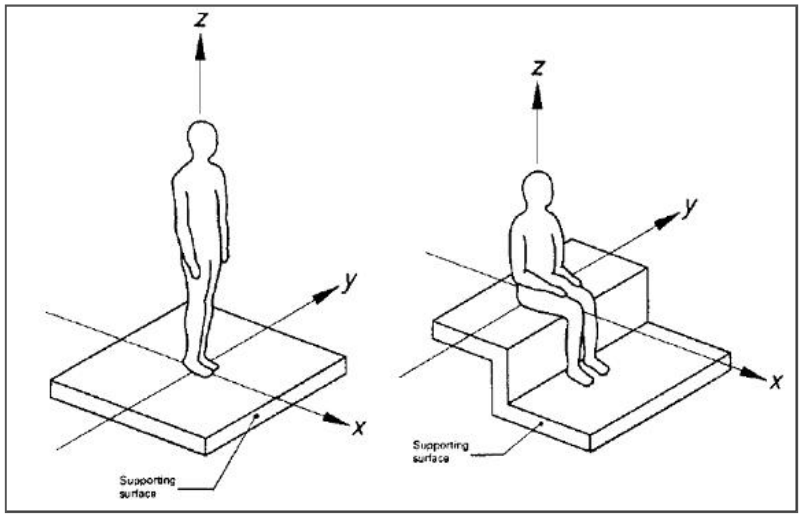

Figure 1.2: Coordinate systems for the direction of vibration influencing the human body

of complaints is considered too low. These criteria are presented as plots of acceleration (or velocity) versus frequency in the three principal directions with respect to the human body: x-axis (back-to-chest); y-axis (side-to-side); z-axis (foot/buttocks-to-head). Although the ISO 2631 also addresses situations in which a person is laying down, this research is focused on floor vibration in z-axis the for a person standing or sitting as illustrated in Figure 1.2. Figure 1.3 is the acceptability chart for z-axis vibration with the ISO base curve envelope plotted to

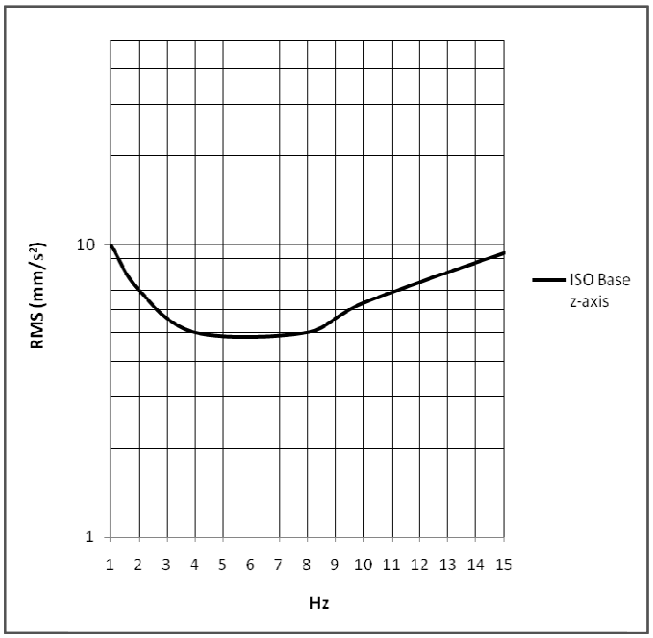

***Figure 1.3*:** ISO Base Curve for 'z'-axis Vibration Acceptability

15 Hz. The ISO base curve represents the threshold of human perception to vibration. The actual acceptable level of vibration depends on whether vibration is continuous or transient, the intended use of the occupancy and damping in the system. As will be discussed CHAPTER 2, the ISO base curve may be adjusted to account for the statistical probability of adverse comment for these various environmental considerations.

1.5. **Guidelines for Vibration Serviceability Design**

1.5.1. ***Composite Steel Framed Concrete Floors***

Among a number of studies that address the issue of vibration serviceability for composite, steel-framed floors, two very successful design guides have been published in the United Kingdom and North America that are commonly referred to and used in practice (Wyatt, 1989, Murray, 1997). The reason these guides are successful in accessing the dynamic serviceability for this type of floor construction is that they provide reasonably accurate methods for calculating the natural frequency and estimating the acceleration response of a floor panel.

1.5.2. ***Cast In-situ Concrete Floors***

Research focused on the dynamic behaviour of cast-in-situ concrete floors is limited. Throughout the 1990s and now in the Twenty-first Century, the most widely used formal guideline for the dynamic analysis and design of flat slab systems was the Concrete Society Technical Report 43 of 1994 (CSTR43, 1994). The *CSTR43* provided a hand calculation method for predicting the frequency and acceleration response factor for post-tensioned floor structures. Reports of over conservative designs resulting from this method having the tendency to underestimate the natural frequency (Caverson, 1994, Pavic A., 2001, Williams, 1994) led to the publication of the *CSTR43, Second Edition* in 2005, in which suggested hand-calculation method for predicting vibration frequency and acceleration response was removed from the guide. More recently, the Concrete Society published the '*Design Guide for Footfall Induced Vibration of Structures'* for the Concrete Centre (Willford, 2006). Although this guide does provide a

comprehensive approach to assessing the vibration performance of structures, it requires users to be proficient with advanced techniques in dynamic structural analysis and finite-element modelling.

1.5.3. ***Design Procedure for PT Floors***

A vibration serviceability check should be an integral part of the design process for in-situ concrete floors, in particular for post-tensioned (PT) systems. A design flowchart is shown in Figure 1.4 as proposed by Pavic (Pavic, 2001). It is clear from this flowchart that the serviceability vibration check is the most important step in the design process and should be undertaken once the slab's geometry, material properties and loads have been selected. Although these parameters provide enough information to estimate the vibration response of a floor, there are no reliable guidelines available to assist designers with accurate estimations of vibration response without the need for sophisticated finite-element methods.

This thesis will describe the development of a new, empirical approach to predicting the frequency and acceleration response of flat, two-way, suspended concrete floors resulting from human-induced impulsive or transient excitation: The Response Coefficient-Root Function Method (RCRF). The RCRF method is a convenient tool structural engineers can use to accurately estimate the vibration serviceability performance of flat, two-way, suspended concrete floors in the design phase of a project (Jetann, 2007, Jetann, 2006).

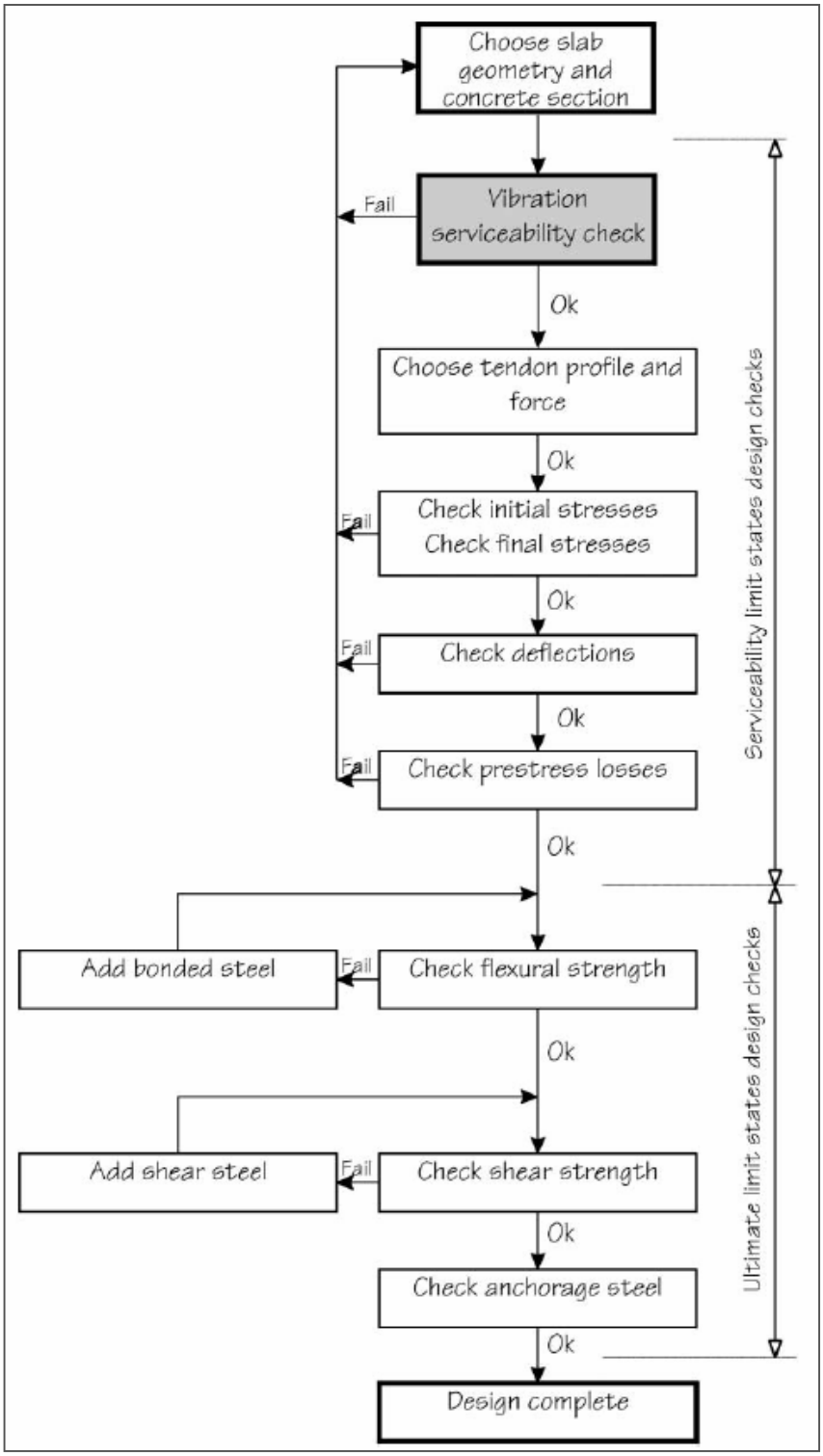

Figure 1.4: Recommended design procedure for PT floors (Pavic 2001)

1.6. **Flat, Two-way, Suspended Concrete Floors**

This thesis addresses the special case of flat, two-way, suspended concrete floors supported on a rectangular column grid as shown in Figure 1.5. For the application of the RCRF method, flat, two-way floor systems should meet the following requirements:

- The soffit of the slab is formed without band beams or ribs (drop panels may be treated with some special considerations);
- A floor panel is defined by the boundary of four columns on a rectangular grid with an aspect ratio no greater than two.

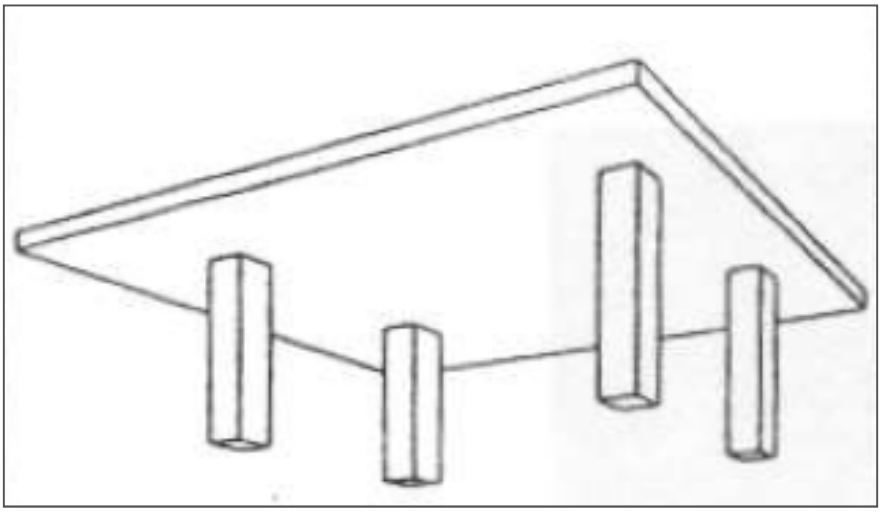

Figure 1.5: Flat, Two-way Floor Panel

1.6.1. ***Reinforced Concrete Floors***

Although reinforced concrete (RC) may be designed as flat-slab construction, vibration serviceability of residential and office spaces is generally not a problem because the span-to-depth ratios are low which provides a stiff system. Vibration

serviceability in RC floors may be a concern if high-strength concrete is used and slender cross sections can be achieved (CSTR43, 2005).

1.6.2. ***Post-tensioned Concrete Floors***

In today's construction industry, the most common type of slender, flat-slab that is susceptible to vibration serviceability problems are of post-tensioned (PT) concrete floors. PT concrete floor systems have been employed in building construction for decades. In recent years, PT floor systems have become a more common solution to the architectural requirements for longer, thinner spans. Post-tensioned floors can help reduce cracking and deflections through pre-compression at anchorages and from draped tendon profiles that produce reversed (balanced) loading, both of which limit tensile stresses. Because post-tensioned slabs are typically thinner than conventionally reinforced systems, an overall reduction in building height can be achieved. Often, PT floors allow the elimination of some supporting columns or walls that would otherwise be necessary. With less construction material and reduced building height, post-tensioned floor systems can potentially decrease the size of footings. Generally, PT floor systems can accelerate construction time and lower construction costs. Although beneficial in some respects, the combination of slenderness and high mass is detrimental to dynamic performance, thus making vibration an important design consideration for post-tensioned concrete slabs.

1.7. **Theoretical Background**

Vibration of floors is typically characterized by cyclic, vertical motion as illustrated in Figure 1.6: Typical damped vibration time-history. In practice, solutions to structural dynamics problems are often simplified by using "equivalent" single degree of freedom (SDOF) systems. These simplifications are based on the experience and assumptions of the engineer. Single degree of freedom, (SDOF), systems under damped, free vibration can be described by the differential equation of motion (Paz, 1997)):

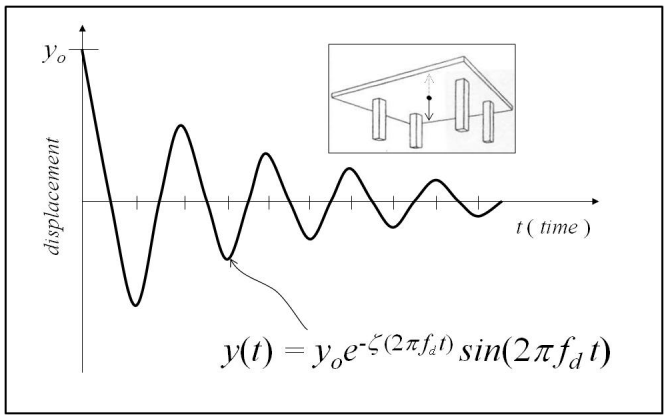

Figure 1.6: Typical damped vibration time-history

$$m\ddot{y} + c\dot{y} + ky = 0 \qquad \textbf{Equation 1-1}$$

Where m = mass; c = viscous damping coefficient; k = stiffness; and y = displacement as a function of time. The frequency to the solution of Equation 1.1 is the damped, natural frequency of the structure, f_d:

$$f_d = f\sqrt{1-\zeta^2} \qquad \textbf{Equation 1-2}$$

From Equation 1.2, two important parameters of floor vibration are revealed. The first is the undamped natural frequency, f, given by Equation 1.3.

$$f = \frac{1}{2\pi}\sqrt{\frac{k}{m}} \qquad \textbf{Equation 1-3}$$

The other parameter given in Equation 1.2 is the damping ratio, ζ, which has the most significant influence on human perception to transient vibration. For

practical purposes, the undamped natural frequency is sufficiently accurate for design, even for floors with relatively large damping ratios (ζ up to 10%). The damping ratio is classically defined as the percentage of inherent damping, c, with respect to critical damping, C_{cr}, given by the following relationship:

$$\zeta = \frac{c}{C_{cr}} = \frac{c}{2\sqrt{km}} \qquad \textbf{Equation 1-4}$$

Suspended concrete floors have continuously distributed mass, damping and stiffness, thus having infinite degrees of freedom. The equation of motion for the free vibration of dynamic systems with multiple degrees of freedom, (MDOF), takes the form:

$$[M]\{y''\}+[C]\{y'\}+[K]\{y\}=\{0\} \qquad \textbf{Equation 1-5}$$

In this case, $[M]$, $[C]$, and $[K]$ are the mass, damping and stiffness matrices respectively, and the nodal displacements, velocities and accelerations are the vectors $\{y\}$ and it's respective derivatives as functions of time.

Cast in-situ concrete floors are immensely complicated MDOF systems that are not easily simplified and demand special attention. Because of the complexity of boundary conditions, material properties and geometry, vibration problems in these types of floors are very difficult solve. The most common approach to solving these problems is the use of finite-element-analysis (FEA). It is common practice to perform Eigen-value natural frequency analysis, in which case the modal frequencies may take the form:

$$f_i = \frac{1}{2\pi}\sqrt{\frac{k_i}{m_i}} \qquad \textbf{Equation 1-6}$$

Now, f_i (Hz) is the modal frequency, k_i represents the modal stiffness and m_i is the modal mass, each for the i^{th} mode of vibration. Recognizing that the modal frequency is proportional to the natural frequency of a SDOF system, the proportionality of the stiffness and mass may be combined with the constant to simplify the expression (Wyatt, 1989):

$$f_i = C_i \sqrt{\frac{k}{m}} = C_i \sqrt{\lambda} \qquad \textbf{Equation 1-7}$$

In this case, C_i is a proportionality coefficient for the i-th mode of vibration. For plate structures, like flat, concrete floors, where by convention the dynamic stiffness-to-mass ratio 'λ (rad/s^2) ' is calculated as follows:

$$\lambda = \frac{k}{m} = \frac{E_{dyn} I}{L_x^4 m} \qquad \textbf{Equation 1-8}$$

Here, E_{dyn} (MPa) is the dynamic, elastic modulus of the concrete, I (mm^3) is the second moment of area per unit width of the slab, L_x (mm) is the short span dimension of the floor panel, and m $(tonne/mm^2)$ is the mass of the floor per unit area. Wyatt's simple approach to calculating the natural frequency of a floor using Equation 1.7 is called the 'Frequency Factor Method', and was developed specifically for one-way, steel-concrete composite floor structures. For this method, the coefficient of proportionality, C_i, is empirically derived for various end-span continuity conditions.

The goal of this research as presented in this thesis is to develop a new simplified approach for two-way suspended concrete floors for various continuity conditions.

1.8. **Original Contribution and Innovation: The RCRF Method**

The main achievement of this research is the development of two empirical expressions for predicting the dynamic response of flat-slab floor structures, which will be referred to as the Response Coefficient-Root Function (RCRF) method. These proposed expressions are similar to those proposed by Wyatt in Equation 1.7, The difference between Wyatt's method and the RCRF method is that the coefficient and root are not constant, instead are functions of the panel aspect ratio, '$\alpha = L_y/L_x$' where L_y is the long span, and L_x is the short span dimension of the panel. The RCRF method consists of two empirically derived expressions, Equations 1.9 and 1.11 below, for estimating the frequency and acceleration response of flat, two-way floor structures subjected to human-induced, impulsive excitation. This new approach to assessing dynamic performance will assist engineers in the designs of suspended floors for vibration serviceability, particularly those of post-tensioned concrete construction.

1.8.1. ***RCRF Frequency***

This research has shown that when the centre of a flat, two-way floor panel is subjected to human-induced impulsive excitation, the primary response frequency of that panel is not exactly proportional to the square-root of 'λ' as suggested in Equation 1.7. In fact, this research has shown that both the root and the proportionally coefficient as given in Equation 1.7 are each functions of the floor panel aspect ratio, 'α'. This concept leads to a new expression for the primary response frequency of a floor panel as follows:

$$f_p(\alpha, \lambda) = C_{f,p}(\alpha) \left(\sqrt[R_{f,p}(\alpha)]{\lambda} \right) \qquad \textbf{Equation 1-9}$$

Now, $f_p(\alpha, \lambda)$ is the Frequency Coefficient-Root Function, (FCRF), for the primary response frequency of the panel, in Hz as a function of 'α' and 'λ' where the subscript 'p' indicates the panel number. While the panel frequency-root function $R_{f,p}(\alpha)$ is dimensionless, the panel frequency-coefficient function $C_{f,p}(\alpha)$ has units of time in seconds 's' raised to the power of '$2/R_{f,p}(\alpha)$ -1' or:

$$Units\ of\ C_{f,p}(\alpha) = \boldsymbol{s}^{\left(\frac{2}{R_{f,p}(\alpha)} - 1\right)} \qquad \textbf{Equation 1-10}$$

Both of these are functions of the panel aspect ratio, $\alpha = L_y/L_x$, where L_y is the long span dimension of the panel.

1.8.2. ***RCRF Acceleration***

This research has also shown that a similar expression for predicting the corresponding acceleration of a floor panel subjected to impulsive excitation may take the form:

$$a_p(\alpha, \lambda) = C_{a,p}(\alpha) \left(R_{a,p}(\alpha)\sqrt{\lambda}\right) \qquad \textbf{Equation 1-11}$$

In this case, $a_p(\alpha, \lambda)$ is the Acceleration Coefficient-Root Function, (ACRF), for the peak acceleration response of the panel as a function of 'α' and 'λ' where the subscript 'p' indicates the panel number. The function $C_{a,p}(\alpha)$ is the panel acceleration-coefficient-function, which has units of distance in millimetres multiplied by time in seconds raised to the power of '$2/R_{a,p}(\alpha)$ - 2', or:

$$Units\ of\ C_{a,p}(\alpha) = \boldsymbol{mm \cdot s}^{\left(\frac{2}{R_{a,p}(\alpha)} - 2\right)} \qquad \textbf{Equation 1-12}$$

Again, $R_{a,p}(\alpha)$ is the dimensionless panel acceleration-root function. Both of these are functions of the panel aspect ratio.

1.8.2.1. ***Adjusted RCRF Slab Depth for Drop-Panels***

Because the RCRF method was derived using finite- element analysis with models having uniform slab depths and no drop-panels, an 'adjusted' slab depth must be considered for slabs with drop-panels. The depth of the slab contributes to both the stiffness and mass of the floor structure. In other words, the depth of the slab affects the stiffness-to-mass ratio 'λ'. To account for the influence of drop-panels on 'λ', a simple slab depth adjustment calculation is proposed as follows:

$$d_{adjusted} = \left[\frac{\left(d\left(L_x - L_{x,drop}\right) + d_{drop}\left(L_{x,drop}\right)\right)}{2L_x} + \frac{\left(d\left(L_y - L_{y,drop}\right) + d_{drop}\left(L_{y,drop}\right)\right)}{2L_y} \right] \quad \textbf{Equation 1-13}$$

where $d_{adjusted}$ is the adjusted depth of the floor plate to account for the influence of drop-panels, d is the depth of the slab, d_{drop} is the depth of the drop-panel, $L_{x,drop}$ is the span of the drop panel in the direction of L_x and $L_{y,drop}$ is the span of the drop panel in the direction of L_y.

1.8.3. ***Scope of Development the RCRF Method***

The RCRF method has been developed for the prediction of serviceability vibration of flat, two-way suspended floor structures resulting from transient human induced loads. Structural engineering practitioners should be aware that the RCRF method has been developed for flat, two-way floor systems as described in Section 1.6 under the scope of analyses described below:

- Material behaviour of the floor was considered isotropic, e.g., the product of modulus of elasticity and second moment of area 'EI' of the floor is the

same in all directions. With that said, for application of the RCRF method, the engineer may choose to use any value of EI' determined to be appropriate considering the effects of time-history degradation of cross-section stiffness due to creep, shrinkage and cracking;

- The damping ratio 'ζ' of the floor structure was 1.2%;
- Floor panels were discretely supported by four columns on a rectangular grid with an aspect ratio 'α' no greater than 2;
- The longer span of any floor panel was less than 12 metres;
- A panel span-to-depth ratio, (L_y/d), was between values of 25 and 45;
- Superimposed loads on the floor were be uniformly distributed;
- Column cross-sections were approximately 5% of the panel span in each direction;
- Cantilevered slab edges were limited in span to no greater than 1 column width.

Despite the above scope of development, research outcomes presented in this thesis are applicable to dealing with the vibration serviceability design of slender, flat-slab systems, which is the type of construction most susceptible to adverse dynamic behaviour arising from human-induced transient loads. Furthermore, this research has addressed the need for providing engineers with a convenient tool that can be used to assess the dynamic performance of flat-slab floor structures in the design phase of a project by developing an empirical method for time-saving hand calculations.

CHAPTER 2

LITERATURE REVIEW

The topic of floor vibration is broad and of interest to a variety of disciplines that include, but are not limited to, structural engineering, mechanical engineering, biomechanics and electrical signals processing. In an effort to focus the scope of this literature review to resources relevant to this study, it has been divided into three categories that adhere to the components of the ISO10137 vibration serviceability assessment introduced in Section 1.2:

1. Acceptability Criteria (the receiver)
2. Human-induced Loads (the source)
3. Natural Frequency of Floor Vibration (the transmission path)

The following sections will provide a literature review how human induced vibrations are assessed, caused and transferred. The order in which these topics will be addressed in this literature review has significance with respect to the goals of this research. With emphasis being placed on the last topic, 'the transmission path', this literature review aims to highlight the fact that of all three topics listed above, the least and most limited information available is on the structural analysis and design of floor vibration.

2.1. **Acceptability Criteria (the receiver)**

There is a large volume of information available on the subject of vibration acceptability criteria. This literature review will concentrate on the aspects of human perceptions of vibration. Information regarding the susceptibility of equipment to vibration is discussed by Ungar and White (Ungar, 1979).

One of the most general tools used in the assessment of human comfort levels are the absorbed-power biomechanical models(Coermann, 1962, Griffin, 1990). Absorbed-power is the rate at which energy is dissipated by the body when subjected to vibration. Biomechanical models simulate the human body as a system of simple mass-spring oscillators in sitting, vertical or horizontal positions as depicted in Figure 2.1: Biomechanical Model (after Pavic 1994). To determine absorbed-power, a biomechanical model is subjected to a periodic, continuous acceleration at the points of contact with the floor (for various positions: sitting, standing or laying) from which the force and velocity on the model can be extracted as functions of time.

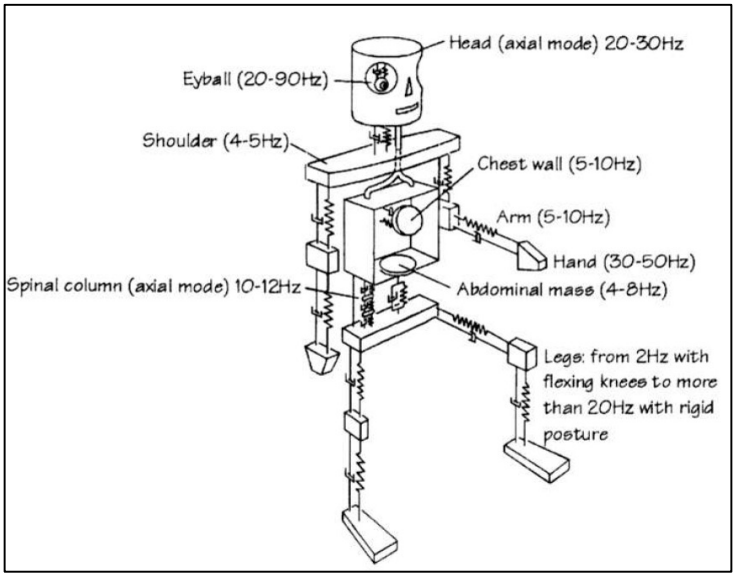

Figure 2.1: Biomechanical Model (after Pavic 1994)

In 1984, Farah published a paper through the American Concrete Institute's symposium on the Deflection of Concrete Structures (Farah, 1986). Farah's paper describes a complex procedure of calculating absorbed-power, as the product of force and the base velocity divided by the period, then integrated over a period of vibration. These calculations reduce to an expression that is a function of the forcing frequency and biomechanical impedance. Figure 2.2 shows the response curve for a simple biomechanical model.

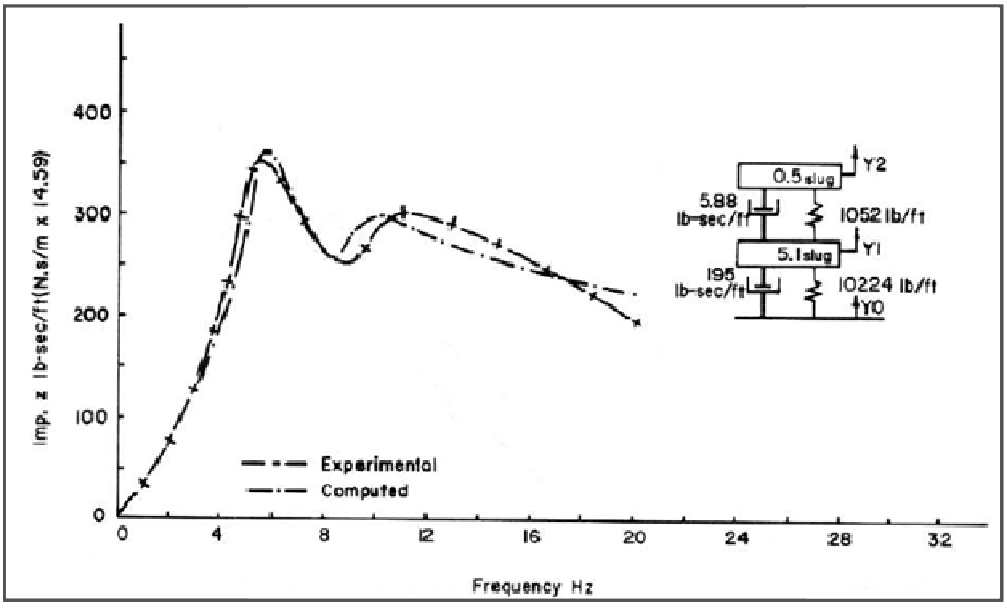

Figure 2.2: Impedance/Frequency Response (after Farah)

Farah's approach considers steady-state or sinusoidal excitations. For transient vibrations, in which damping plays a significant role, and is more appropriate for the dynamic serviceability of floor structures, Farah suggests the following inequality:

$$\frac{e^{\frac{-\delta}{2}}\left(1-e^{-n\delta}\right)}{n\left(1-e^{-\delta}\right)}\left(\frac{I}{2\pi aM}\right)^2 < 1 \qquad \textbf{Equation 2-1}$$

Where δ = logarithmic decrement, I = reference impulse taken as 15 lb-sec, a = a human response parameter, M = the mass of the system, and n = number of peak responses during a time of three seconds. Although this approach may be used as acceptability criteria for serviceability vibrations, absorbed-power is mainly of interest in the field of biomechanics.

2.1.1. ***Composite Floor Structures***

Reiher and Meister conducted some of the first research on human response to vibration in the early 1930's (Bachmann, 1987). One of the most significant outcomes of these studies was the Reiher-Meister Scale that rated the levels of perception to vibration from 'imperceptible' to 'painful'. This scale is presented

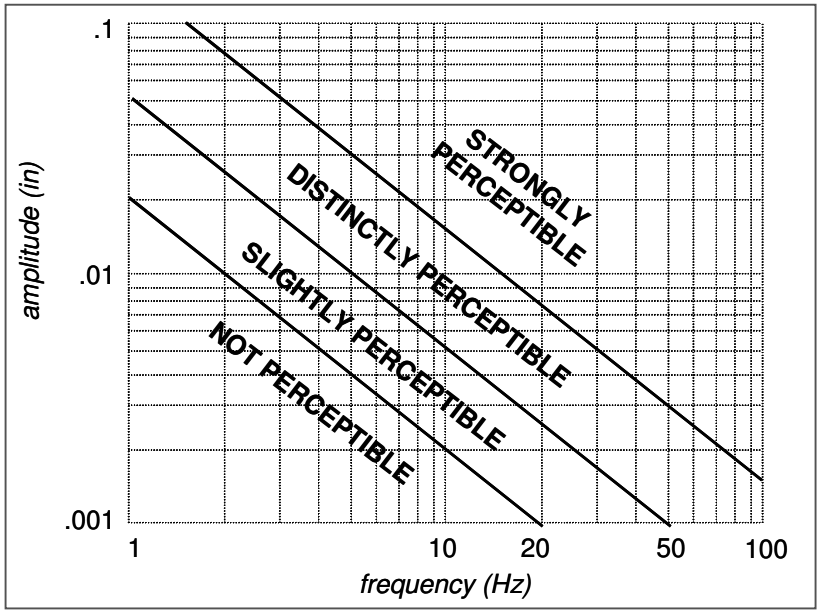

Figure 2.3: Modified Reiher-Meister Scale (after Naeim)

on a chart of displacement amplitude versus frequency is a basis from which modern acceptability criteria has evolved. During the 1960's the Reiher-Meister

Scale was modified by Lenszen to account for floor systems subjected to transient vibrations and having realistic damping of approximately 5% (Naeim, 1991). The Modified Reiher-Meister Scale in Figure 2.3, is useful for the concrete floors supported on steel beams.

The primary difference between the original and the modified scale is that the validity for the application of the modified scale is qualified with an inequality for damping ratio proposed by Murray as follows(Murray, 1975):

$$\zeta > 35 A_o f + 2.5 \qquad \textbf{Equation 2-2}$$

Where, ζ = percent damping ratio, A_o = the peak amplitude established from a heal-drop test measured in inches, and f = the first mode natural frequency of the floor.

In the 1990's it became more common for the criterion of human comfort with respect to floor vibration to be expressed in terms of acceleration. Figure 2.4

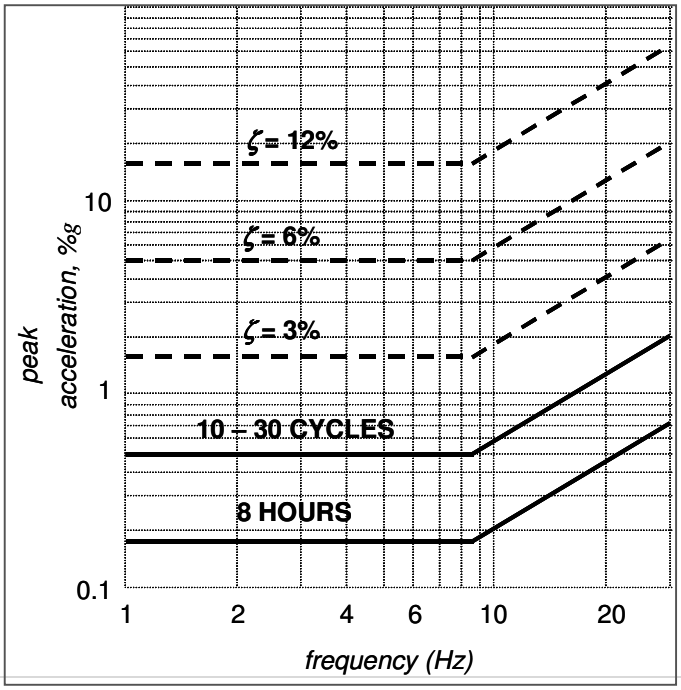

Figure 2.4: Acceleration Criteria for Buildings (after Allen)

shows a plot of acceptable levels of perceptible peak acceleration as a percentage of gravity, g. The solid curves are for the limits for continuous vibration, while the dashed curves are the limits for impulsive vibration for various degrees of damping (Allen, 1990). It is apparent from this graph that higher levels of acceleration are acceptable for systems with higher damping ratios for impulsive vibration. This is because the transient response diminishes rapidly with greater values of damping. It may also be gathered from Figure 2.4 that continuous vibrations are less tolerable than transient vibrations.

The International Standards Organization has established design criteria for the serviceability vibrations of floors (ISO10137, 2007, ISO2631.2, 2003, ISO2631.1, 1997). In the early 1990's Murray and Allen recognised that there was an opportunity to simplify the approach of assessing acceptable acceleration limits. Because a majority of floors susceptible to vibration in North America were of composite steel-deck construction, Murray and Allen modified the ISO acceleration scale by setting limits for various uses of tenancies. The Modified ISO scale in Figure 2.5 also took into consideration the behaviour of this type of floor construction with respect to damping (Murray T. M., 1993). This ISO scale does not explicitly require the designer to consider the damping ratio, however, the scale is based on typical magnitudes for modal damping between 1.0% and 5.0%.

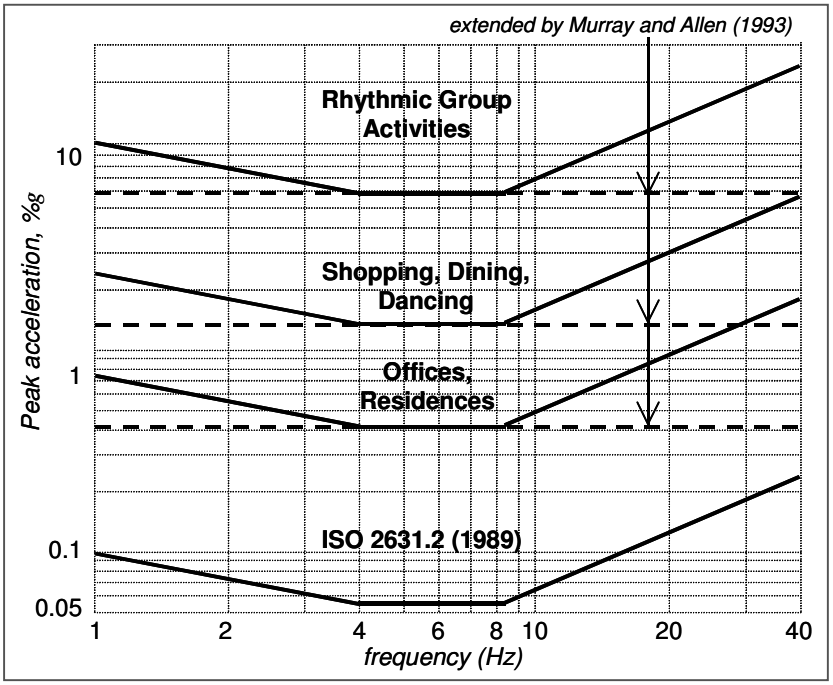

Figure 2.5: *Modified ISO scale*

For more refined calculations and to account for the effects of variable damping, the following inequality has been suggested (Murray, 1997):

$$\frac{P_o e^{(-0.35 f_n)}}{\zeta W} \leq \frac{a}{g} \qquad \textbf{Equation 2-3}$$

Where, depending of the use of the floor, 0.29 (kN) < P_o < 0.45 (kN), f_n = natural frequency, ζ = damping ratio, W = the estimated weight of the floor panel and a/g = acceleration limits from Figure 2.5. The criteria for acceptable acceleration may also be compared with the frequency ratio, which is the ratio of excitation frequency, f_o, with respect to the natural frequency, f, of the floor. Allen suggested the following inequality for group activities (Allen, 1990):

$$\frac{1.3\alpha\left(\frac{w_p}{W}\right)\sin(2\pi f t)}{\sqrt{\left[\left(\frac{f_o}{f}\right)-1\right]^2+\left[2\zeta\left(\frac{f_o}{f}\right)\right]^2}} \leq \frac{a}{g} \qquad \textbf{Equation 2-4}$$

In the above equation, α = a dynamic load factor and w_p = the weight of a person. The other factors are as previously defined. In this form, it is apparent that as the excitation frequency approaches the natural frequency of the structure, the dynamic response is at maximum. It will be explained in Section 2.3 that it is desirable to shift the natural frequency of the floor away from the expected excitation frequency for continuous vibrations in particular. The obvious limitation to the modified ISO approach is the fact that its use is intended specifically for composite steel-deck construction.

The Concrete Society Technical Report 43 of 1994 also outlined a complex procedure for deriving response factors for post-tensioned floors supported on a rectangular grid. The *CSTR43* approach was the first published attempt to formulate a hand calculation method for addressing dynamic serviceability issues for cast-in-situ concrete floor construction. The response factors derived by the Concrete Society's approach are restricted to the same magnitudes as those prescribed by the ISO. Calculations for these response factors are a tedious process that makes provisions for solid, coffered and ribbed slabs. In addition, *CSTR43* response factors, which are functions of several factors, must be determined for two orthogonal directions, x and y. Letting the subscript 'r' represents x or y, the component response factor takes the form:

$$R_r = \frac{C_r N_r}{m n_x n_y n_x l_x l_y} \qquad \textbf{Equation 2-5}$$

Table 2.1: CSTR43 1st Ed., Maximum Response Coefficients

Maximum Response Coefficient	Floor Frequency Range
$C_r = \frac{224.8}{f_r^2 \zeta}$	$f_r \leq 3Hz$
$C_r = \frac{27.2}{\zeta}$	$3Hz < f_r \leq 4Hz$
$C_r = \frac{83.2 - f_r}{\zeta}$	$4Hz < f_r \leq 5Hz$
$C_r = \frac{0.88(20 - f_r)}{\zeta} + 2(f_r - 5)$	$5Hz < f_r \leq 20Hz$
$C_r = 30$	$f_r > 20Hz$

The factor, C_r = maximum response coefficient is given in Table 2.1: CSTR43 1st Ed., Maximum Response Coefficients, N_r = modal response coefficient, which is a function of the then damping ratio, ζ, and effective aspect, a_r, ratio for floor panels in the r-direction:

$$N_r = 1 + [0.5 - 0.1\ln(\zeta)]a_r \quad \text{(for solid or coffered slabs)} \qquad \textbf{Equation 2-6}$$

$$N_r = 1 + [0.65 - 0.1\ln(\zeta)]a_r \quad \text{(for ribbed slabs)} \qquad \textbf{Equation 2-7}$$

The rest of the terms in Equations 2.5 will be thoroughly explained in Section 2.3.2. When the both component response factors have been calculated, they are superimposed for the overall response. Unfortunately, the response factor method prescribed by the *CSTR43* came under heavy criticism for being over conservative. It has been reported that vibration considerations based on the *CSTR43* result in over design and increased construction costs. In addition to

producing conservative designs, the *CSTR43 First Edition* does not provide any commentary on the development of the hand calculation method.

Acceptability charts and variations of the ISO scales have been developed in a number of countries. The United Kingdom has vibration limits published though the British Standard (BS6472, 2008). In the United States limits are provided in the American National Standards (ANSI-S2.71, 2006), and in Australia similar limits are based on the ISO and provided in the Australian Standard, (AS2670, 1990). In addition to peak acceleration, the acceleration criterion used by these standards is the root-mean-square (RMS) acceleration. The RMS acceleration is calculated from a weighted acceleration, $a_w(t)$, time-history record as follows:

$$RMS = \sqrt{\frac{\int_{t_1}^{t_2} a_w^2(t)dt}{(t_2 - t_1)}} \qquad \textbf{Equation 2-8}$$

Where, t_1 and t_2 are the limits of integration. However, it has been reported that RMS acceleration may not be an appropriate gage for human comfort because of the transient nature of loads caused by humans (Pavic A., 2001). For this reason a more recent measure has been developed known as the vibration-dose-value (VDV):

$$VDV = \sqrt[4]{\int_{t_1}^{t_2} a_w^4(t)dt} \qquad \textbf{Equation 2-9}$$

Although the VDV does not have any physical meaning, as the resulting units are ($m/s^{1.75}$), research has shown that this method is suitable for all types of

vibration, particularly for the transient nature of occupant imposed dynamic loading when measured over long durations (Pavic A., 2001).

Today, the most widely adopted approach used to access vibration acceptability is the use of response-factor multipliers on the ISO base curve. This relatively straightforward approach involves measuring or calculating the vibration response of a floor and comparing that response with a limiting value based on the intended use of the floor. Figure 2.6 graphically illustrates the several selected response factor multipliers of the ISO Base Curve envelope.

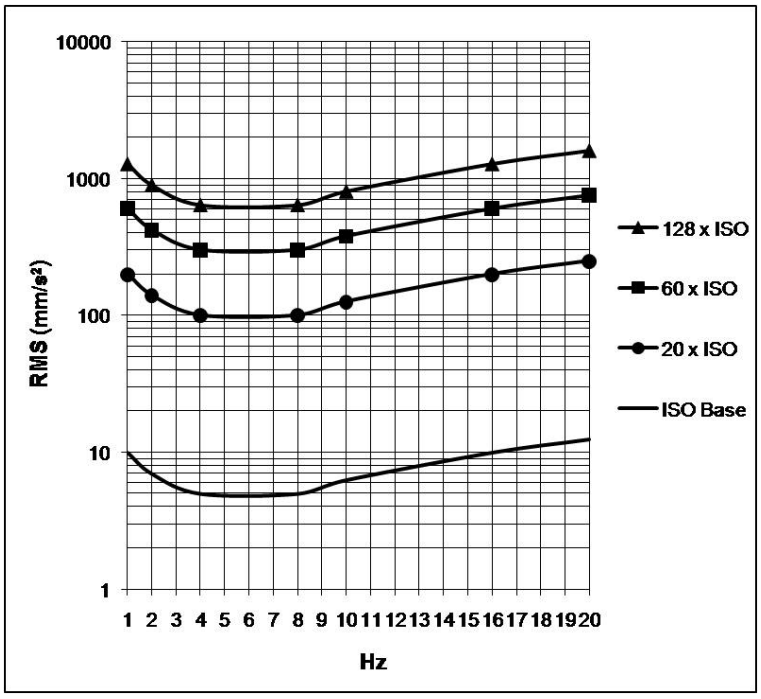

Figure 2.6: Selected Response Factor Multipliers of the ISO BASE Curve

Figure 2.7 is an excerpt from AS2870.2 which defines the range of response factors along with associated description for each application.

Place	Time	Continuous or intermittent vibration [2]	Transient vibration excitation with several occurrences per day
Critical working areas (for example some hospital operating-theatres, some precision laboratories, etc.)	Day Night	1	1 [2), 3)]
Residential	Day	2 to 4 [4)]	30 to 90 [4), 5), 6), 7)]
	Night	1,4	1,4 to 20
Office	Day Night	4 [5)]	60 to 128 [8)]
Workshop [9)]	Day Night	8 [5), 10)]	90 to 128 [8), 10)]

1) Table 2 leads to magnitudes of vibration below which the probability of reaction is low. (Any acoustic noise caused by vibrating walls is not considered.)

2) Also includes quasi-stationary vibrations caused by repetitive shocks. Shock is defined in ISO 2041:1975, clause 3, and is sometimes referred to as transient (impulsive) vibration.

3) Magnitudes of transient vibration in hospital operating-theatres and critical working places pertain to periods of time when operations are in progress or critical work is being performed. At other times, magnitudes as high as those for residence are satisfactory provided that there is due agreement and warning.

4) Within residential areas there are wide variations in vibration tolerance. Specific values are dependent upon social and cultural factors, psychological attitudes and expected interference with privacy.

5) The "trade-off" between number of events per day and magnitudes is not well established. The following provisional relationship shall be used for cases of more than three events a day pending further research into human vibration tolerance. This involves further multiplying by a number factor $F_n = 1{,}7\ N^{-0.5}$ where N is the number of events per day. This "trade-off" equation does not apply when values are lower than those given by the factors for continuous vibration. When the range of event magnitudes is small (within a half amplitude of the largest), the arithmetic mean can be used. Otherwise only the largest need be considered.

6) For discrete events with durations exceeding 1 s, the factors can be adjusted by further multiplying by a duration factor, F_d:

$F_d = T^{1.22}$ for concrete floors and T is between 1 and 20

$F_d = T^{0.32}$ for wooden floors and T is between 1 and 60

where T is the duration of the event, in seconds, and can be estimated from the 10 percentage (–20 dB) points of the motion time histories.

7) In hard rock excavation, where underground disturbances cause higher frequency vibration, a factor of up to 128 has been found to be satisfactory for residential properties in some countries.

8) The magnitudes for transient vibration in offices and workshop areas should not be increased without considering the possibility of significant disruption of working activity.

9) Vibration acting on operators of certain processes, such as drop forges or crushers which vibrate working places, may be in a separate category from the workshop areas considered here. Vibration magnitudes, for the operators of the exciting processes, which are specified in ISO 2631-1, will then apply.

Figure 2.7: TABLE 2 from AS2870.2 –Response Factors for z-axis vibration

2.1.2. **Comments on Acceptability Criteria**

In summary, acceptability criteria for floor vibrations have been subjectively derived from extensive research on the tolerance levels of the receiver. The frequency of vibration and associated damping are common factors for any assessment method under consideration. Although research on damping is ongoing, typical damping ratios for floors have been well established, particularly for composite steel-deck construction and generally fall within a narrow range. As will be explained in Section 2.3, there are also well established techniques available for evaluating the fundamental frequency of composite, steel-framed floor systems. Because the first edition of the *CSTR43* has proven to be unreliable, its approach to assessing the natural frequency of floors has been removed in the second edition, strictly limiting the available guidance for evaluating the natural frequency of cast-in-situ floors with hand calculations. Therefore the most challenging task for an engineer to perform when assessing vibration acceptability is predicting the natural frequency of suspended concrete floors.

2.2. **Human Induced Dynamic Loads (the source)**

As the case is with acceptability criteria, there has been a great deal of research on dynamic loads and sources of vibration. Dynamic loads on structures may be harmonic, periodic or non-periodic and are either transient or continuous. This literature review will concentrate on human sources of dynamic loads. Human perception of vibration also depends on the nature of vibration which may be

continuous or transient. Sources of continuous vibration are often mechanical, external or caused by internal group activity. Transient sources of floor vibration are usually imposed internally by the footfalls of occupants. This research is focused on the vibration response of floor structures subjected to human-induced transient or impulsive excitation

Human induced dynamic loads are usually transient in nature. Because human induced dynamic loads are also periodic, they may be mathematically modelled as forcing functions with relative ease. Figure 2.8 shows typical data obtained from an instrumented treadmill (Brownjohn, 2004). Between steps, or footfalls, a person's body rises and falls. With each heel contact, impulsive energy is transferred from the walker to the floor. It is apparent from Figure 2.8 that the forces from the left and right footfalls may be superimposed, resulting in a single periodic function of footfall force in Newtons versus time in seconds.

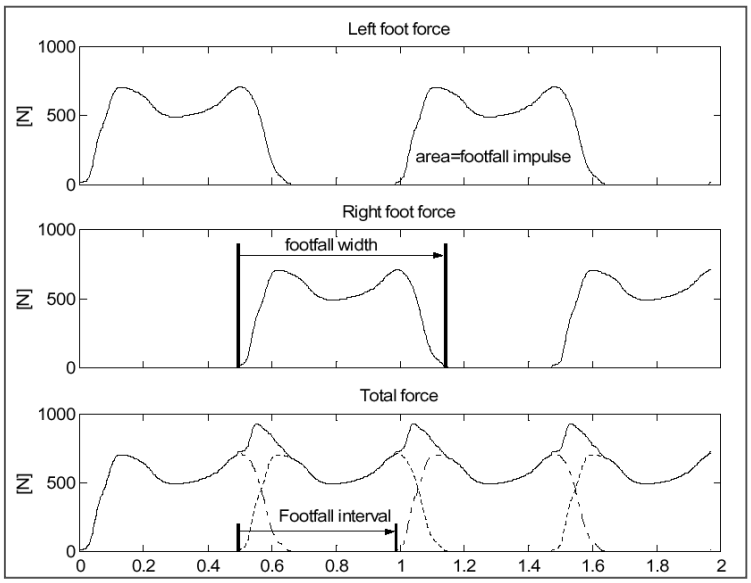

Figure 2.8: Foot**f**all forcing function (after Brownjohn)

The periodic nature of these forcing functions allows them to be decomposed into sinusoidal components and expressed mathematically as a Fourier Series. Rainer, Pernica and Allen conducted a Canadian study on footbridge loading and produced the Fourier coefficients shown in Figure 2.9. The coefficients derived

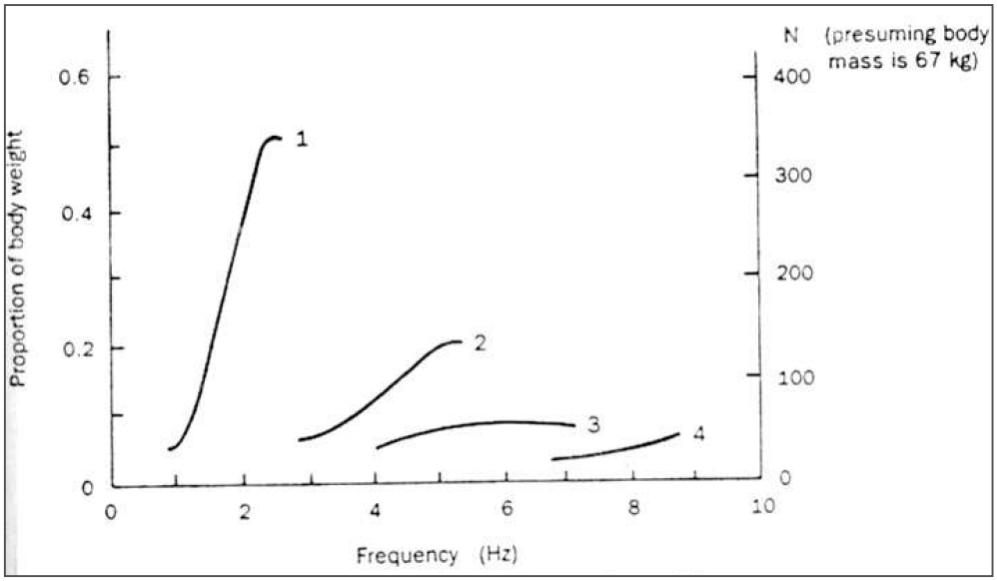

Figure 2.9: Fourier coefficients for walking loads (after Wyatt)

from this study are the results of a single person walking with regular pace (Rainer, 1988). Other types of human induced dynamic loading result in Fourier coefficients of various magnitudes, but the nature of developing mathematical models for load functions is the same.

Eriksson conducted a comprehensive study that investigated the dynamic loads imposed on floors from human activities including walking, running and jumping. His study investigated combinations loading by individuals and crowds at various frequencies and coordination (Errikson, 1994). An outcome of Eriksson's research was a set of two types of force models. The first type of model he

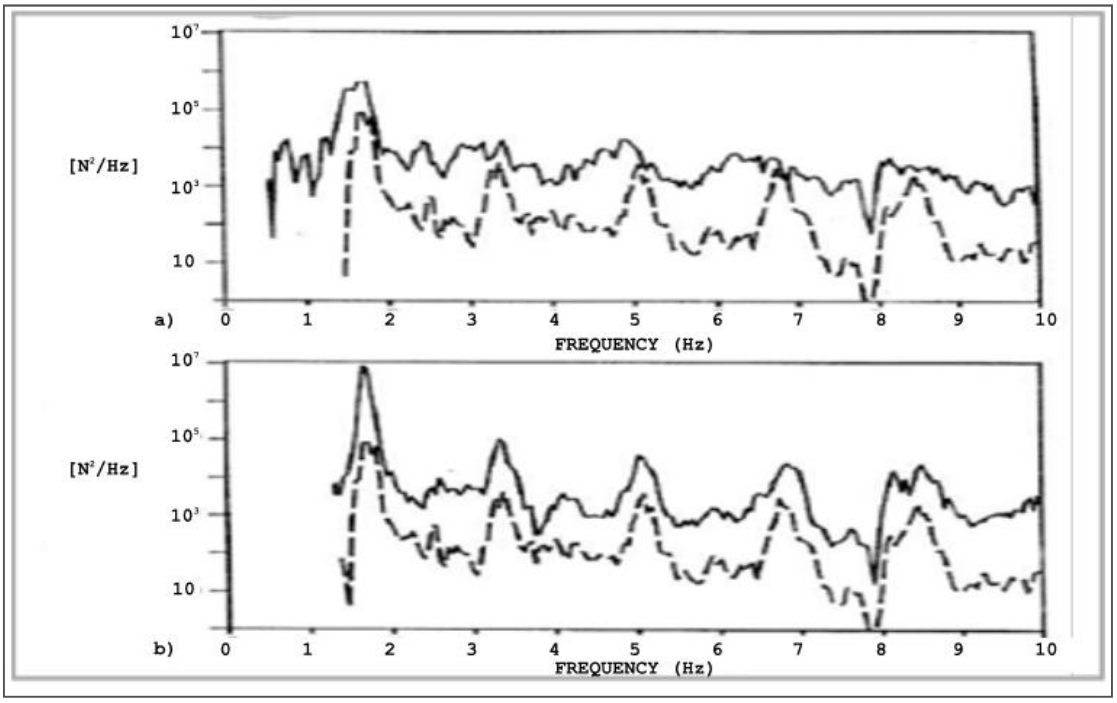

Figure 2.10: Spectral density functions for a group of 11 persons at: a) coordinated walking, b) uncoordinated walking. The dashed line represents the spectral density function for an individual walking at 1.7Hz (after Eriksson)

referred to as an 'RMS force model'. The RMS load model was established for low-frequency forces from individual pedestrians or crowds moving with a considerable degree of coordination like exercise or dancing. For crowd type loadings that exhibit a low degree of coordination, Eriksson adopted a 'Broad-band force model'. The reason for this distinction is that the spectral density functions for uncoordinated motions are relatively flat compared to the spikes observed in spectra obtained from more coordinated, periodic excitation and can be seen in Figure 2.10. In the cases of running, jumping and dance, the character of footfall impacts is different to that of walking. It can be observed from Figure 2.8 that there is an overlap in time between the steps of a walker. Instead, when running, jumping or dancing, there is a space in time between individual contacts between a person's feet and the ground. Galambos refers to

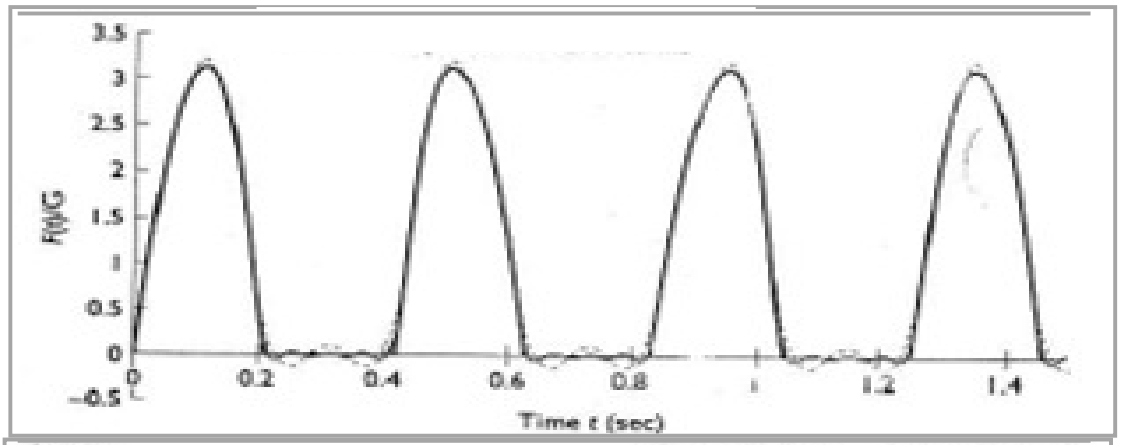

Activity	Contact Ratio α	Impact Factor K_p
Pedestrian movements, low impact aerobics	2/3	2.4
Rhythmic exercises, high impact aerobics	1/2	3.1
Normal jumping	1/3	4.7
High jumping	1/4	6.3

Figure 2.11 *Jumping and group forcing function (after Smith)*

this phenomenon as 'flying time' and Wyatt has coined the term 'free flight'(Galambos, 1988, Wyatt, 1989). This space in time is clearly illustrated in Figure 2.11, which the typical plot of a load function for group activity. Additionally, as would be expected, the impulse delivered to the floor with each contact is higher than from walking. This combination of factors requires special attention. Pernica in the early 1990's developed load functions for these activities (Pernica, 1990, Smith, 2002). These load functions incorporate an impact factor and a contact factor, each of which are associated with the type of activity under consideration. Soon after, Ji and Ellis recommended an analytical procedure that will not be repeated here (Ji, 1994). However, the shape of the normalized load function and table of factors are also presented in Figure 2.11.

2.2.1. **Comments on Human Induced Dynamic Loads**

There are a number of ways in which humans impose dynamic loads on floors. Extensive research has been conducted on the measurement and modelling these loads. The primary purpose of developing load models is for their application in dynamic structural analysis and design. Even so, Ebrahimpour concluded that the sophisticated load models that resulted from his research were too complex to be applied directly in design. As a consequence recommendations were made that significantly simplified the mathematical modelling of loads as functions to load intensity factors instead (Ebrahimpour, 1996).

In conclusion to this section on human-induced loads, having a representative load model is not sufficient to provide a complete assessment of floor vibration. It was explained in Section 2.1 that acceptability criterion is a function of the frequency and acceleration response of the floor structure. Therefore, without reliable methods to determine the response frequency and acceleration of suspended concrete floors, dynamic analysis is a significant challenge for engineers may not have the required technical background to competently employ high-powered computational tools such as transient dynamic finite element analysis.

2.3. **Vibration Response (the transmission path)**

This section of the literature review will emphasise that although there is an abundant amount of information relevant to the dynamic analysis and design of composite, steel framed floors, there is very little directly related to predictive methods for the structural analysis and design of suspended concrete floor vibration. Awareness of the problem of floor vibration has existed at least since the early nineteenth century. There are a number of recent papers that quote some of the first advice provided on the subject offered by Thomas Tredgold in 1828:

> "Girders should always, for long bearings, be made as deep as they can be got; an inch or two taken from the height of a room is of little consequences compared with a ceiling disfigured with cracks, besides the inconvenience of not being able to move on the floor without shaking everything in the room."

The nature of Tredgold's statement underlines the fact that floor vibration is a structural issue that demands a structural engineering solution. Although it is unknown whether Tredgold gave his advice based on a first- principal analytical approach, he did recognize that increasing the stiffness of the structure by increasing the depth of the girder served to increase the frequency response of the floor. It is obvious from Equation 1.7 that the frequency response of a structure is proportional to the system stiffness. The technique of adjusting the stiffness of the structure, as proposed by Tredgold is known today as 'frequency

tuning'. Floor structures can be 'high' or 'low' tuned by respectively increasing or decreasing the stiffness. Usually high tuning is favourable for strength considerations, in spite of associated increased costs. Tuning may also be accomplished by adjusting the mass attached to the structure (Bachman, 1995).

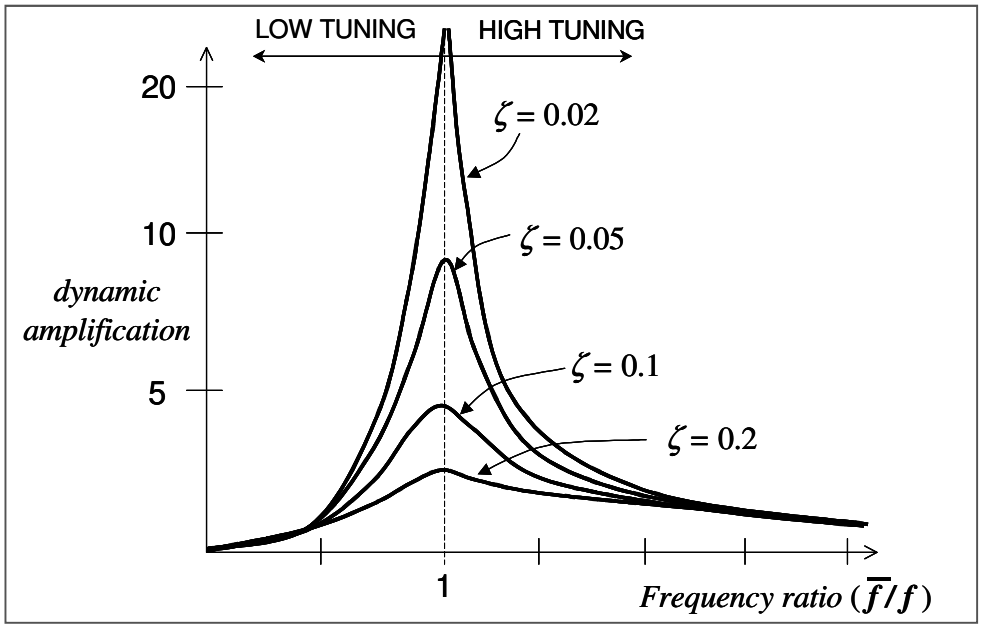

Figure 2.12: Frequency tuning (after Bachmann)

The effect of frequency tuning is to shift the natural frequency of a structure away from a resonance situation. This can be observed on a dynamic amplification curve as shown in Figure 2.12. For harmonic loading with a given force amplitude, resonance occurs as the ratio of the forcing frequency approaches the natural frequency of the structure. For any frequency ratio, the dynamic deflections increase as a multiple of the deflection that would be caused by a static force of the same magnitude as the forcing function depending on the damping of the system.

Without the ability to predict the dynamic performance of floors, vibration assessment becomes retrospective. If vibration is determined to be a

serviceability problem after the floor has been constructed, then costly structural retrofit could be required that may interrupt or change the originally intended function of the tenancy. Bendickson gives examples of remedial solutions (Bendickson, 1993).

2.3.1. ***Composite Floor Construction***

Predictive determination of the natural frequency of a floor structure is crucial for assessing dynamic serviceability during the design phase of a project. There have been a number of studies that addressed this issue for composite, steel-framed floors. The United Kingdom has published the 'Design Guide on the Vibration of Floors' through the Steel Construction Institute that deals with composite, steel-framed floor construction (Wyatt, 1989). Because steel-framed floors are comprised of main beams (girders), secondary beams (joists), and the concrete slab, the interaction of these elements must be considered in the overall dynamic behaviour. Steel-framed floors obey the classic equation for spring-mass oscillators in series, otherwise known as the Dunkerly method:

$$\frac{1}{f_0^2} = \sum \frac{1}{f_g^2} + \sum \frac{1}{f_j^2} + \sum \frac{1}{f_s^2} \qquad \textbf{Equation 2-10}$$

Where f_0 = the system natural frequency, f_g = the natural frequency of the girders, f_j = the natural frequency of the joists and f_s = the natural frequency of the slab.

By considering the load path and the elastic behaviour of girders and joists in steel-framed floors, this guide considers four levels of practical approach for evaluating natural frequency:

a) static computer analysis – In situations where the layout of steel framing is not regular, the fundamental mode shape can be difficult to obtain. For this situation, a more refined degree of calculations is required and lends itself to numerical solutions. Concisely stated, the designer must iterate a deflected shape and loading such that the product of deflection, y_i, and mass, m_i, is in equal proportion to point loads, P, at all locations along each span by a constant of proportionality, q_i. The resulting equation for the natural frequency of a floor from a discrete formulation takes the form of the following finite sum:

$$f = \frac{1}{2\pi}\sqrt{P\sum \frac{q_i y_i}{m_i y_i^2}} \qquad \textbf{Equation 2-11}$$

b) dynamic computer analysis – This method includes matrix formulation software and finite element analysis. Although these computational tools have the potential to be highly accurate, the results are influenced by he assumptions of the modeller. Special care must be used when estimating connectivity between members, material properties, distribution of loads and steel-concrete interaction.

c) *self-weight deflections* - This method employs the basic formula for natural frequency given in Equation 2.12. The weighted average value of deflection, Δ_w (mm), from an equivalent beam is assumed to be ¾ (three-fourths) of the maximum total component deflections, Δ_o (mm), and the value for gravity, $g \sim 9810$ (mm/s^2), are in place of mass and stiffness:

$$f = \frac{1}{2\pi}\sqrt{\frac{g}{\Delta_w}} = \frac{18}{\sqrt{\Delta_0}} \qquad \textbf{Equation 2-12}$$

d) *frequency-coefficient method* – The frequency-coefficient method, is suitable for one-way floor systems in which continuous spans with various span ratios should be considered. The formula for natural frequency in this case makes use of a constant referred to as the frequency factor, C_B, and is the same as Equation 1.7:

$$f = C_B \sqrt{\frac{k}{m}} \qquad \textbf{Equation 2-13}$$

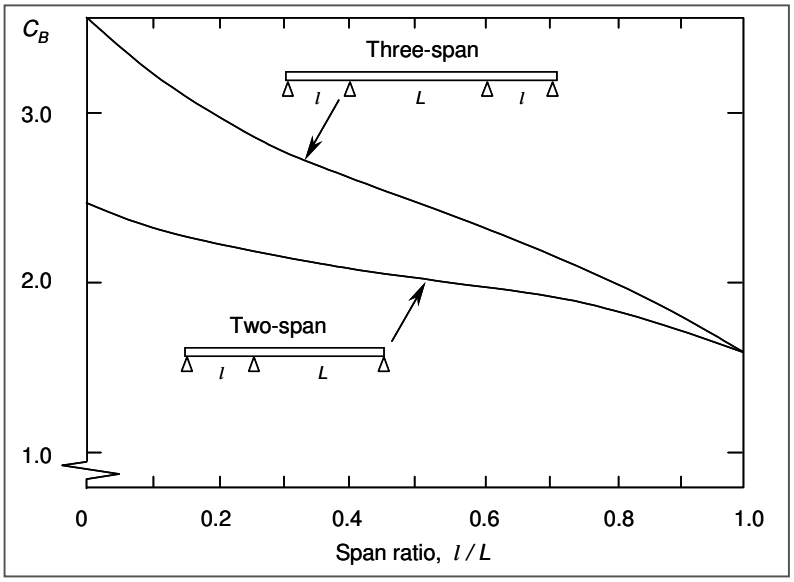

Figure 2.13: *Frequency Factor, C_B, for continuous beams to use with reference to Equation 2.13 (after Wyatt)*

Collaborative research between the United States and Canada has also been successful in publishing a design guide for steel-frame supported concrete floors through the American Institute of Steel Construction entitled, “Floor Vibrations Due to Human Activity”(Murray, 1997). The approach to determining the design frequency is virtually identical to the British self-weight deflections approach.

Instead of separating the frequencies of the girders, joists and slab, this approach considers the behaviour of an individual floor panel bounded by the main beams or girders. There are, however, some subtle differences. One difference is that Murray's method neglects the slab contribution to the system dynamic behaviour. The other is simply the presentation of the equation for fundamental frequency:

$$f = 0.18\sqrt{\frac{g}{\Delta_g + \Delta_j}} \qquad \textit{Equation 2-14}$$

In this formulation, the constant, 0.18, is derived on the same assumptions as the British guide in that the self-weight deflections are ¾ (three-fourths) of the maximum calculated deflections of the girders as in Equation 2.12, Δ_g (mm), and the joists, Δ_j (mm):

$$f = \frac{1}{2\pi}\sqrt{\frac{g}{\frac{3}{4}\left(\Delta_g + \Delta_j\right)}} \approx 0.18\sqrt{\frac{g}{\left(\Delta_g + \Delta_j\right)}} = 0.18\sqrt{\frac{9810}{\left(\Delta_g + \Delta_j\right)}} \approx \frac{18}{\sqrt{\Delta_0}}$$

The natural frequencies calculated from to Equation 2.14 are suitable for accessing acceptability that were discussed in Section 2.1. It should be emphasized that the stiffness used for these equivalent beam formulations is based on the composite action between the steel supporting frame members and the concrete slab.

2.3.2. **Cast-In-Situ Concrete Floor Construction**

Research focused on the dynamic behaviour of cast-in-situ concrete floors is limited, particularly for post-tensioned systems. The only available formal

guideline for the dynamic analysis and design of post-tensioned system is the Concrete Society Technical Report 43 (CSTR43) of 1994 (1994). Since its publication, there have been numerous complaints that it produces over conservative designs when used for assessing vibration serviceability. This is primarily a result of the *CSTR43* method having the tendency to underestimate the design frequency.

It was previously mentioned in Section 2.1 that the CSTR43 method makes provisions for solid (of coffered) and ribbed slabs. The method for calculating design frequency begins by assuming a multi-panel floor geometry that is supported on a rectangular grid, which has two orthogonal fundamental families of vibration. The assumed floor geometry is shown in Figure 2.14.

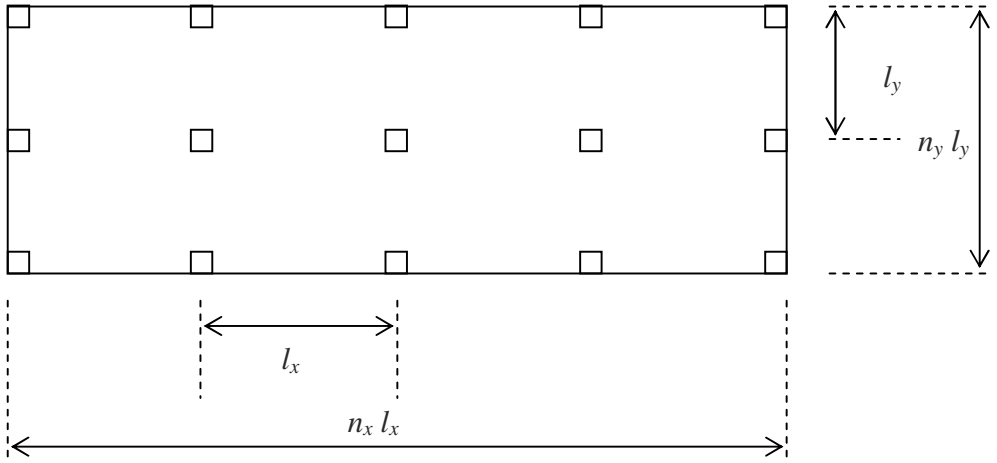

Figure 2.14: *CSTR43 Floor Geometry*

The design frequency is calculated for each direction in the following manner. An aspect ratio, λ, is determined for each orthogonal direction:

$$\lambda_x = \frac{n_x l_x}{l_y}\sqrt[4]{\frac{I_y}{I_x}} \quad ; \quad \lambda_y = \frac{n_y l_y}{l_x}\sqrt[4]{\frac{I_x}{I_y}} \qquad \textbf{Equation 2-15}$$

Where, n_x and n_y are the number of bays; l_x and l_y are the lengths of and individual bay; and I_x and I_y are the second moments of area per unit width spanning, in the x and y directions respectively. The second moments of area for solid, flat slabs are equal in each direction. However, for coffered and ribbed slabs, extremely high differences between moments of inertia may be encountered. The aspect ratios are used to calculate a weighting factor, k_r, letting the subscript, r, represent the directions x or y:

$$k_r = 1 + \frac{1}{\lambda_r^{\,2}} \quad \text{(for solid or coffered slabs)} \qquad \textbf{\textit{Equation 2-16}}$$

$$k_r = \sqrt{1 + \frac{1}{\lambda_r^{\,4}}} \quad \text{(for ribbed slabs)} \qquad \textbf{\textit{Equation 2-17}}$$

The weighting factor is then used to determine the primary orthogonal frequencies, $f\,'_r$:

$$f'_x = k_x \frac{\pi}{2}\sqrt{\frac{EI_y}{ml_y^4}} \;\; ; \;\; f'_y = k_y \frac{\pi}{2}\sqrt{\frac{EI_x}{ml_x^4}} \qquad \textbf{\textit{Equation 2-18}}$$

Where, E = the modulus of elasticity of the concrete; m = the mass per unit area including 10% of the superimposed live load mass and the other terms are as previously defined. Next, the basic frequency, f_b, of a single panel is calculated:

$$f_b = \frac{\frac{\pi}{2}\sqrt{\frac{EI_x}{ml_x^4}}}{\sqrt{1+\frac{l_y^4}{l_x^4}}} = \frac{\frac{\pi}{2}\sqrt{\frac{EI_x}{ml_x^4}}}{\sqrt{1+\frac{l_y^4}{l_x^4}}} \quad \text{(for solid or coffered slabs)} \qquad \textbf{\textit{Equation 2-19}}$$

$$f_b = \frac{\frac{\pi}{2}\sqrt{\frac{EI_x}{ml_x^4}}}{\sqrt[4/3]{1+\left(\frac{I_x l_y^4}{I_y l_x^4}\right)^{2/3}}} = \frac{\frac{\pi}{2}\sqrt{\frac{EI_x}{ml_x^4}}}{\sqrt[4/3]{1+\left(\frac{I_y l_x^4}{I_x l_y^4}\right)^{2/3}}} \quad \text{(for solid or coffered slabs)} \qquad \textbf{\textit{Equation 2-20}}$$

Once the basic frequency, f_b, and the fundamental frequency, f, have been calculated, then the system design frequency for each orthogonal direction is:

$$f_r = f_r' - (f_r' - f_b)\left(\frac{1/n_x + 1/n_y}{2}\right) \qquad \textbf{Equation 2-21}$$

Although the CSTR43 method appears to be extremely comprehensive in its approach, several studies have shown that it can be just as extremely unreliable. In 1994, Williams and Waldron conducted a very interesting survey on the available methods of predicting vibrations in concrete floors, one of which was the CSTR43 (Williams, 1994). For their study, a database of existing data was compiled from previous experimental modal analyses on real floor structures. In all, 12 (twelve) cast-in-situ floor structures were investigated. Nine of these floors were post-tensioned systems of various configurations. The aim of their study was to compare the predicted values of natural frequencies to those actually

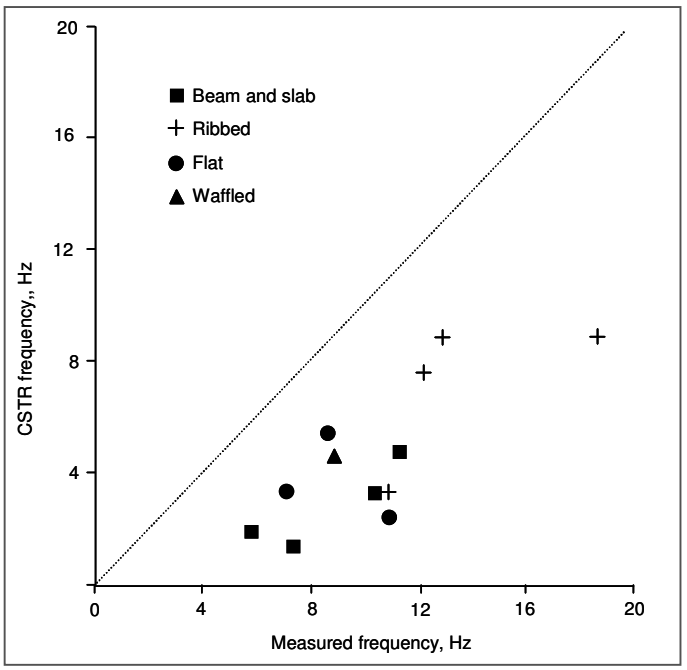

Figure 2.15 *Frequency Comparison (after Williams and Waldron)*

measured. Figure 2.15 Frequency Comparison (after Williams and Waldron) shows very clearly that the CSTR43 method under predicted the natural frequencies of every floor structure in their database.

More recent research on the deficiencies of the Concrete Society method has been conducted in the United Kingdom (Pavic, 2002, Caverson, 1994). One study involved field-testing a 600 tonne, ribbed, post-tensioned concrete floor (Reynolds P., 1998). The measured natural frequency was compared to the calculated frequency following the recommendations of the CSTR43. Furthermore, the predicted and measured RMS accelerations were also obtained and compared to the ISO2631-2 acceptability criteria shown in . This study showed that the measured values for natural frequency were more than 2.5 times greater than predicted by CSTR43 hand calculations. It also illustrated the potential for the CSTR43 method to produce over conservative designs.

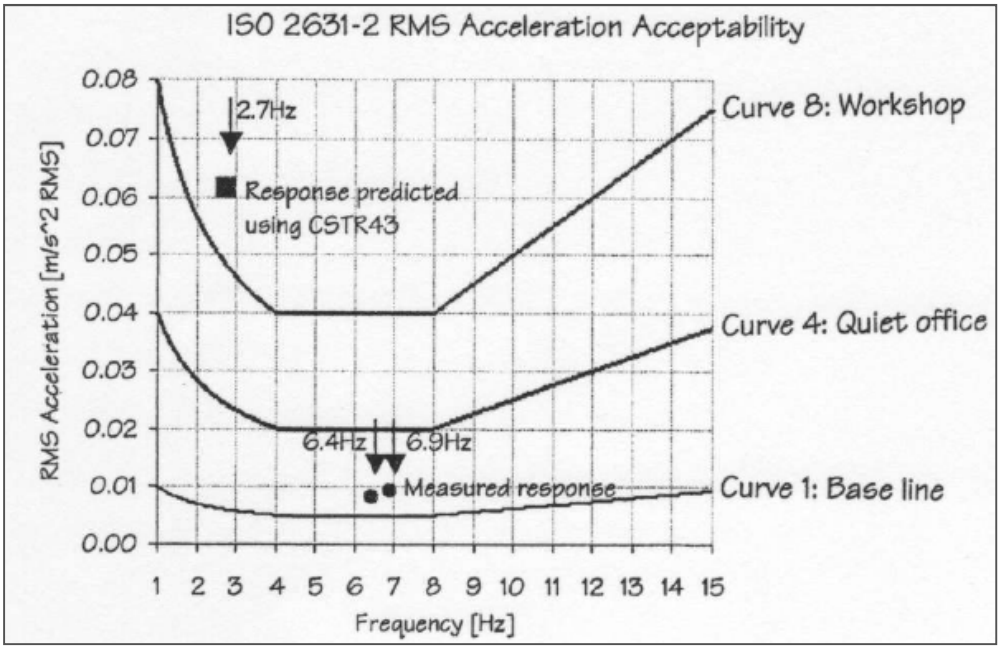

Figure 2.16: *Acceptability Comparison (after Pavic)*

2.4. **Comments on Floor Vibration**

The Australian Standard, AS 3600-2001, and the British Standard, BS 8110-1, for concrete structures simply mention the need to consider vibration serviceability criteria without any specific design guidance(AS3600, 2009, BS8110-1, 1997). The American concrete code, ACI 318-05, makes no reference to serviceability vibrations whatsoever (ACI318-05, 2005). Also in the United Kingdom, the Concrete Society's Technical Report No 43 (CSTR43) suggests modified guidelines for vibration that were originally derived for steel-framed, composite concrete floors. The most significant problem with the CSTR43 guidelines on vibration is that there was no research or experimental studies to validate the suggested modifications prior to its publication. As a consequence, there have been reports of overconservative designs resulting from the use of the CSTR43 for vibration design considerations.

Recent research on the vibration of floors conducted at the University of Sheffield in the United Kingdom involved a one-way, post-tensioned concrete strip (Pavic, 1998). The deficiency here is that many PT floor systems are designed for two-way behaviour. Furthermore, this particular study was focused on the use of false floors in buildings. It did not explicitly investigate approaches to the design or theoretical analysis of floor vibration. Other studies have considered vibration in floors from a finite-element-modelling standpoint. These previous FEM studies on the vibration of floors were mainly concerned with the practice of modal testing and model updating techniques applied to civil engineering structures.

Traditionally, modal testing is a tool employed in the disciplines of mechanical and aerospace engineering for which structures or components are susceptible to continuous, high-frequency fatigue. For most circumstances, this is not the typically expected serviceability load case for floors in buildings; however, the outcomes of these studies are a valuable stepping stone for this proposed research because they have shown that it is suitable to use isotropic shell elements and smeared stiffness for FEM studies on the vibration of floors (Reynolds P., 1998, Pavic A., 2001, Pavic, 2003, Errikson, 1994) Although these studies dealt with floor vibration, they were retrospective, and none addressed the problem from a theoretically predictive approach.

Although these resources have produced a comprehensive set of dynamic serviceability criteria, none provide reliable analysis and design tools for the prediction of vibration response cast in-situ floor structures and hence the need for this research program.

CHAPTER 3

LABORATORY TESTING

3.1. **Overview**

There are several important aspects of laboratory testing in this research program. It is important to understand that the significance of laboratory testing must be considered in conjunction with subsequent finite element analysis which will be discussed thoroughly in CHAPTER 4. Generally, these laboratory tests have provided insight on the vibration response of a full-scale, post-tensioned, two-way, suspended concrete floor structure. These laboratory tests have also been essential in enabling the accurate calibration of material models for elasticity and damping in subsequent finite-element analysis. In particular, these laboratory tests, in conjunction with finite-element analysis, have provided a means to gauge the dynamic modulus of elasticity of concrete, '$E_{c,dyn}$', which is an important parameter needed for assessing vibration serviceability performance.

3.2. **Test Specimen and Set-up**

To simulate a slab geometry typically encountered in slender floor structures of actual industry projects, a full-scale floor plate was constructed in the university's structures laboratory. The specimen was a post-tensioned, two-way, flat plate panel, simply supported at the corners. The panel was square with 5.7 metre spans and a thickness of 170mm which is shown in Figure 3.1.

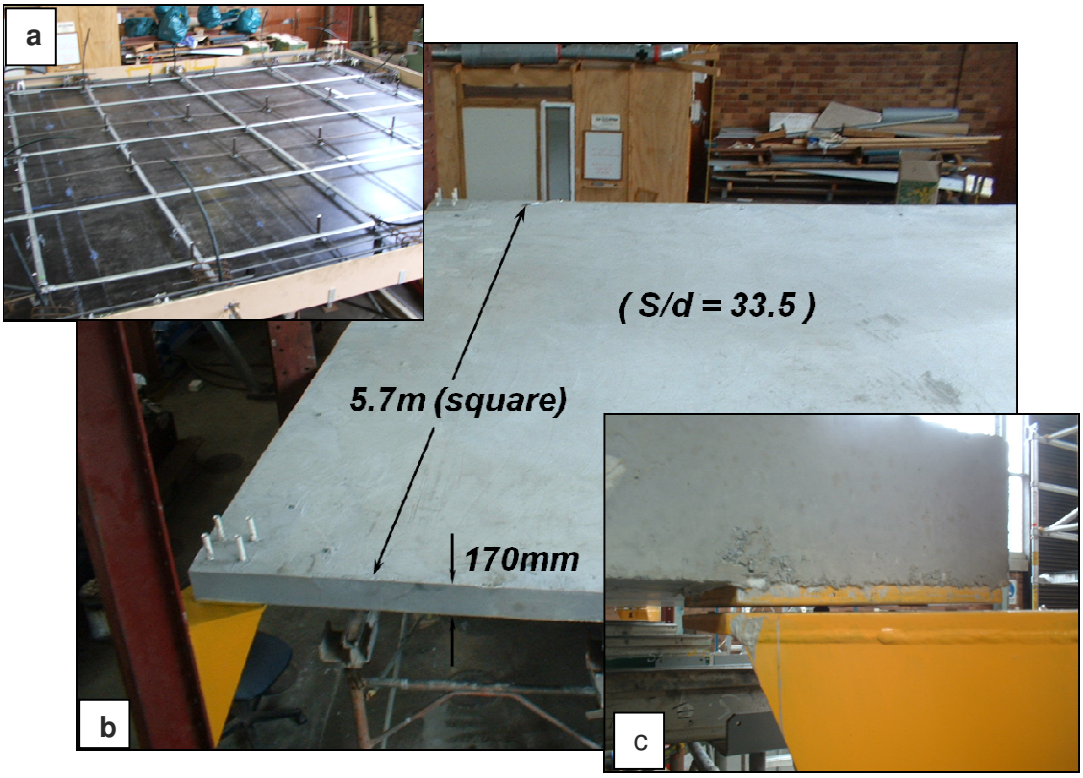

Figure 3.1: *Laboratory Specimen – a) formwork with reinforcement and post-tensioning tendons installed; b) completed slab showing dimensions; c) steel support bracket showing pin-supported plate.*

This laboratory specimen was necessary in providing baseline results for the calibration of finite element computer models for static and dynamic behaviour. The overall geometry and post-tensioning layout is shown in Figure 3.3.

Following the normal timeframe and procedure for post-tensioned floor construction in real buildings, seven days after the slab was poured the tendons were stressed to 154 kN per strand. The ends of the live-end strands were then cut and the stressing pockets were packed and sealed so tendons could be grouted.

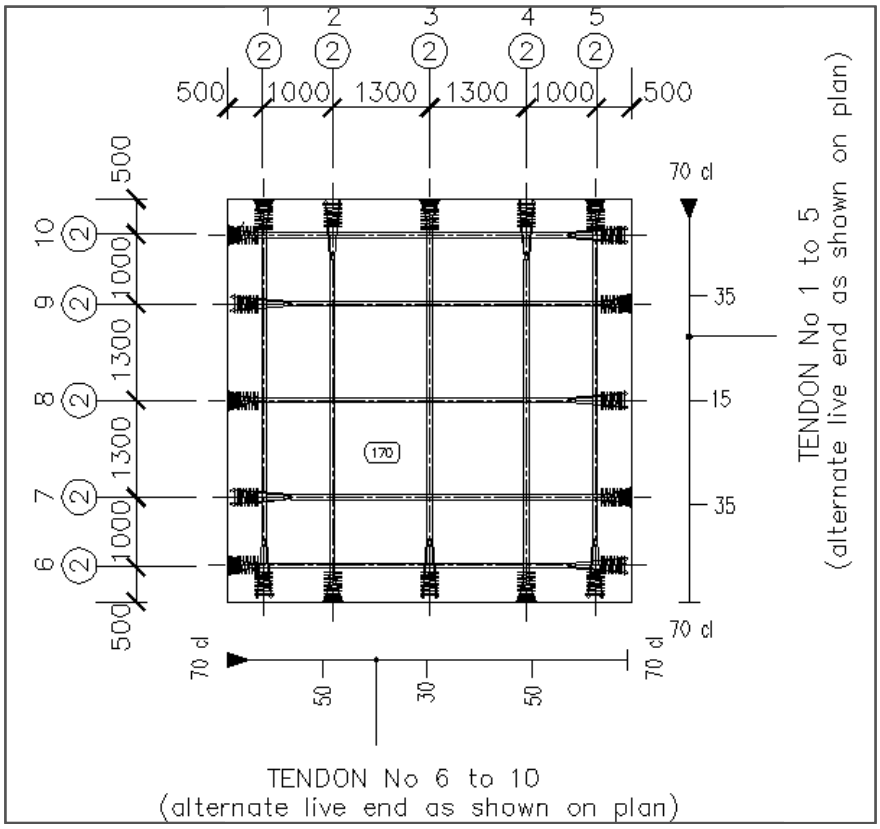

Figure 3.2 *Specimen Plan and Tendon Layout)*

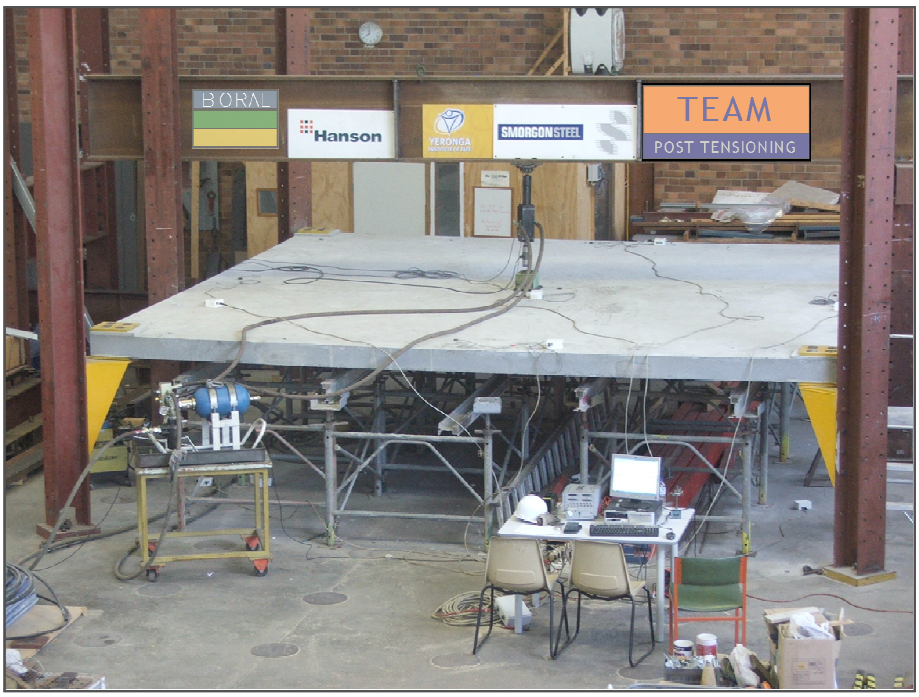

Figure 3.3: : *Specimen Test Set-up: Hydraulic pump and actuator (bottom left); Data acquisition system (bottom right); Hydraulic ram/load cell fixed to header beam (top)*

After casting the concrete the specimen was surface hydrated for a period of 28days prior to the formwork being stripped and props removed. Surface hydration was achieved by thoroughly wetting the specimen then covering it completely with 0.2mm plastic sheeting. The complete test set-up is shown in Figure 3.2. The specimen was designed for a concentrated load of 50kN and factored, super imposed dead and live loads of 1kPa and 2kPa respectively. This specimen required the following material:

- 5.5 cubic metres of concrete
- 35 square metres of formwork
- 140 metres of 12.7 post-tensioning strand
- 48 metres of N16 reinforcement
- 500 kg of steel plate for support brackets.

One of the special features of this test specimen set-up was the support system, which was designed to provide pinned support conditions. The specimen was

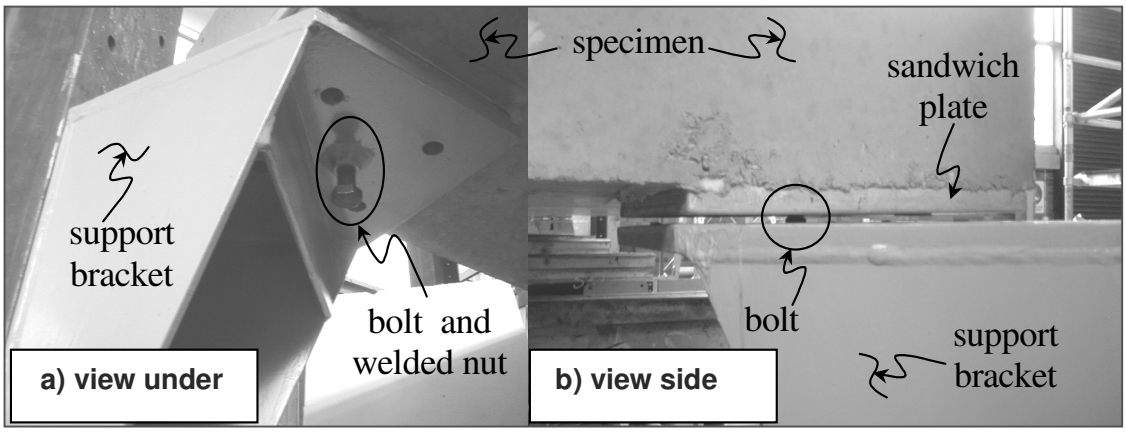

Figure 3.4: *Support Bracket Details*

supported on its corners by four steel support brackets. The details of the support brackets are shown in Figure 3.4. The specimen was cast onto free

floating, 20mm sandwich plates that were placed on the top of each support bracket. To achieve a pinned connection, a hardened, high-strength steel nut was welded to the underside of the 20mm top plate of each support bracket. A round-tipped, threaded rod is then turned through the nut until the sandwich plate is raised above the top plate. In this position, the specimen is supported entirely by the point contact between the threaded rod and the sandwich plate thus resulting in a relatively frictionless, ideal pinned support.

Static loads were applied to the centre of the panel by a hydraulic ram that was fixed to a header beam which was suspended over the specimen by columns fixed to the laboratory reaction floor. Images of the ram and load cell assembly are shown in Figure 3.5. To protect the load cell from rigid contact with the specimen, a softwood timber block was place beneath the load cell. Prior to testing the load cell was lowered into contact with a steel plate placed on top of the block to distribute the load onto the block.

Linear potentiometer displacement transducers were used to measure vertical 'z-axis' deflections of the specimen during static and dynamic tests. Displacement transducers were supported by clamps fixed to frames on the underside of the specimen at midspan along each edge and at the centre of the panel. An image of a displacement transducer is shown in Figure 3.6.

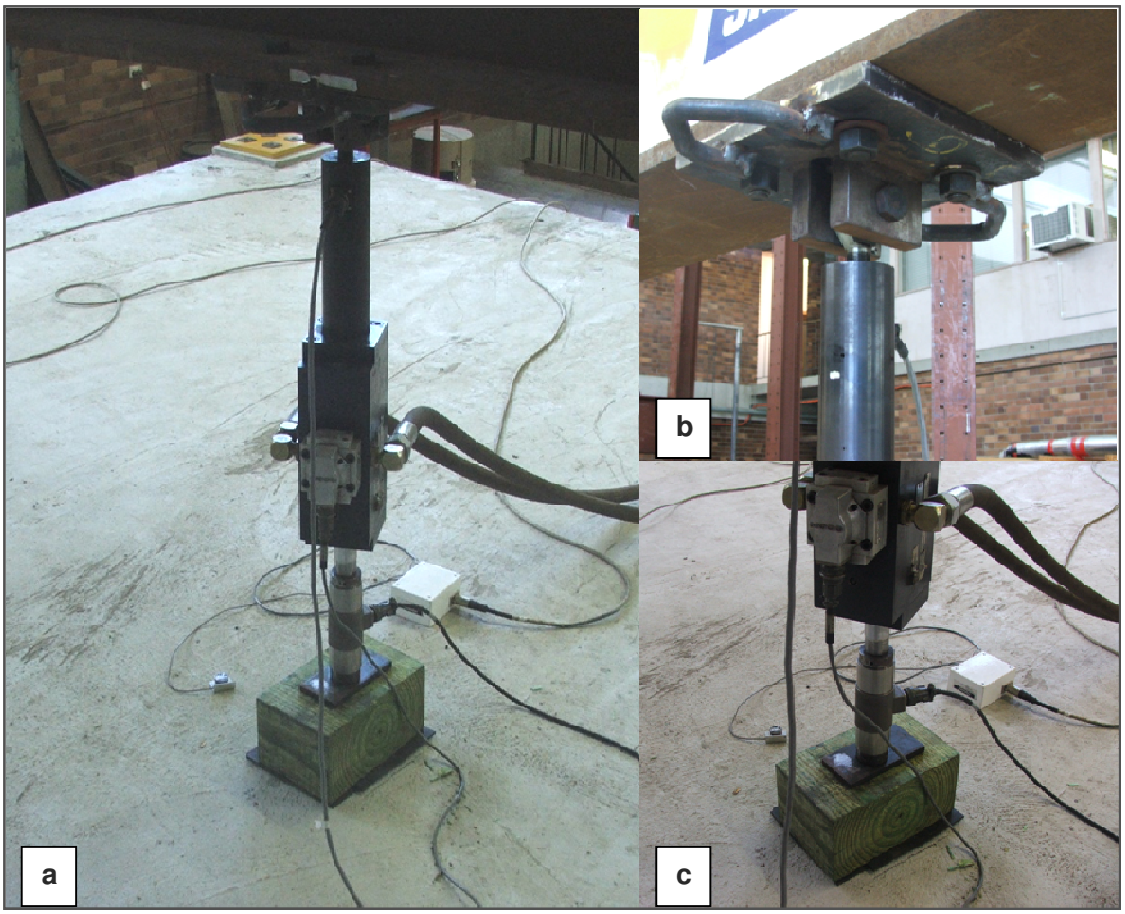

Figure 3.5: *Hydraulic Ram and Load Cell – a) assembly; b) ram fixing to header beam; c) load cell mounted to ram and contact with floor on steel plate and timber block.*

Figure 3.6: *Linear potentiometer displacement transducer.*

Figure 3.5: Laboratory *Data Acquisition Workstation.*

Accelerations during dynamic tests were measured by five accelerometers which were fixed directly to the top of the specimen with epoxy adhesive at the midspan of each side and at the centre of the panel. Each accelerometer and displacement transducer was assigned a channel and connected to a common 'eDAQ 'data acquisition hardware unit. These displacement and acceleration channels were calibrated by 'zeroing' each instrument before each test commenced. This was done by pulling cables out and back into each socket. The data collected by the eDAQ system was relayed to a desktop computer and was processed by the data acquisition software package 'InFIELD.' Figure 3.7 is a picture of the data acquisition workstation with the eDAQ unit on the table.

3.3. **Concrete Compression Tests and Modulus of Elasticity**

The Australian Standard for Concrete Structures AS3600 allows the strength and modulus of elasticity of concrete at particular age to be determined by testing using concrete cylinder compression tests. Stress-strain curves from cylinder compression tests were used for this research to establish the static modulus of elasticity of concrete, '$E_{c,stat}$', on 28 day old samples. Three concrete cylinder tests were used to determine an

Figure 3.6: Concrete Compression Test Cylinder.

average '$E_{c,stat}$', representative of the specimen. An image of a crushed cylinder following a compression test is shown in Figure 3.6. The static modulus, '$E_{c,stat}$' was calculated as the ratio of 40% of maximum stress divided by the corresponding strain (AS1012.17, 1997). Table 3.1 provides a summary of concrete cylinder properties and test results for strength and '$E_{c,stat}$'.

	Diameter (mm)	Height (mm)	Weight (kg)	Peak Load (kN)	$E_{c,stat}$ (MPa)
Cylinder 1	100	198	3.61	419	30267
Cylinder 2	100	200	3.63	435	34331
Cylinder 3	100	200	3.63	431	29328
Average	100	199	3.62	428	31309

Table 3.1: Concrete Compression Test Cylinder Properties and Results.

It is also interesting that the 40MPa concrete mix specified for the design of this specimen had an actual strength of 52MPa at 28 days with a corresponding ultimate strain of 2000$\mu\varepsilon$. The average '$E_{c,stat}$' resulting from compression testing was 31309MPa. For normal weight concrete the static modulus of elasticity may be alternatively calculated from AS3600 Clause 6.1.2 as follows:

Equation 3-1

Where f_c = the assumed compressive strength of concrete at a relevant age which is usually 28 days. It is important to note that '$E_{c,stat}$' may range ± 20%. For the case of a 40MPa concrete mix, which would be the assumed 28 day strength of this specimen, the corresponding ''$E_{c,stat}$' is 32GPa as calculated by the Australian Standard formula of Equation 3.1. The difference between this

value and the average '$E_{c,stat}$' value determined from laboratory testing is -2%, which is well within the ± 20% range. It turns out that the static modulus of elasticity required by finite-element analysis to reproduce the results of static tests was 32.5GPa, a 1.5% variation.

Laboratory tests were carefully planned to be conducted 28 days from the day that the specimen was poured to coincide with the 28 day results of concrete cylinder compression tests on samples from the specimen. To establish an estimate of '$E_{c,dyn}$' for vibration serviceability problems, both static and dynamic tests were conducted in the laboratory. The load-deflection stiffness from static tests in the laboratory was replicated with finite element models of the specimen using a value for Young's Modulus that corresponded to the static modulus of elasticity '$E_{c,stat}$'. The free vibration response of the specimen subjected to heel-drop impacts during dynamic tests were also replicated with finite-element analysis. To obtain the same frequency of the vibration response measured on the laboratory specimen with finite element modelling, Young's Modulus had to be adjusted by a factor of 1.04. This 4% increase in the modulus of elasticity required by finite element analysis corresponds to the dynamic modulus of elasticity, '$E_{c,dyn}$'.

3.4. **Static Tests**

The purpose of conducting static tests was to establish the elastic load/deflection behaviour of the specimen. Results from these static tests performed in the

laboratory were used to calibrate Young's Modulus of Elasticity for material modelling in subsequent finite-element analysis.

These static, laboratory tests involved applying a gradually increasing load to the top of the specimen at a rate of 0.4kkN/s up to 40kN, then decreasing the load back to 1kN at the same rate over three (3) cycles. The load applied with the hydraulic ram was measured by the load cell while the corresponding deflection

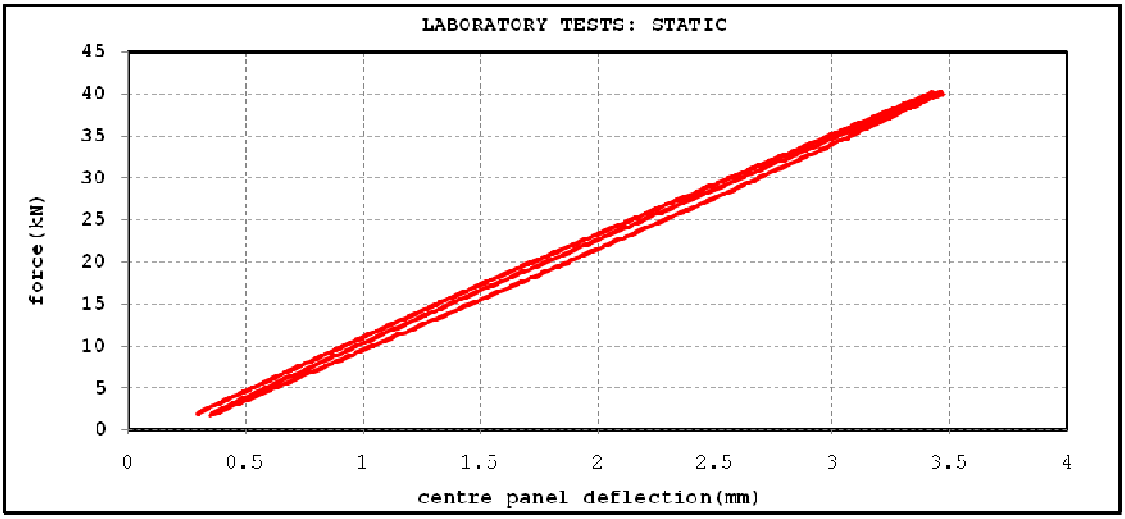

Figure 3.7: Laboratory Static Load – Deflection Results (12.2 kN/mm centre panel stiffness)

of the underside of the specimen was measured with the centre panel linear potentiometer displacement transducer. Three cycles were completed to ensure that the behaviour was indeed linear-elastic and consistent without hysteresis. A typical force vs. deflection graph of these static laboratory tests is shown as Figure 3.7. The static stiffness of the specimen was determined to be 12.22kN/mm. This value was used during the calibration of a FE model of the specimen and corresponded to a value of 'E_{stat}' of 32.5GPa.

3.5. **Dynamic Tests**

Two types of dynamic tests were conducted: heel-drop and group-activity. Heel-drop tests are the primary type of human-induced load of interest in this research; however, group-activity tests were also conducted to show that the panel response frequency was not affected by other types of human-induced dynamic loads. Time-history acceleration records from laboratory tests in conjunction with preliminary finite element analysis were useful in developing the material model for damping ratio and '$E_{c,dyn}$' for the pin-supported specimen.

3.5.1. **Heel-Drop Tests**

Heel-drop tests were performed to establish the free vibration behaviour of the specimen (Murray, 1975). To conduct heel-drop tests for this research, a person would stand at the centre of the specimen, rise to their toes and wait still until the acceleration caused by prior movement was reduced to zero. The person would then drop to their heels suddenly, striking the floor. The acceleration response caused by the heel-drop was measured using an accelerometer located in the centre of the specimen approximately 100mm from the feet of the person performing the heel-drop. The natural frequency of the specimen was determined from the power spectral density, and the presence of damping was observed as the gradual decay of acceleration shown in the time-history record. The power spectral density function and time-history record for a heel-drop test are shown in Figure 3.8. The power spectrum reveals the peak frequency responses of the specimen to be 7.6Hz.

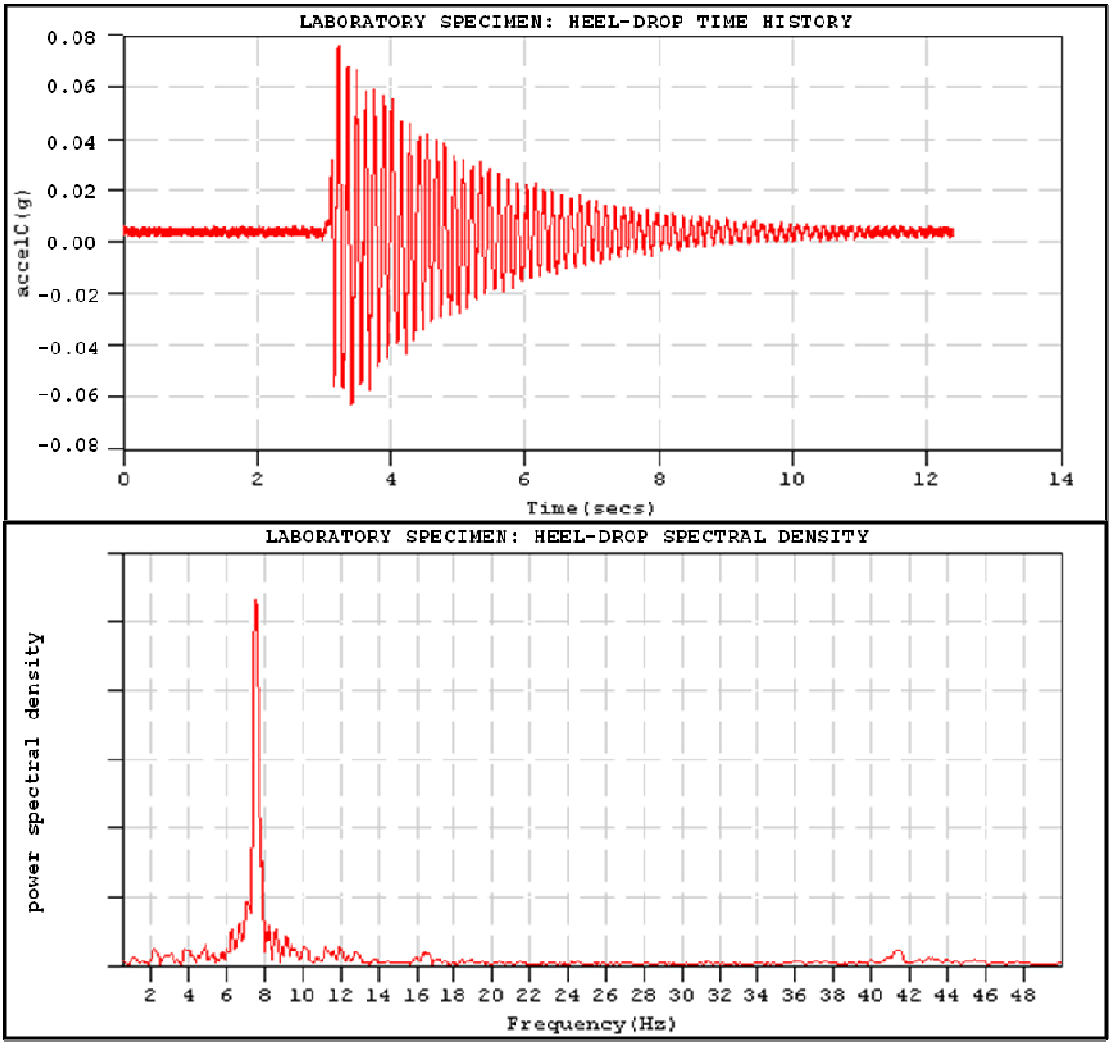

Figure 3.8: Heel-DropTime-History Acceleration Record and Spectral Density Results (7.6 Hz)

3.5.2. ***Group-Activity Tests***

Two types of group-activity tests were performed to show that the primary frequency response of the specimen was not influenced by different types of human-induced dynamic loads: walking and jumping. Both walking and jumping tests were conducted with ten (10) people on the specimen. Walking tests were uncoordinated while jumping tests were synchronized at a rate of approximately 2Hz. Time-history records and spectral density results for these tests are provided in Figure 3.9: Group-Activity Time-History Acceleration Records.

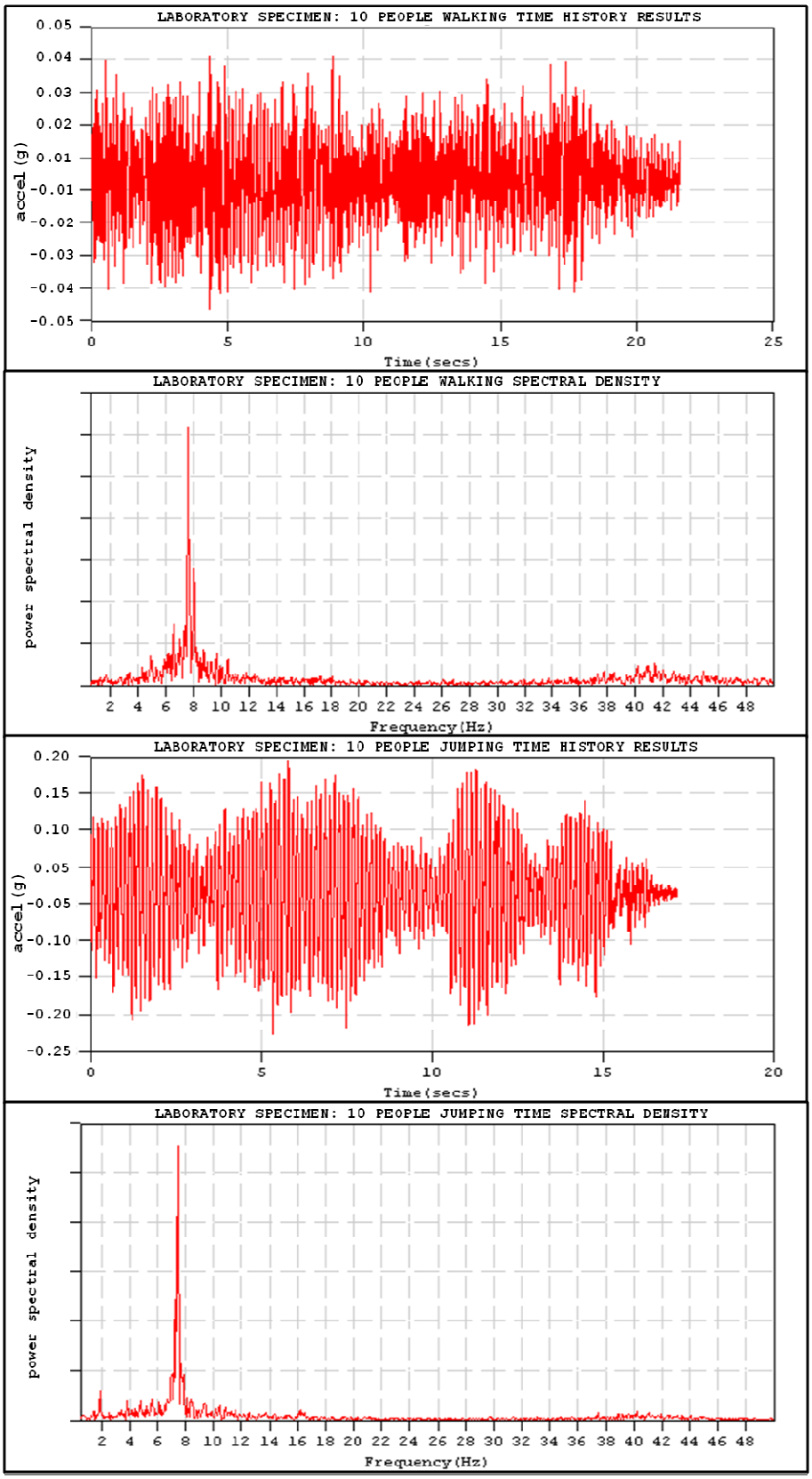

Figure 3.9: Group-Activity Time-History Acceleration Records and Spectral Density Results (walking and jumping - 7.6 Hz)

3.6. **Summary of Laboratory Results**

Laboratory tests in this research were conducted on a full-scale, post-tensioned concrete specimen. Both static and dynamic tests were performed. Static tests results showed that the specimen had a centre panel load-deflection stiffness of 12.2kN/mm. Dynamic tests were comprised of two types of loads: heel-drop and group-activity. Heel-drop tests revealed that the free vibration primary response frequency of the specimen was 7.6Hz. Two types of group-activity tests were conducted with ten (10) people on the specimen. The first type of group-activity test was of uncoordinated walking, and the second type was of synchronized jumping at a rate of approximately 2Hz. Both types of group-activity tests also revealed that the primary response frequency of the specimen was 7.6Hz.

Results for static and dynamic laboratory tests will be used to calibrate material models for use in finite-element analysis that reproduces the behaviour of the specimen. Finite-element analysis will be expanded to study the behaviour of a variety of floor panel configurations typically encountered in real buildings.

CHAPTER 4

FINITE-ELEMENT ANALYSIS & RCRF DEVELOPMENT

For most structural engineering problems, reliable guidelines are available to assist the engineer in arriving at reasonable solutions. This is not the present case with regard to the serviceability design for vibration of suspended concrete floors. Those guidelines that are available are inadequate to address real floor structures without the use of sophisticated computer methods (Pavic, 1998). Guidelines for convenient applications that do not require computer solutions have shown to be unreliable, producing design requirements that are over conservative and have since been withdrawn. A number of studies that have dealt with floor vibration of cast in-situ, concrete floors are mostly retrospective, and none addressed the problem from a predictive approach. Developing an empirical guideline for predicting the vibration response of suspended flat-slab, concrete floors is the essence of this research. This chapter will describe how the Response Coefficient-Root Function Method was innovated.

Although the aim of this research was to develop an empirical guideline for the serviceability design of floor vibration that does not require the engineer to rely on sophisticated computer methods, finite-element analysis (FEA) has been a fundamental part of this research and necessary for development of the RCRF method. Because vibration is a dynamic problem, having a finite element package capable of performing Eigen-value and transient dynamic analyses was

very important. The finite element software employed for this research was STRAND7 by G+D Computing Pty Ltd (Strand7, 2003). This FEA software has sophisticated, three-dimensional, multi-modal natural frequency analysis, time-step and non-linear capabilities. STRAND7 also has an extensive catalogue of finite elements and the capability of combining materials, which is necessary for modelling composite structures like the post-tensioned concrete.

4.1. **Preliminary Finite Element Analysis**

The first step in this computational phase of research was to replicate the behaviour of the laboratory specimen. Because the research plan for the extended scope of this computational phase was to study a variety of floor plate configurations, it was important to simplify the complexity of modelling and reduce calculation time by using homogeneous shell elements in finite-element analysis. Since the laboratory specimen was of post-tensioned concrete construction, it was important to ensure that modelling the material with homogeneous elements was appropriate. To do this, a comparison of both composite and homogeneous models of the specimen was necessary.

4.1.1. **Static FEA Calibration of Composite and Homogeneous Models**

Because real post-tensioned floors are comprised of concrete and stressed steel tendons, it is necessary to model composite, elastic behaviour with a material having a homogeneous cross-section. First, the elastic stiffness, of a simply supported two-way floor system having the same geometry as the laboratory specimen was studied using a composite finite-element model. Four-node, shell

elements were used to model the concrete and two-node, cable elements were used to model the steel post-tensioning strands. The cable elements were profiled and prestressed to simulate the post-tensioning tendons of the laboratory specimen. Composite behaviour was simulated by using link elements between the cable and shell element nodes for lateral and transverse degrees of freedom. Three independent load cases were considered: self-weight dead load (DL), post-tensioning (PT) and concentrated mid-span load (P). The performance of the model was gauged to have extremely high accuracy when comparing hand calculated top and bottom fibre stresses to those calculated from FEA for each load case. Then the elastic stiffness was taken as the load-deflection ratio, P/Δ_P, where 'Δ_P ' is the deflection caused by the load 'P' subsequent to the initial deflection from the combination of self-weight and post-tensioning. The static modulus of elasticity, '$E_{c,stat}$', required to achieve the elastic stiffness behaviour of the laboratory specimen, e.g., P/Δ_P = (40)/(3.27) = 12.2 kN/mm, was 32.5GPa. Figure 4.1 is a graphical image of the deflection and results of static analysis for the composite finite-element model (FEM) of the laboratory specimen.

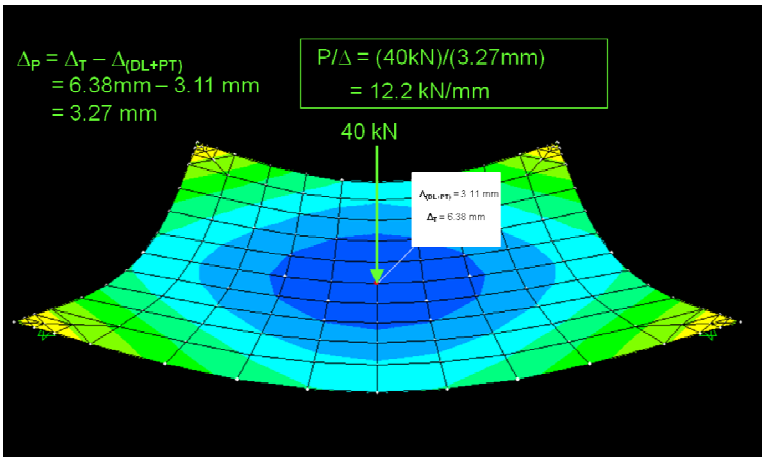

***Figure 4.1*:** Deflection Contours of a Composite Finite-Element Model of the Laboratory Specimen

Similarly, the elastic behaviour of a finite-element model using a homogeneous material with no post-tensioning cables or rigid links was studied. In this case, only four-node, shell elements were used to model the concrete. The same geometry and values for the concrete density and modulus of elasticity assumed for the composite FEM were used. Only two independent load cases were considered: self-weight dead load (DL) and a concentrated load (P) at the centre of the panel. Then the elastic stiffness was taken as the load-deflection ratio, P/Δ_P, where 'Δ_P ' is the deflection caused by the load 'P' subsequent to the initial deflection from the self-weight. This exercise produced nearly identical results as the analysis using composite modelling.

Comparing the results between the two types of models showed that the only difference was the magnitude of deflection prior to applying the superimposed concentrated load, 'P'. The composite model exhibited less initial deflection because the post-tensioning load served to counter the self-weight deflections. However, the difference in elastic stiffness was less than 0.5%. Considering that AS3600, clause 6.1.2, recognises that the values for the modulus of elasticity for concrete may vary $+/-20.0\%$, and the concrete cylinder tests for this specimen produced similar results for the static modulus of elasticity it was determined reasonable for this study to proceed with dynamic FEA using homogeneous finite element modelling techniques.

4.1.2. ***Dynamic FEA Calibration***

Dynamic analysis using a heel-drop load function on the finite element model of the laboratory specimen was calibrated against results from the preliminary free vibration from heel-drop tests conducted in the laboratory discussed in Section 3.5. Murray's triangular load function for heel-drop simulation was used to obtain the dynamic response of the finite element model shown in Figure 4.2. The heel-drop load function is a 2,670 Newton force initially applied then linearly decreasing decreased to zero over a period of 0.05 seconds, which corresponds to an impulse of 67 Newton-seconds.

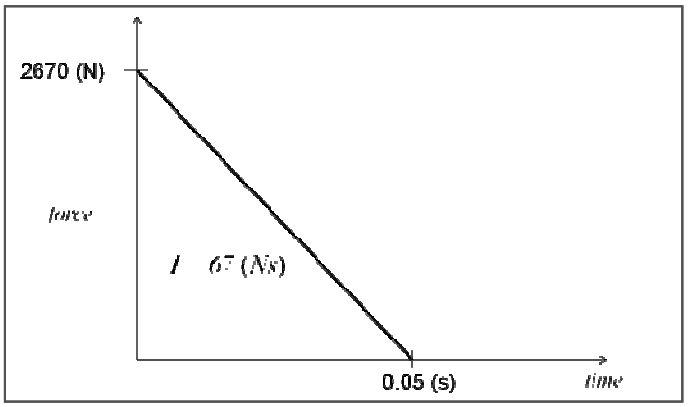

Figure 4.2: Heel-Drop Load Function *(Murray 1975)*

Calibration of the finite element model was an iterative process to determine the dynamic modulus of elasticity, '$E_{c,dyn}$', and the damping ratio, ζ, of the specimen to be estimated. Estimation of the dynamic modulus '$E_{c,dyn}$' was accomplished by adjusting the FEM modulus until the power spectral density function of the model matched the power spectral density function obtained from laboratory tests. The dynamic response of the finite-element model of the specimen using the static

modulus of elasticity of the concrete '$E_{c,stat}$ = 32.5GPa' determined from static analysis described in Section 4.1.1 underestimated the 7.6Hz primary response frequency of the specimen. Increasing the FEM modulus of elasticity to a value of 33.3GPa resulted in good agreement with the laboratory response. Figure 4.3 shows the comparison of measured and calculated power spectra against the first five Eigen-value natural frequencies.

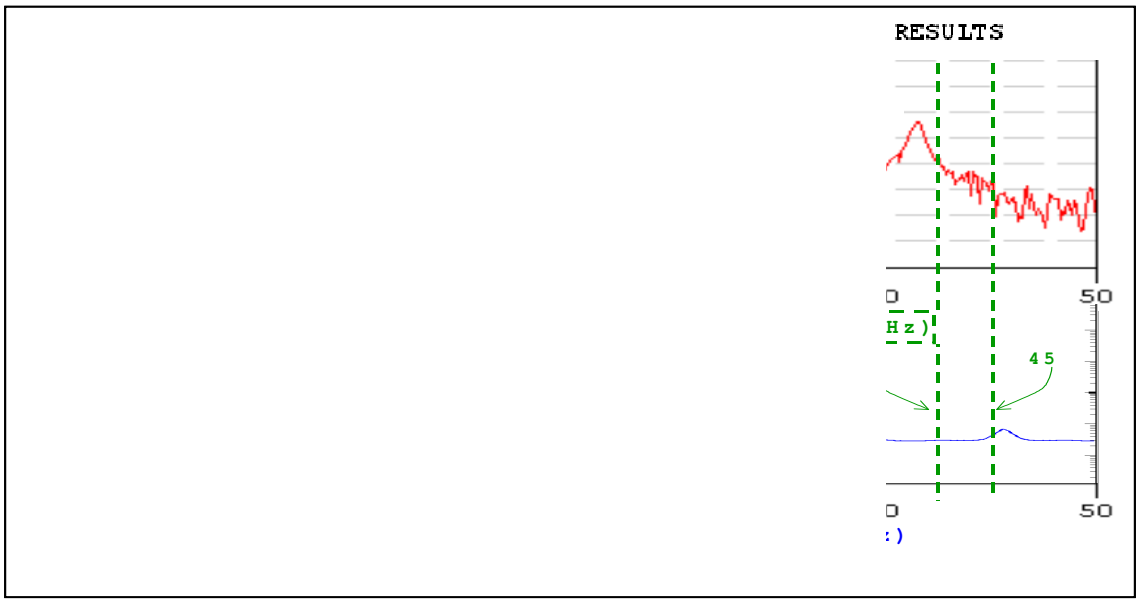

***Figure 4.3**: Computed and Measured Spectral Density and Eigen-value Natural Frequency*

The damping ratio was of the laboratory specimen was estimated by adjusting the damping ratio of the finite-element model until the time-history response of the laboratory specimen was replicated with reasonable accuracy using the Rayleigh Damping Coefficient Method. The computed decay of acceleration from a transient dynamic analysis showed good agreement with the time-history acceleration record. Using the Rayleigh damping method to model damping resulted in an equivalent damping ratio of ζ = 1.2%, which is typical for a bare

floor structure. The computed and measured time-history acceleration records are shown in Figure 4.4.

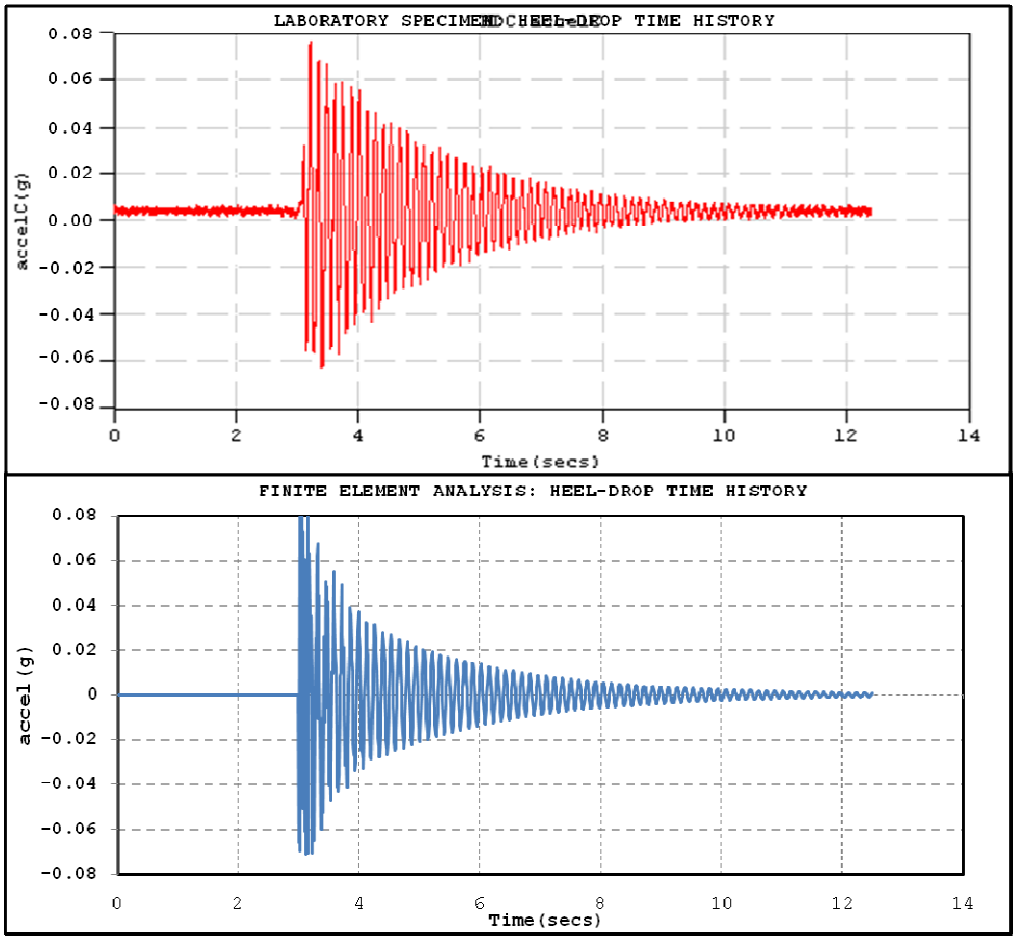

Figure 4.4: *Computed and Measured Time History Records*

Both Figure 4.3 and Figure 4.4 serve to illustrate that the calibrated finite element model showed excellent agreement with the laboratory tests, particularly with regard to the primary response frequency of 7.6 Hz and damped acceleration response. Further finite-element studies adopted homogeneous material models having $E_{c,dyn}$ = 33.3GPa and ζ = 1.2%.

4.1.3. ***Initial Panel Variation Investigation***

The frequency coefficient approach for calculating the natural frequency of composite floors, which uses empirically determined coefficients was introduced in Section 2.3.1. The intent of this research is to develop a similar method for predicting the response (or design) frequencies and accelerations of cast in-situ concrete floors. To do so, the behaviour of a single panel was first investigated followed by analysis of a floor structure with 9 (nine) panels.

4.1.3.1. ***Single Panel***

Figure 4.5 provides a graphic example of the manner in which a frequency coefficient approach may be applied to two-way concrete floors. In this example, the FEA from a single floor panel with square plan dimensions was expanded and analysed for various values of the stiffness-to-mass ratio, '$\lambda = (EI)/(L^4 m)$.' To obtain various values of 'λ' the spans and depths were adjusted. In addition, the corner support conditions were also varied between the extremes of ideal full fixities and simple pins. A linear regression curve fit was performed for the results of each model, resulting in a formula for the response frequency. The original regression curve equations were rearranged to resemble the basic formula for natural frequency. The resulting frequency factors, $C_{fixed} = 3.95$ *and* $C_{pinned} = 3.17$, are the constants in the numerator outside the radical for each formula in Figure 4.5. Ideal supports are a theoretical restraint and not practically possible in real structures. The support condition provided by columns in real floor structures would fall somewhere between the two extremes. For this reason

an average curve is also plotted giving a frequency factor of C_{avg}= 3.56. This empirical approach was extended to investigate floor structures with multiple panels.

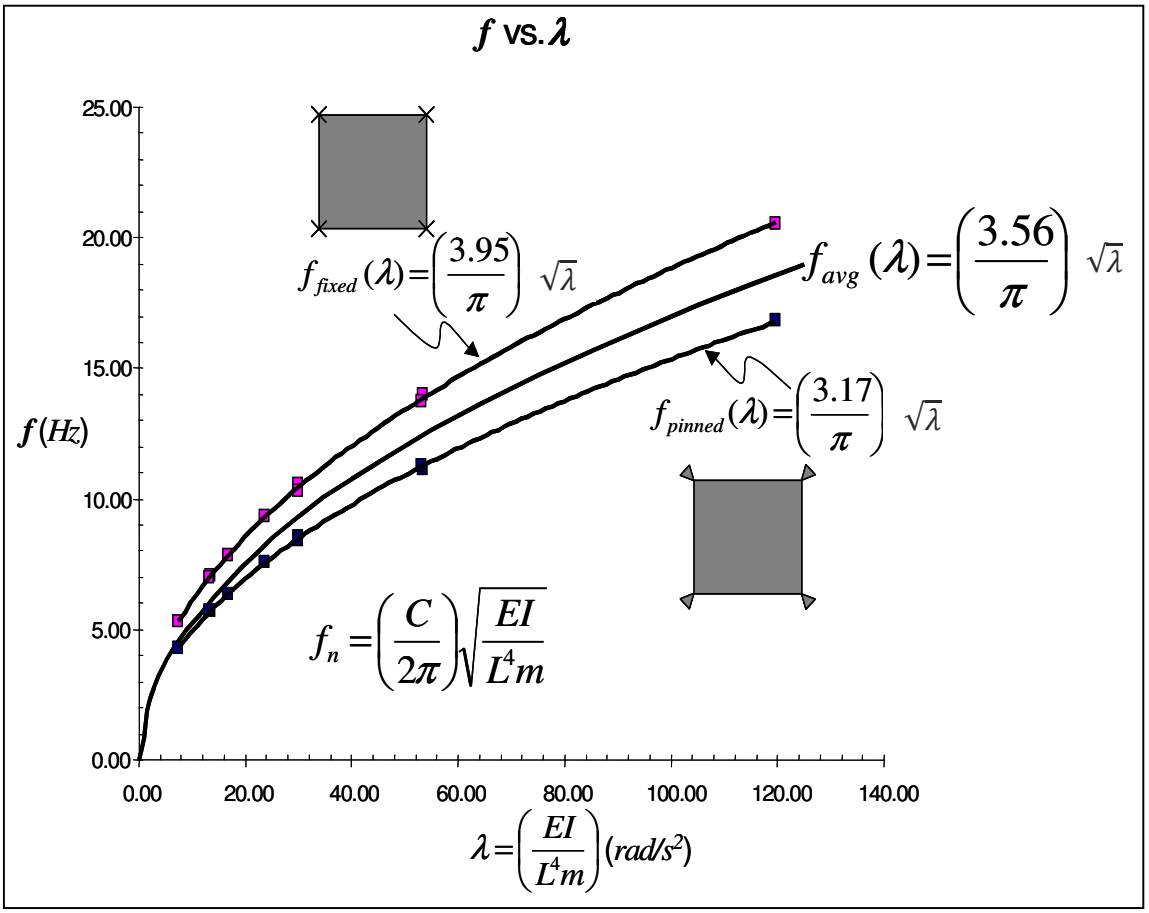

***Figure 4.5**: Frequency factors for a single square panel with pinned and fixed corner supports*

4.1.3.2. ***Nine Panel***

Observations of preliminary FEA results on multiple panel floors during the beginning of this research provided insight on the potential for developing a dynamic serviceability guideline for the design of suspended concrete floor structures. One's intuition may lead to an expectation that the free vibration

response of a floor subjected to transient excitation, like a heel-drop, should correspond to the first-mode natural frequency calculated from an Eigen-value analysis. This is not always true. Three finite element models of a nine-panel floor with a square support grid were analysed for transient dynamic response and Eigen-value natural frequency. The geometry for the 9-panel model is shown in Figure 4.6. Only pinned supports were studied for this phase of initial investigation. The panel span-to-depth ratio was held constant at: $S/d = 33.5$, which is the same as for the single panel specimen. The individual panel

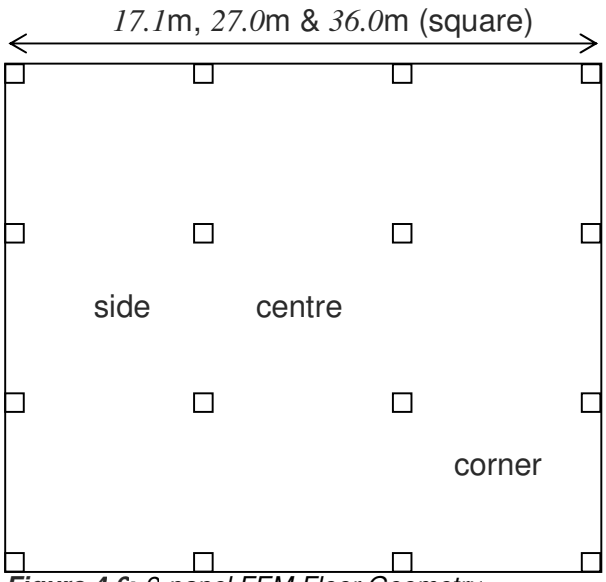

***Figure 4.6**: 9-panel FEM Floor Geometry*

dimensions *were* 5.7m, 9.0m and 12.0m with corresponding values of $\lambda = 33.7$, 12.7 and 7.15 respectively. Three separate transient dynamic analyses were conducted on each of the three models by applying a heel-drop excitation to the side, centre and corner floor panels. Eigen-value natural frequency analyses were also conducted for each model. The power spectra resulting from transient analyses corresponding to a centre panel response and Eigen-value frequencies for each of the three finite element models are presented in Figure 4.7.

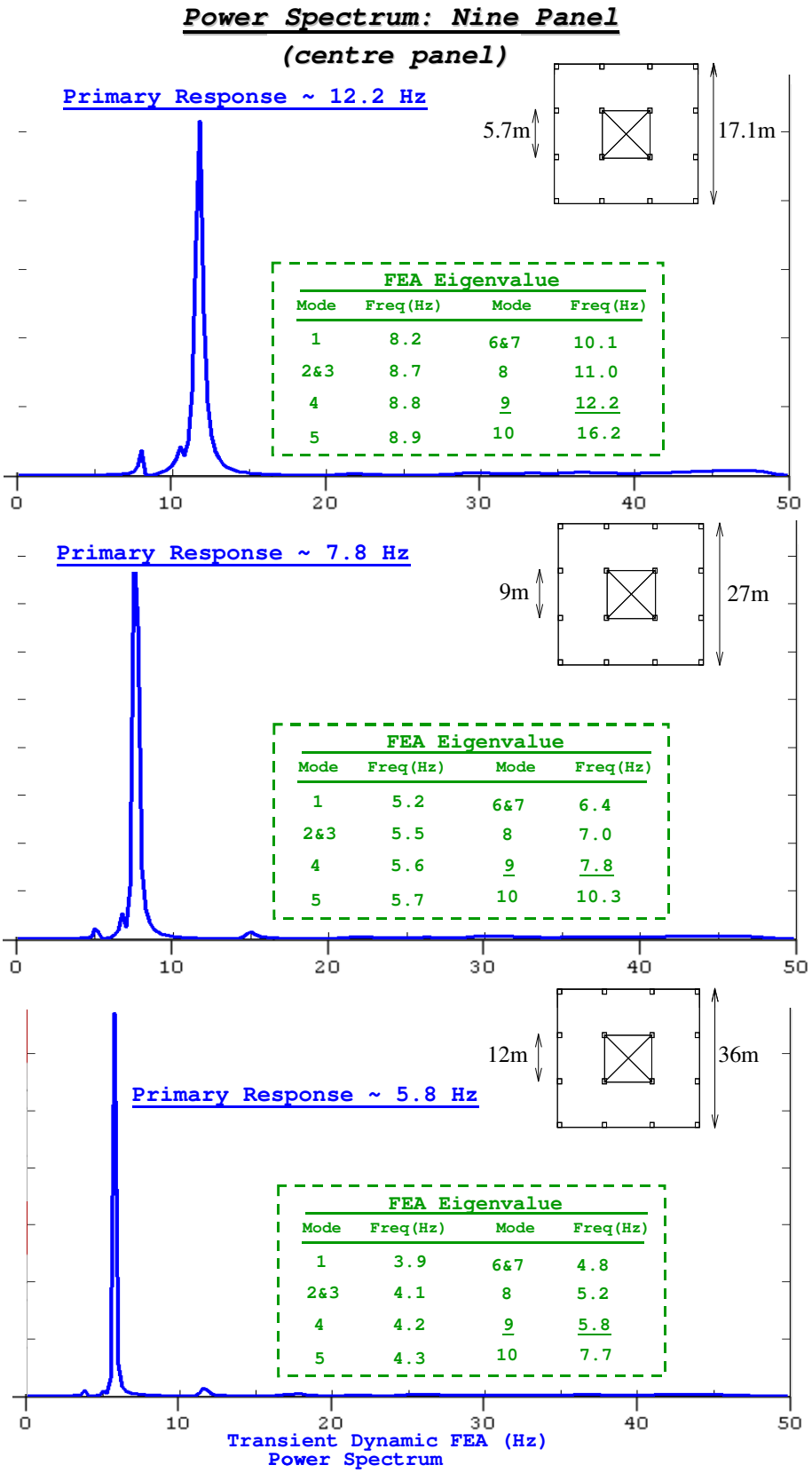

Figure 4.7: Transient and Eigen-value FEA for a 9-panel floor

It turns out that the primary free vibration response of the centre panel, for this special case, dominantly corresponds to the 9^{th} (ninth) Eigen-value natural frequency. Similar trends were also apparent from the analyses conducted on the side and corner panels. By plotting the primary frequency response for each case against the stiffness-to–mass ratio, λ , the resulting frequency factors are easily derived as $C_{centre}= 6.82$, $C_{side}= 5.56$ *and* $C_{corner}= 4.87$. These factors are plotted in Figure 4.8.

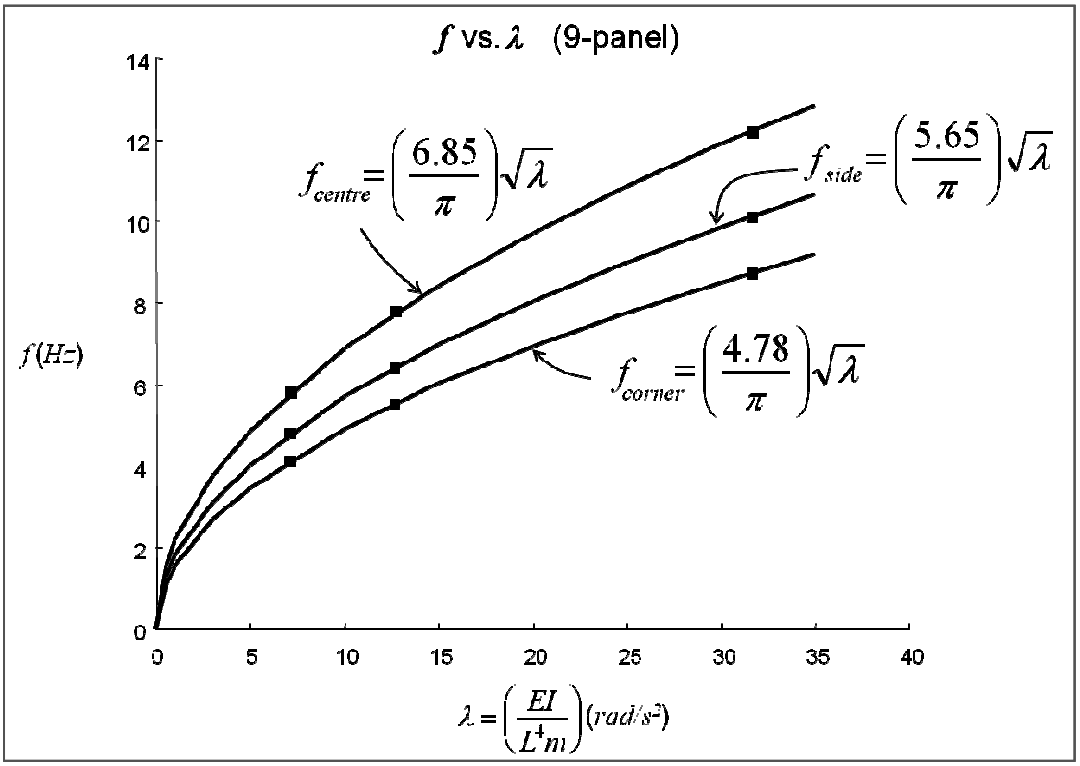

***Figure 4.8*:** Panel Frequency Functions Example for a 9-panel Floor

The preliminary finite-element analysis of the simply supported, single and multiple panel floor systems described in this section were expanded to investigate the behaviour of floor structures with various aspect ratios and the effects of modelling realistic column supports.

4.2. **Derivation of the RCRF Method**

4.2.1. ***Overview***

An introduction to the Response Coefficient-Root Function (RCRF) method was given in Section 1.8. This section will describe the systematic approach used to derive the expressions of the RCRF method. The objective of this phase of the research was to investigate the response frequency of a variety of floor panel configurations. These configurations were based on the floor plate configurations used to derive bending moment and deflection coefficients from

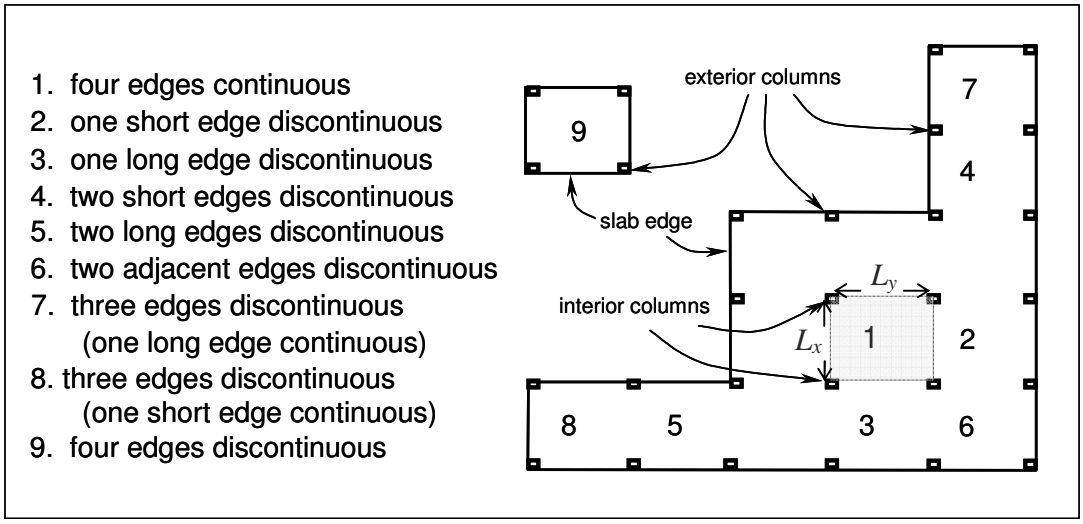

Figure 4.9: RCRF Panel Configuration Program

yield-line theory, which account for edge continuity conditions for wall-supported floor plates which are used in the Australian Standard for Concrete Structures, AS3600 (Warner R., 1998, AS3600, 2009). This research, however, is focused on the dynamic serviceability performance of column-supported floors. A plan sketch of and list of these edge conditions are shown in Figure 4.9. Each of the panel configuration numbers shown in Figure 4.9 was analysed for its response to a heel-drop excitation at the centre of each panel. Using the finite-element

material model, which was calibrated from laboratory tests as described CHAPTER 3, e.g., $E_{c,dyn}$ = 33.3GPa and ζ =1.2%, a finite-element analysis program was established. This analysis program involved a series of models for which the span-to-depth, L_y/d, and aspect ratios, $\alpha = L_y / L_x$, varied. Table 4.1 shows how the stiffness-to-mass ratio 'λ' changes with L_y/d and α.

Aspect Ratio α	***Span-to-Depth Ratio L_y/d***	***Stiffness-to-Mass Ratio λ (rad/s^2)***
1	45	7.05
	35	11.91
	25	22.84
1.5	45	35.69
	35	60.31
	25	115.625
2	45	112.79
	35	190.6
	25	365.43

Table 4.1*:* RCRF Derivation FEA Parameters - Variation of 'λ' ($E_{c,dyn}$ = 33.3GPa and L_y = 9m)

For each set of models, the long spans, L_y, of the floor panels were held constant at nine meters (9m) while the short spans, L_x, were adjusted to vary the aspect ratio, $\alpha = L_y/L_x$, at 1, 1.5 and 2. For each model in a set, the parameter 'λ' was investigated by adjusting the span-to-depth ratio. As an example, for α = 1, and L_y/d = 25, 35 and 45, the corresponding variation in the stiffness-to-mass ratio is λ = 7.05, 11.91, 22.84 respectively. To simulate the effect of support stiffness in real buildings, columns were modelled above and below the slab with eight-node solid brick elements having an elastic modulus of $E_{c,stat}$ = 35GPa to reflect 50MPa concrete. Columns heights were three meters (3m) above and below mid-depth of the slab elements, and all translational degrees of freedom at the end nodes

were restrained to provide fixed supports. Column cross-sections were dimensioned at 5.0% of the panel span in each direction at the panel corner to provide reasonable geometry for nominal punching shear considerations. These models were analysed using time-stepped, transient dynamic analysis for the panel primary response to a 'heel-drop' load function for both frequency and acceleration functions given by Equation 1.9 and Equation 1.11 respectively.

4.2.2. ***Panel 1 FEA Overview***

For clarity and brevity of discussion, only the series of results related to the edge continuity conditions of Panel '1', depicted in Figure 4.9, will be described in this section. A complete set of results for all other panel edge conditions will be outlined at the end of this section. An isometric view of one of the finite-element models analysed during the course of this investigation is shown in Figure 4.10.

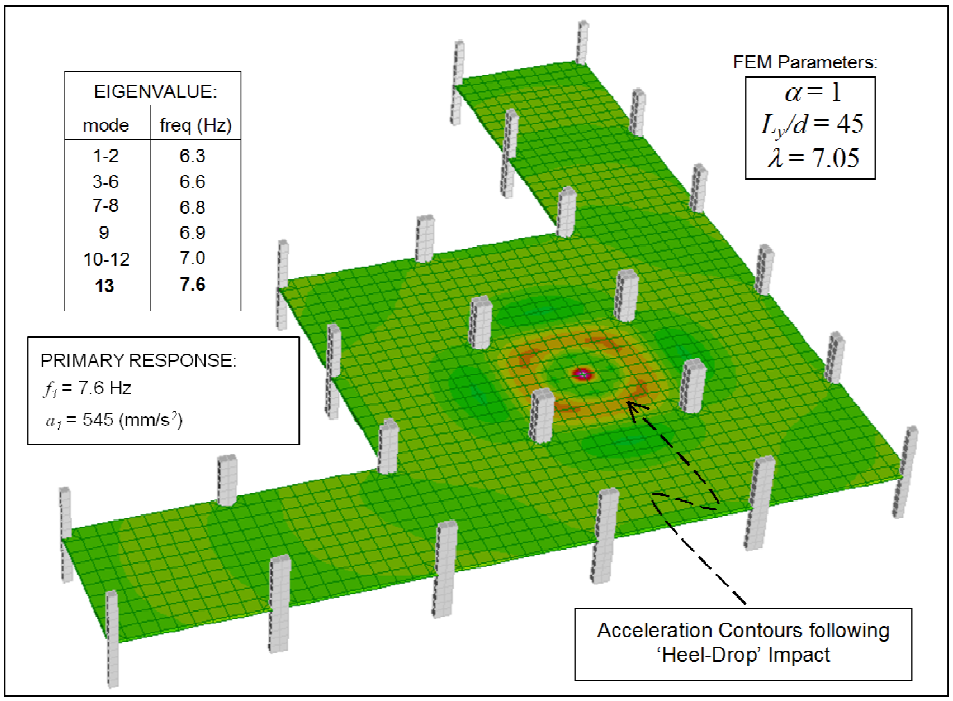

Figure 4.10: RCRF Panel Configuration – Typical Finite-Element Model

This particular model has the following parameters: α = 1, L_y/d = 45 and λ = 7.05. Results for this analysis are also provided in Figure 4.10, which are the set of Eigen-value natural frequencies for the first through the thirteenth modes, the acceleration contours immediately following a heel-drop excitation and transient dynamic response frequency and acceleration resulting from a heel-drop excitation. It can be observed that the primary response frequency of Panel 1, corresponds to the thirteenth Eigen-value frequency of 7.6*Hz* and the peak response frequency is 545 mm/s^2.

It should be emphasized here that in current practice, engineers generally assume that the first mode frequency as calculated from an Eigen-value analysis is the critical frequency for acceptability criteria requirements. Results from this investigation prove that this assumption is not necessarily true for multi-panel floor structures. The results given in Figure 4.10 show that the panel primary natural frequency of 7.6*Hz* would be underestimated by 17% if the first mode Eigen-value natural frequency of 6.3*Hz* were assumed to be the governing response for this panel, which could lead to an over conservative dynamic serviceability design.

4.2.3. ***Panel 1 Primary Response Functions: Frequency and Acceleration***

To obtain the primary response for frequency and acceleration from the transient dynamic analysis, a time-history record of acceleration was extracted the FEA output. From the time-history record the peak acceleration could be identified, and the power-spectral density function (power spectrum) was then analysed

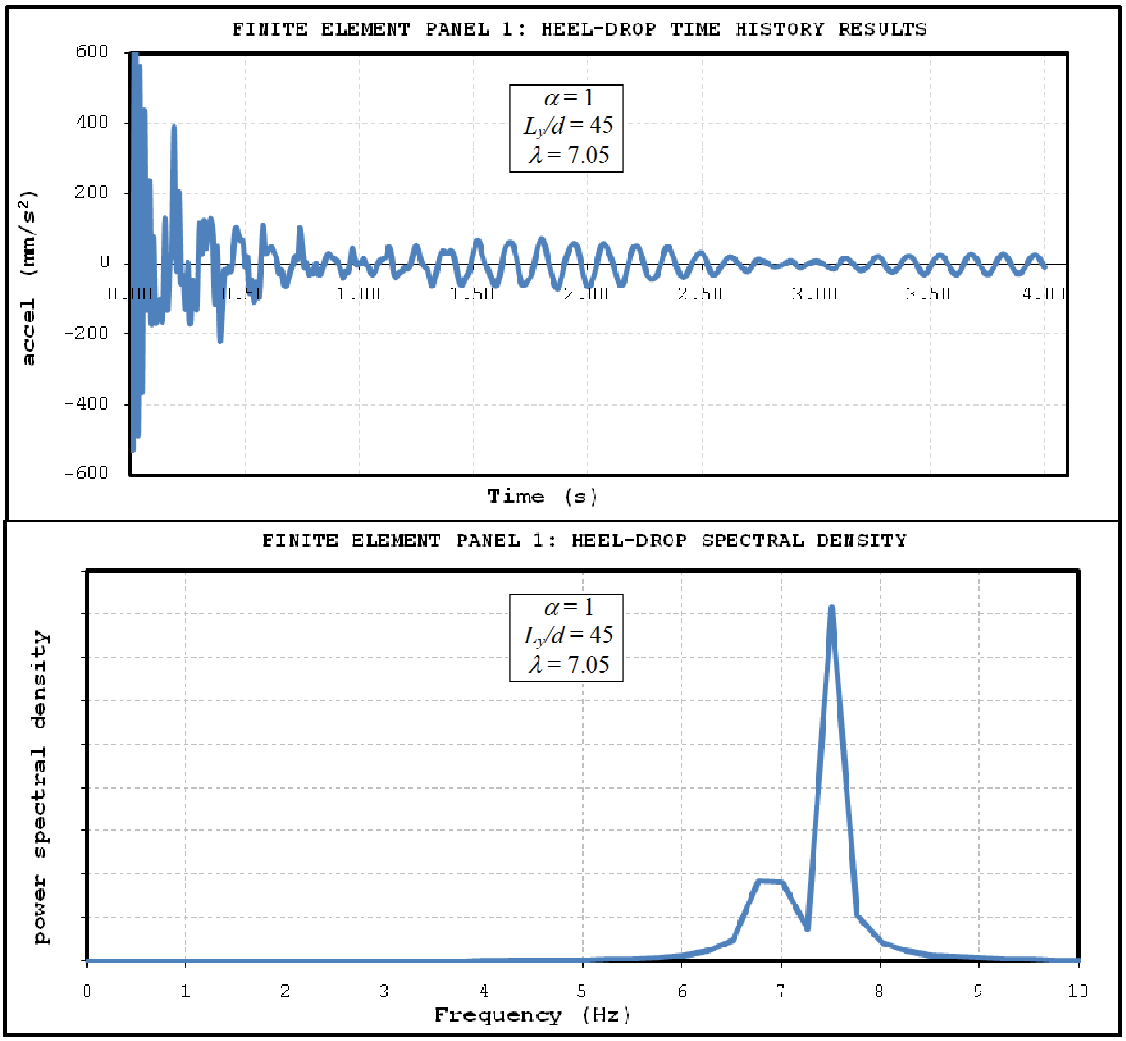

Figure 4.11: Time History Record and Spectral Density for Panel 1 ($\alpha = 1$, $\lambda = 7.05$)

using MatLAB (MatLab, 2003). The time-history acceleration record and the power-spectrum for Panel 1 having $\alpha = 1$ and $\lambda = 7.05$ are plotted in Figure 4.11. Further analyses were conducted by adjusting the span-to-depth ratio, L_y/d, from 45, to 35 and 25. Using the same methodology described previously, the primary panel frequencies and accelerations responses were obtained for Panel 1 having aspect ratios of '$\alpha =$ 1, 1.5 and 2' and values of stiffness-to-mass-ratios

'λ (rad/s^2) = 7.05, 11.91 and 22.84' as per Table 4.1. A summary of these results is provided in Table 4.2.

	Aspect Ratio α	Span-to-Depth Ratio L_v/d	Stiffness-to-Mass Ratio λ (rad/s^2)	Frequency Response f (Hz)	Acceleration Response a (mm/s^2)
PANEL 1		45	7.05	**7.6**	**545**
	1	35	11.91	**9.5**	**355**
		25	22.84	**11.8**	**206**
		45	35.69	**10.5**	**704**
	1.5	35	60.31	**13.0**	**462**
		25	115.63	**16.8**	**256**
		45	112.79	**13.2**	**694**
	2	35	190.6	**16.7**	**476**
		25	365.43	**20.3**	**246**

Table 4.2: Panel 1 Response Frequencies and Accelerations

The primary response frequencies of Panel 1 are plotted in Figure 4.12 along with a regression curve-fit which provided an expression for each of these frequencies as a function of 'λ'. For example, the curve-fit function that best describes the primary response frequency of Panel 1 with $\alpha = 1$ is given by:

$$f_1(\alpha = 1, \lambda) = 3.6204^{(2.6337)}\sqrt{\lambda} \qquad \textit{Equation 4-1}$$

Here, $f_1(\alpha = 1, \lambda)$ is the primary frequency response of the Panel 1 in Hz as a function of 'λ' with '$\alpha = 1$'. The constants 3.6204 and 2.6337 are the panel

frequency coefficient and root of 'λ' respectively. By substituting 'λ = 7.05', into Equation 4.1 it is obvious that the resulting frequency becomes 7.6Hz

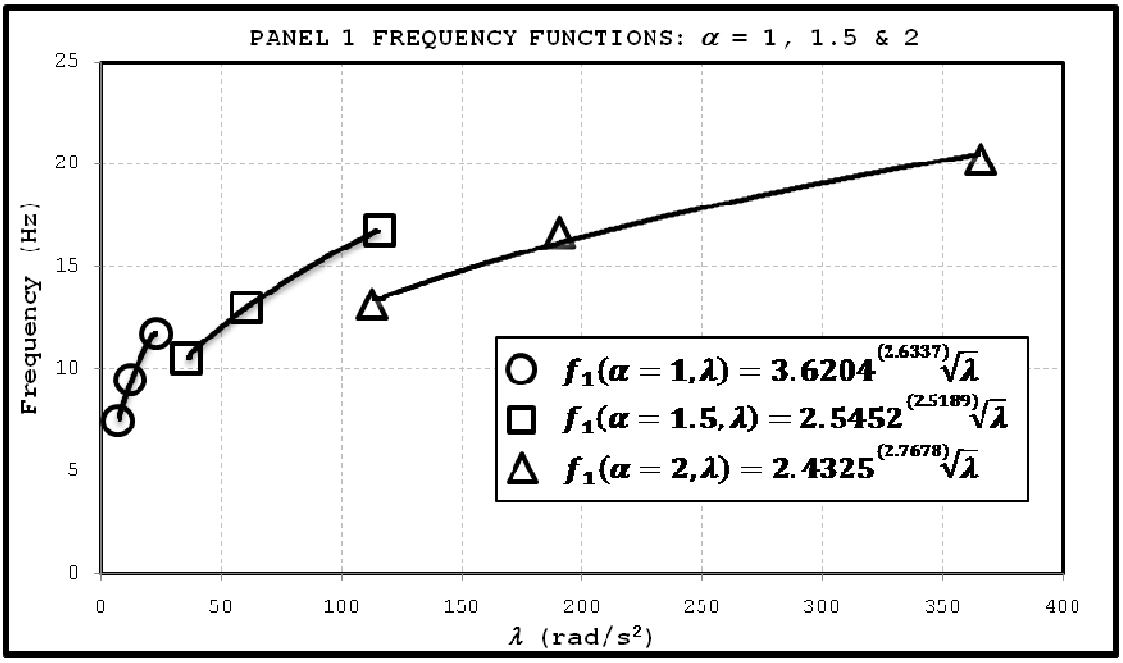

Figure 4.12: Panel 1 - Panel 1 Frequency Functions

Similarly, an expression was derived for the primary acceleration response. For example, the curve-fit function that best describes the primary response acceleration of Panel 1 with α = 1 is given by:

—

Equation 4-2

In this case, $a_1(\alpha$=1,$\lambda)$ is the primary acceleration response of the Panel 1 in mm/s^2 as a function of 'λ' with 'α = 1'. The constants 2.76 and -1.2063 in this expression are the panel acceleration coefficient and root of 'λ' respectively. The Panel 1 primary response accelerations are plotted in Figure 4.13 along with a regression curve-fit which provided an expression for each of these frequencies

as a function of 'λ'. By substituting 'λ = 7.05', Equation 4.2 it is obvious that the resulting acceleration becomes 545 mm/s^2.

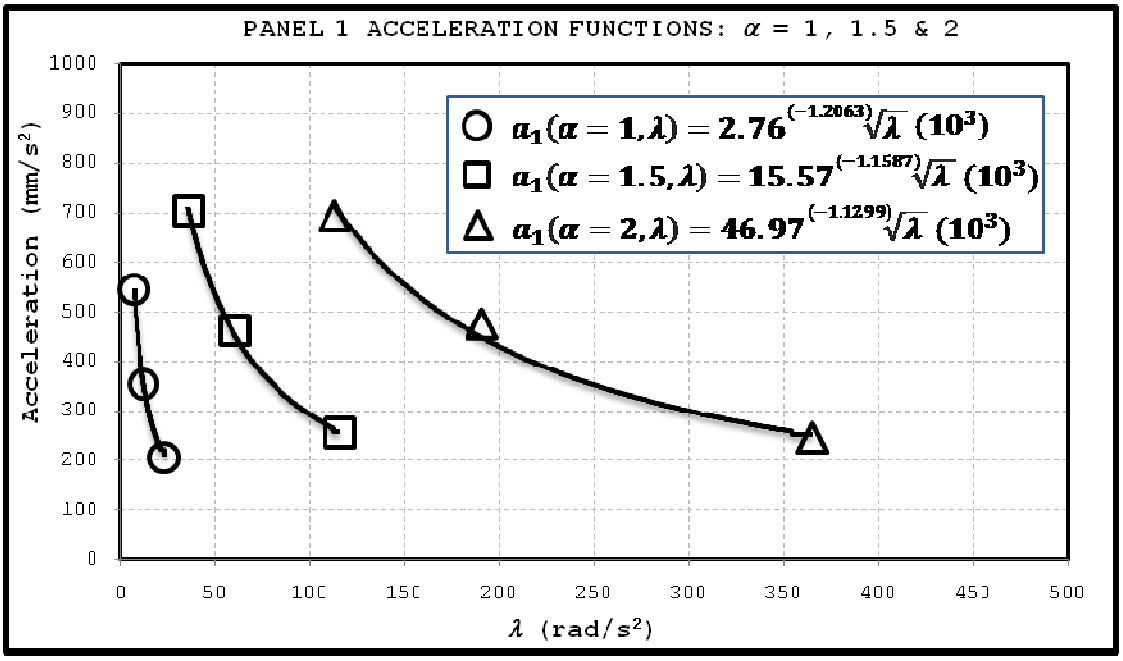

Figure 4.13: Panel 1 - Panel 1 Acceleration Response Functions

4.2.4. ***Panel 1 RCRF Functions***

From the frequency and acceleration response functions illustrated in Figure 4.12 and Figure 4.13, it is clear that the respective coefficients and roots change with various magnitudes of the aspect ratio 'α'. Table 4.3 summarizes the coefficients and roots for Panel 1.

	Aspect Ratio α	***Frequency Coefficient*** $C_{f,1}$	***Frequency Root*** $R_{f,1}$	***Acceleration Coefficient*** $C_{a,1}$	***Acceleration Root*** $R_{a,1}$
PANEL 1	1	3.6204	2.6337	2.76 x10^3	-1.2063
	1.5	2.5452	2.5189	15.57 x10^3	-1.1587
	2	2.4325	2.7678	46.97 x10^3	-1.1299

Table 4.3: Panel 1 – Response Frequency and Acceleration Function Coefficients and Roots

By plotting these coefficients and roots with respect to the aspect ratio 'α', and performing a regression analysis curve-fit to these data, an expression for each as a function of 'α' can be derived. These functions are:

- $C_{f,1}(\alpha)$ - the Frequency Coefficient Function for Panel 1
- $R_{f,1}(\alpha)$ - the Frequency Root Function for Panel 1
- $C_{a,1}(\alpha)$ - the Acceleration Coefficient Function for Panel 1
- $R_{a,1}(\alpha)$ - the Acceleration Root Function for Panel 1

where the subscript of '1' indicates the special case of Panel 1. Graphs of $C_{f,1}(\alpha)$ and $R_{f,1}(\alpha)$ are plotted together in Figure 4.14, and graphs of $C_{a,1}(\alpha)$ and $R_{a,1}(\alpha)$ are plotted separately in Figure 4.15. Each of these figures shows the regression curve-fit equations. These regression equations are the respective coefficient and root functions for the frequency and acceleration formulas of the RCRF method given by Equation 1.9 and Equation 1.11 for Panel '1' summarized as follows:

RCRF Frequency –

$$f_1(\alpha, \lambda) = C_{f,1}(\alpha) \left(R_{f,1}(\alpha)\sqrt{\lambda}\right) \qquad \textit{Equation 1.9}$$

- $C_{f,1}(\alpha) = 1.925(\alpha)^2 - 6.9629(\alpha) + 8.6583$
- $R_{f,1}(\alpha) = 0.7273(\alpha)^2 - 2.0478(\alpha) + 3.9542$

RCRF Acceleration –

$$a_1(\alpha, \lambda) = C_{a,1}(\alpha) \left(R_{a,1}(\alpha)\sqrt{\lambda}\right) \qquad \textit{Equation 1.11}$$

- $C_{a,1}(\alpha) = (37.152(\alpha)^2 - 67.251(\alpha) + 33.858) \times 10^3$
- $R_{a,1}(\alpha) = -0.0374(\alpha)^2 - 0.1886(\alpha) + 1.3575$

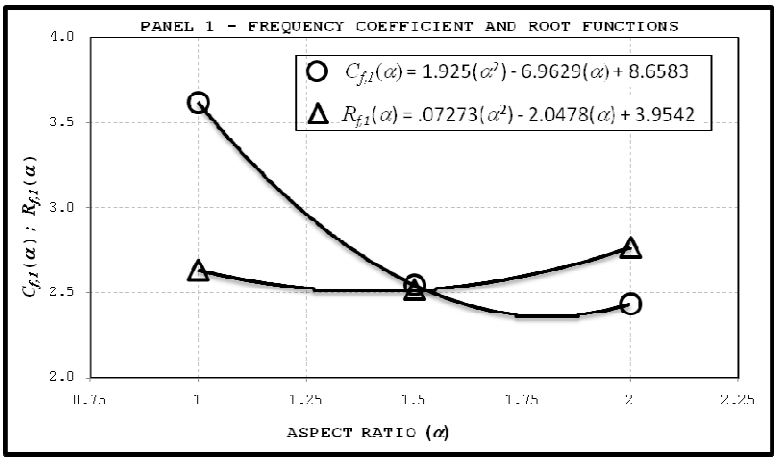

Figure 4.15: Panel 1 - Frequency Coefficient and Root Functions

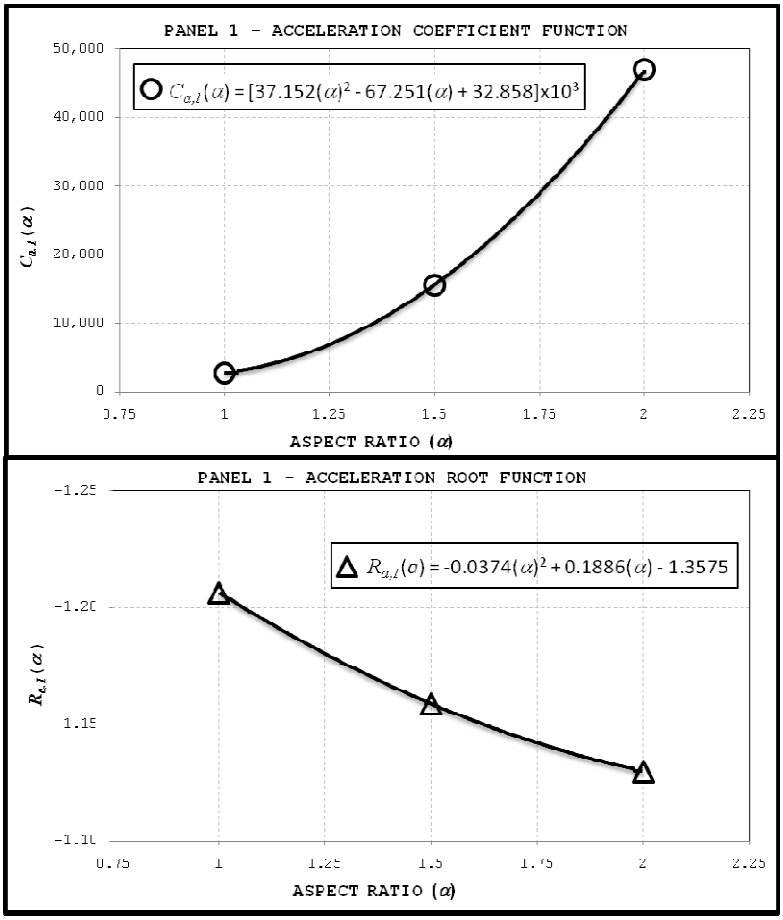

Figure 4.14: Panel 1 - Acceleration Coefficient and Root Functions

Finally, assembling these above expressions into the form of the RCRF method for Panel 1 gives the Frequency Coefficient-Root Function (FCRF), $f_1(\alpha,\lambda)$, and the Acceleration Coefficient-Root Function (ACRF), $a_1(\alpha,\lambda)$, which can be used to estimate the primary natural frequency, of a floor with the edge continuity conditions of Panel 1, as depicted Figure 4.9, for any value of $'\alpha'$ or $'\lambda'$:

Panel 1 Frequency (FCRF) –

$$f_1(\alpha,\lambda) = \left(1.925(\alpha)^2 - 6.9629(\alpha) + 8.6583\right)\left[\left(0.7273(\alpha)^2 - 2.0478(\alpha) + 3.9542\right)\sqrt{\lambda}\right] \quad \textit{Equation 4-3}$$

Panel 1 Acceleration (ACRF) –

$$a_1(\alpha,\lambda) = \left(37.152(\alpha)^2 - 67.251(\alpha) + 33.858\right)x10^3\left[\left(-0.0374(\alpha)^2 + 0.1886(\alpha) - 1.3575\right)\sqrt{\lambda}\right] \quad \textit{Equation 4-4}$$

4.3. **Summary of FEA Results for the RCRF Method**

Section 4.2 described the methodology used to derive the RCRF expressions for the frequency and acceleration response of Panel 1 as shown in Figure 4.9. The same methodology was also used to derive the RCRF expressions for the frequency and acceleration response of all nine panels. Table 4.4 summarizes the coefficient and Root functions for the frequency and acceleration response of all nine panels. Tables 4.5 to 4.14 provide the finite-element analysis results which were used to derive the RCRF method developed by this research program.

TABLE 4.4: RESPONSE COEFFIEIENT-ROOT FUNCTIONS

PANEL 1	$C_{f,1}(\alpha)$	$1.925(\alpha)^2 - 6.9629(\alpha) + 8.6583$
	$R_{f,1}(\alpha)$	$0.7273(\alpha)^2 - 2.0478(\alpha) + 3.9542$
	$C_{a,1}(\alpha)$	$[37.152(\alpha)^2 - 67.251(\alpha) + 33.858]\ x10^3$
	$R_{a,1}(\alpha)$	$-0.0374(\alpha)^2 + 0.1886(\alpha) - 1.3575$
PANEL 2	$C_{f,2}(\alpha)$	$-1.101(\alpha) + 4.2051$
	$R_{f,2}(\alpha)$	$-0.1822(\alpha)^2 + 0.728(\alpha) + 1.91$
	$C_{a,2}(\alpha)$	$[-12.223(\alpha)2 + 70.694(\alpha) - 55.998]\ x10^3$
	$R_{a,2}(\alpha)$	$-0.6259(\alpha)^2 + 1.9674(\alpha) - 2.5899$
PANEL 3	$C_{f,3}(\alpha)$	$1.277(\alpha)^2 - 5.4743(\alpha) + 7.3032$
	$R_{f,3}(\alpha)$	$0.2408(\alpha)^2 - 0.6273(\alpha) + 2.8423$
	$C_{a,3}(\alpha)$	$[34.025(\alpha) - 30.534]\ x10^3$
	$R_{a,3}(\alpha)$	$-0.6259(\alpha)^2 + 1.9674(\alpha) - 2.5899$
PANEL 4	$C_{f,4}(\alpha)$	$0.5328(\alpha)^2 - 3.3064(\alpha) + 5.7388$
	$R_{f,4}(\alpha)$	$-0.5317(\alpha)^2 + 1.6406(\alpha) + 1.3511$
	$C_{a,4}(\alpha)$	$[-2.0802(a)^2 + 39.095(\alpha) - 34.592\ ]\ x10^3$
	$R_{a,4}(\alpha)$	$0.5033(\alpha)^2 + 1.6089(\alpha) - 2.3714$
PANEL 5	$C_{f,5}(\alpha)$	$0.6376(\alpha)^2 - 3.3508(\alpha) + 5.6784$
	$R_{f,5}(\alpha)$	$-0.1178(\alpha)^2 + 0.5559(\alpha) + 2.022$
	$C_{a,5}(\alpha)$	$[-104.17(\alpha)^2 + 320.91(\alpha) - 213.37]\ x10^3$
	$R_{a,5}(\alpha)$	$-1.5707(\alpha)^2 + 4.1947(\alpha) - 3.7327$
PANEL 6	$C_{f,6}(\alpha)$	$0.9314(\alpha)^2 - 4.3115(\alpha) + 6.3277$
	$R_{f,6}(\alpha)$	$0.0087(\alpha)^2 + 0.1223(\alpha) + 2.3248$
	$C_{a,6}(\alpha)$	$[60.903(\alpha)^2 + 200.87(\alpha) - 137.45]\ x10^3$
	$R_{a,6}(\alpha)$	$-1.123(\alpha)^2 + 3.2565(\alpha) - 3.365$
PANEL 7	$C_{f,7}(\alpha)$	$1.4786(\alpha)^2 - 6.4055(\alpha) + 8.2328$
	$R_{f,7}(\alpha)$	$0.5897(\alpha)^2 - 2.0852(\alpha) + 4.3924$
	$C_{a,7}(\alpha)$	$[-61.951(\alpha)^2 + 205.36(\alpha) - 140.67]\ x10^3$
	$R_{a,7}(\alpha)$	$-1.0596(\alpha)^2 + 3.0627(\alpha) - 3.2079$
PANEL 8	$C_{f,8}(\alpha)$	$1.0454(\alpha)^2 - 5.1037(\alpha) + 7.3642$
	$R_{f,8}(\alpha)$	$0.205(\alpha)^2 - 0.9213(\alpha) + 3.6131$
	$C_{a,8}(\alpha)$	$[-69.051(\alpha)^2 + 225.24(\alpha) - 153.46]\ x10^3$
	$R_{a,8}(\alpha)$	$-1.0779(\alpha)^2 + 3.0573(\alpha) - 3.1842$
PANEL 9`	$C_{f,9}(\alpha)$	$0.3644(\alpha)^2 - 2.6116(\alpha) + 5.1646$
	$R_{f,9}(\alpha)$	$-0.2177(\alpha)^2 + 0.6341(\alpha) + 2.2973$
	$C_{a,9}(\alpha)$	$[-49.558(\alpha)^2 - 188.67(\alpha) + 136.21]\ x10^3$
	$R_{a,9}(\alpha)$	$-1.1885(\alpha)^2 + 3.7121(\alpha) + 3.8677$

TABLE 4.5: RCRF RESULTS - PANEL 1 ($E_{c,dyn}$ = 33.3 GPa; L_y = 9m)								
Aspect Ratio α	***Span-to-Depth Ratio*** L_y/d	***Stiffness-to-Mass Ratio*** $\lambda\ (rad/s^2)$	***Frequency Response*** $f\ (Hz)$	***Acceleration Response*** $a\ (mm/s^2)$	***Frequency Coefficient*** $C_{f,1}$	***Frequency Root*** $R_{f,1}$	***Acceleration Coefficient*** $C_{a,1}$	***Acceleration Root*** $R_{a,1}$
1	45	7.05	**7.6**	**545**	3.6204	2.6337	2.76 $x10^3$	-1.2063
	35	11.91	**9.5**	**355**				
	25	22.84	**11.8**	**206**				
1.5	45	35.69	**10.5**	**704**	2.5452	2.5189	15.57 $x10^3$	-1.1587
	35	60.31	**13.0**	**462**				
	25	115.63	**16.8**	**256**				
2	45	112.79	**13.2**	**694**	2.4325	2.7678	46.97 $x10^3$	-1.1299
	35	190.6	**16.7**	**476**				
	25	365.43	**20.3**	**246**				

TABLE 4.6: RCRF RESULTS - PANEL 2 ($E_{c,dyn}$ = 33.3 GPa; L_y = 9m)								
Aspect Ratio α	*Span-to-Depth Ratio* L_y/d	*Stiffness-to-Mass Ratio* $\lambda\ (rad/s^2)$	*Frequency Response* $f\ (Hz)$	*Acceleration Response* $a\ (mm/s^2)$	*Frequency Coefficient* $C_{f,1}$	*Frequency Root* $R_{f,1}$	*Acceleration Coefficient* $C_{a,1}$	*Acceleration Root* $R_{a,1}$
1	45	7.05	**6.8**	**550**	3.1059	2.4558	2.47 $x10^3$	-1.2484
	35	11.91	**8.7**	**345**				
	25	22.84	**11.0**	**200**				
1.5	45	35.69	**9.8**	**733**	2.5499	2.5920	22.54$x10^3$	-1.0471
	35	60.31	**12.0**	**460**				
	25	115.63	**15.4**	**239**				
2	45	112.79	**12.0**	**611**	2.0049	2.6371	36.50 $x10^3$	-1.1587
	35	190.6	**14.8**	**399**				
	25	365.43	**18.8**	**222**				

TABLE 4.7: RCRF RESULTS - PANEL 3 ($E_{c,dyn}$ = 33.3 GPa; L_y = 9m)								
Aspect Ratio α	*Span-to-Depth Ratio* L_y/d	*Stiffness-to-Mass Ratio* $\lambda\ (rad/s^2)$	*Frequency Response* $f\ (Hz)$	*Acceleration Response* $a\ (mm/s^2)$	*Frequency Coefficient* $C_{f,1}$	*Frequency Root* $R_{f,1}$	*Acceleration Coefficient* $C_{a,1}$	*Acceleration Root* $R_{a,1}$
1	45	7.05	**6.8**	**550**	3.1059	2.4558	3.39 $x10^3$	--1.1001
	35	11.91	**8.7**	**345**				
	25	22.84	**11.0**	**200**				
1.5	45	35.69	**8.5**	**809**	1.9650	2.4432	27.5 $x10^3$	-1.0471
	35	60.31	**10.5**	**447**				
	25	115.63	**13.8**	**250**				
2	45	112.79	**9.3**	**665**	1.4626	2.5510	22.2 $x10^3$	-1.1587
	35	190.6	**11.5**	**399**				
	25	365.43	**14.8**	**273**				

TABLE 4.8: RCRF RESULTS - PANEL 4 ($E_{c,dyn}$ = 33.3 GPa; L_y = 9m)								
Aspect Ratio α	***Span-to-Depth Ratio*** L_y/d	***Stiffness-to-Mass Ratio*** $\lambda\ (rad/s^2)$	***Frequency Response*** $f\ (Hz)$	***Acceleration Response*** $a\ (mm/s^2)$	***Frequency Coefficient*** $C_{f,1}$	***Frequency Root*** $R_{f,1}$	***Acceleration Coefficient*** $C_{a,1}$	***Acceleration Root*** $R_{a,1}$
1	45	7.05	**6.5**	**525**	2.9562	2.4600	2.42 $x10^3$	-1.2658
	35	11.91	**8.3**	**334**				
	25	22.84	**10.5**	**207**				
1.5	45	35.69	**7.8**	**723**	1.9780	2.6157	19.37 $x10^3$	-1.0905
	35	60.31	**9.5**	**459**				
	25	115.63	**12.2**	**247**				
2	45	112.79	**8.3**	**613**	1.2572	2.5056	35.28 $x10^3$	-1.1669
	35	190.6	**10.3**	**394**				
	25	365.43	**13.2**	**224**				

TABLE 4.9: RCRF RESULTS - PANEL 5 ($E_{c,dyn}$ = 33.3 GPa; L_y = 9m)								
Aspect Ratio α	***Span-to-Depth Ratio*** L_y/d	***Stiffness-to-Mass Ratio*** $\lambda\ (rad/s^2)$	***Frequency Response*** $f\ (Hz)$	***Acceleration Response*** $a\ (mm/s^2)$	***Frequency Coefficient*** $C_{f,1}$	***Frequency Root*** $R_{f,1}$	***Acceleration Coefficient*** $C_{a,1}$	***Acceleration Root*** $R_{a,1}$
1	45	7.05	**6.5**	**602**	2.9652	2.4600	3.37 $x10^3$	-1.1086
	35	11.91	**8.3**	**334**				
	25	22.84	**10.5**	**207**				
1.5	45	35.69	**8.3**	**861**	2.0868	2.5907	33.61 $x10^3$	-0.9747
	35	60.31	**10.3**	**495**				
	25	115.63	**13.0**	**257**				
2	45	112.79	**9.0**	**664**	1.5272	2.6624	11.77 $x10^3$	-1.6260
	35	190.6	**11.0**	**440**				
	25	365.43	**14.0**	**320**				

TABLE 4.10: RCRF RESULTS - PANEL 6 ($E_{c,dyn}$ = 33.3 GPa; L_y = 9m)								
Aspect Ratio α	***Span-to-Depth Ratio*** L_y/d	***Stiffness-to-Mass Ratio*** $\lambda\ (rad/s^2)$	***Frequency Response*** $f\ (Hz)$	***Acceleration Response*** $a\ (mm/s^2)$	***Frequency Coefficient*** $C_{f,1}$	***Frequency Root*** $R_{f,1}$	***Acceleration Coefficient*** $C_{a,1}$	***Acceleration Root*** $R_{a,1}$
1	45	7.05	**6.5**	**522**	2.9476	2.4558	2.51 x10^3	-1.2315
	35	11.91	**8.2**	**325**				
	25	22.84	**10.5**	**200**				
1.5	45	35.69	**8.0**	**780**	1.9561	2.5278	26.81 x10^3	-1.0070
	35	60.31	**10.0**	**448**				
	25	115.63	**12.8**	**242**				
2	45	112.79	**8.8**	**635**	1.4303	2.6042	20.67 x10^3	-1.3447
	35	190.6	**10.8**	**394**				
	25	365.43	**13.8**	**263**				

TABLE 4.11: RCRF RESULTS - PANEL 7 ($E_{c,dyn}$ = 33.3 GPa; L_y = 9m)								
Aspect Ratio α	***Span-to-Depth Ratio*** L_y/d	***Stiffness-to-Mass Ratio*** $\lambda\ (rad/s^2)$	***Frequency Response*** $f\ (Hz)$	***Acceleration Response*** $a\ (mm/s^2)$	***Frequency Coefficient*** $C_{f,1}$	***Frequency Root*** $R_{f,1}$	***Acceleration Coefficient*** $C_{a,1}$	***Acceleration Root*** $R_{a,1}$
1	45	7.05	**6.5**	**565**	3.3059	2.8969	2.73 $x10^3$	-1.2048
	35	11.91	**7.8**	**322**				
	25	22.84	**9.8**	**211**				
1.5	45	35.69	**7.8**	**776**	1.9514	2.5913	27.97 $x10^3$	-0.9980
	35	60.31	**9.5**	**463**				
	25	115.63	**12.2**	**239**				
2	45	112.79	**8.3**	**634**	1.3362	2.5806	*22.23 $x10^3$*	*-1.3210*
	35	190.6	**10.3**	**400**				
	25	365.43	**13.1**	**259**				

TABLE 4.12: RCRF RESULTS - PANEL 8 ($E_{c,dyn}$ = 33.3 GPa; L_y = 9m)								
Aspect Ratio α	*Span-to-Depth Ratio* L_y/d	*Stiffness-to-Mass Ratio* $\lambda\ (rad/s^2)$	*Frequency Response* $f\ (Hz)$	*Acceleration Response* $a\ (mm/s^2)$	*Frequency Coefficient* $C_{f,1}$	*Frequency Root* $R_{f,1}$	*Acceleration Coefficient* $C_{a,1}$	*Acceleration Root* $R_{a,1}$
1	45	7.05	**6.5**	**565**	3.3059	2.8969	$2.73x10^3$	-1.2048
	35	11.91	**7.8**	**322**				
	25	22.84	**9.8**	**211**				
1.5	45	35.69	**7.8**	**888**	2.0608	2.6925	$29.04\ x10^3$	-1.0235
	35	60.31	**9.5**	**526**				
	25	115.63	**12.0**	**282**				
2	45	112.79	**8.3**	**682**	1.3384	2.5907	$20.82\ x10^3$	-1.3812
	35	190.6	**10.3**	**461**				
	25	365.43	**13.0**	**291**				

TABLE 4.13: RCRF RESULTS - PANEL 9 ($E_{c,dyn}$ = 33.3 GPa; L_y = 9m)								
Aspect Ratio α	***Span-to-Depth Ratio*** L_y/d	***Stiffness-to-Mass Ratio*** $\lambda\ (rad/s^2)$	***Frequency Response*** $f\ (Hz)$	***Acceleration Response*** $a\ (mm/s^2)$	***Frequency Coefficient*** $C_{f,1}$	***Frequency Root*** $R_{f,1}$	***Acceleration Coefficient*** $C_{a,1}$	***Acceleration Root*** $R_{a,1}$
1	45	7.05	**6.0**	**711**	2.9174	2.7137	2.90 $x10^3$	-1.3441
	35	11.91	**7.3**	**420**				
	25	22.84	**9.3**	**294**				
1.5	45	35.69	**7.5**	**886**	2.0671	2.7586	35.29 $x10^3$	-0.9737
	35	60.31	**9.3**	**537**				
	25	115.63	**11.5**	**266**				
2	45	112.79	**8.0**	**886**	1.3990	2.6947	42.89 $x10^3$	-1.1976
	35	190.6	**10.0**	**447**				
	25	365.43	**12.4**	**328**				

CHAPTER 5

FIELD INSTRUMENTATION

5.1. **Overview**

The aim of this phase of research was to measure the response frequencies of two-way, flat slab concrete floor structures in real buildings, and to compare the measured response frequencies and accelerations with the those predicted by the RCRF method. This chapter will briefly discuss the correlation of natural response measurements to the RCRF predicted response for three floor structures having edge continuity conditions corresponding to Panel 1 as depicted in Figure 4.9 for which the derivation of RCRF method was explained in Section 4.2. For confidentiality purposes, the names of these properties will not be disclosed and will be referred to as floor structures '1', '2' and '3'.

5.2. **Floor Structure '1'**

The first floor structure to be instrumented was a suspended, post-tensioned, basement carpark of a high-rise residential building under construction. Because this floor structure was a construction site, careful coordination and planning was necessary to gain access to conduct tests at times when the floor was not being used for access of construction equipment or personnel. At the time of testing, the floor panel was clear of any stacking materials. This floor structure and its RCRF parameters are shown in Figure 5.1. This figure is taken from the as-constructed structural drawings for the project. It can be seen that the supporting

columns are not all the same size or shape; therefore, the weighted average distances to the geometric centroids of the columns was used to define the spans in each direction. Given that this floor panel is continuous on all four edges, it may be categorized as a Panel type '1' according to Figure 4.9.

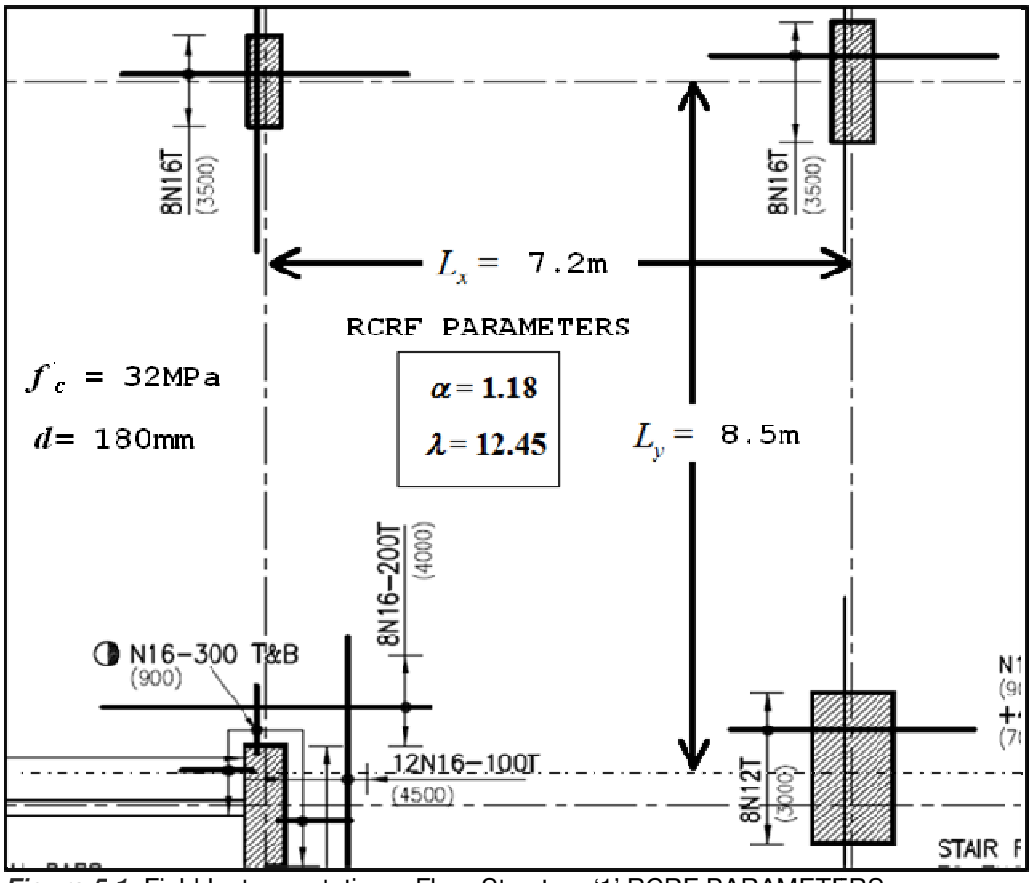

Figure 5.1: Field Instrumentation – Floor Structure '1' RCRF PARAMETERS

5.2.1. ***Measured Response***

An accelerometer was rigidly fixed to the top surface of the concrete slab at the centre of the panel. Heel-drop tests were conducted on the panel, and a portable data acquisition system was used to obtain the acceleration time-history record and power-spectrum on site. Several Heel-Drop tests were conducted to ensure

that the data acquisition equipment was working properly and that the response measurements were consistent. The typical power-spectrum and acceleration

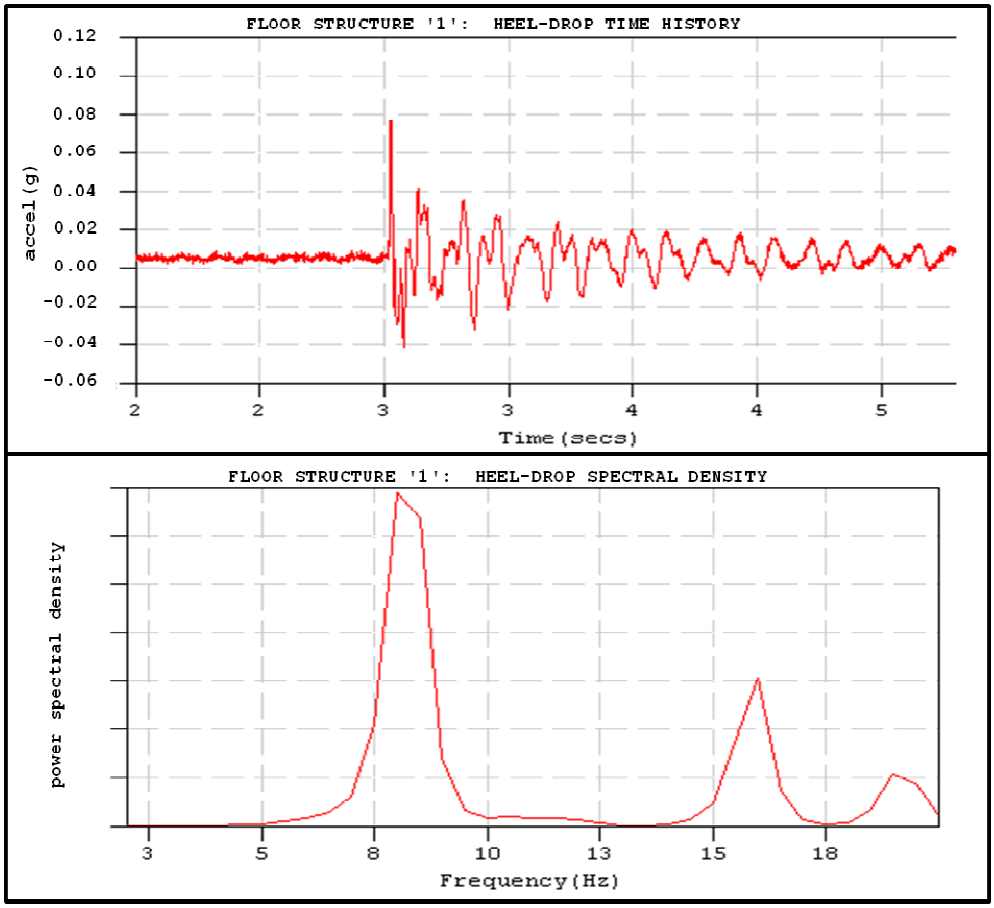

Figure 5.2: Field Instrumentation – Floor Structure '1' HEEL-DROP Time History and Spectral Density Results

time-history acceleration records for Heel-Drop tests conducted on this panel are given in Figure 5.2. It can be seen from the time-history acceleration record that there is an initial peak response of approximately $785 mm/s^2$ ($0.08 gravity$) and the measured response frequency for Floor Structure '1' was approximately $8.5 Hz$.

5.2.2. ***RCRF Correlation***

The geometric and material properties of Floor Structure '1' are as follows:

- L_x (*mm*) = 7200
- L_y (*mm*) = 8500
- d (*mm*) = 180
- I (mm^3) = $d^3/12$ = $486x10^3$
- m (*tonne*/mm^2) = $432x10^{-9}$
- f'_c = $32MPa$
- $E_{c,dyn}$ = $1.04(5055.75)(f'_c)^{.5}$ = $29.74GPa$

These properties correspond to the RCRF method parameters:

- α = 1.18
- λ = 12.45

By substituting the values of 'α' and 'λ' into Equation 6, the RCRF predicted response of Floor Structure '1' would be calculated as follows:

Frequency (FCRF) –

$$f_1(\alpha,\lambda) = \left(1.925(1.18)^2 - 6.9629(1.18) + 8.6583\right)\left[\left(0.7273(1.18)^2 - 2.0478(1.18) + 3.9542\right)\sqrt{12.45}\right] = \underline{\mathbf{8.4}\boldsymbol{Hz}}$$

Acceleration (ACRF) –

$$a_1(\alpha,\lambda) = \left(37.152(1.18)^2 - 67.251(1.18) + 33.858\right)x10^3\left[\left(-0.0374(1.18)^2 + 0.1886(1.18) - 1.3575\right)\sqrt{12.45}\right] = \underline{\mathbf{740}\boldsymbol{mm/s^2}}$$

Although the RCRF predicted acceleration underestimates the measured peak acceleration by 6%, the RCRF predicted frequency is within 2% of measurements. It can be concluded that in the case of Floor Structure '1 that the RCRF calculated response shows reasonably good agreement with the measured response.

5.3. **Floor Structure '2'**

The second floor structure to be instrumented was the post-tensioned, floor of a commercial building under construction. Because this floor structure was a construction site, careful coordination and planning was necessary to gain access to conduct tests at times when the floor was not being used for access of construction equipment or personnel. At the time of testing, the floor panel was clear of any stacking materials. This floor structure and its RCRF parameters are shown in Figure 5.3, which is a sketch replicated from the as-constructed structural drawings for the project. The supporting columns are all the same size and shape on a square grid of 8.2m in each direction. The drop panels over the columns can also be observed in Figure 5.3 as 1.8m square thickenings each with a depth of 325mm. Because the RCRF method was derived using finite-

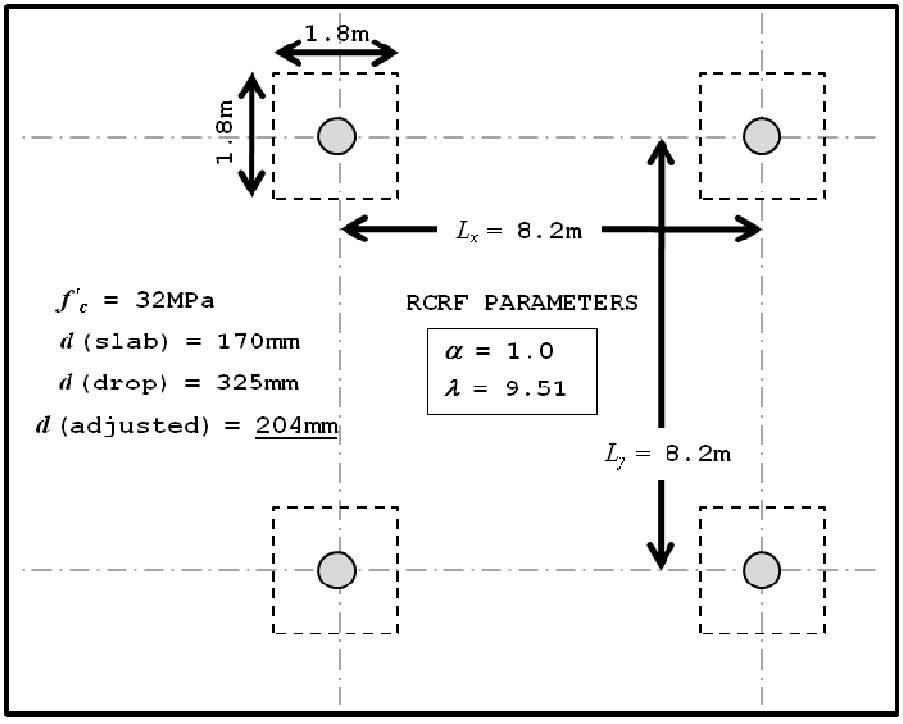

Figure 5.3: Field Instrumentation – Floor Structure '2' RCRF PARAMETERS

element analysis with models having uniform slab depths and no drop-panels, an 'adjusted' slab depth must be considered. The adjusted slab depth for Floor Structure '2' is 204mm as calculated by Equation 1.13. Because this floor structure is continuous on all sides, it may be categorized as Panel type '1' according to Figure 4.9 for RCRF calculation purposes.

5.3.1. ***Measured Response***

An accelerometer was rigidly fixed to the top surface of the concrete slab at the centre of the panel. Heel-drop tests were conducted on the panel, and a portable

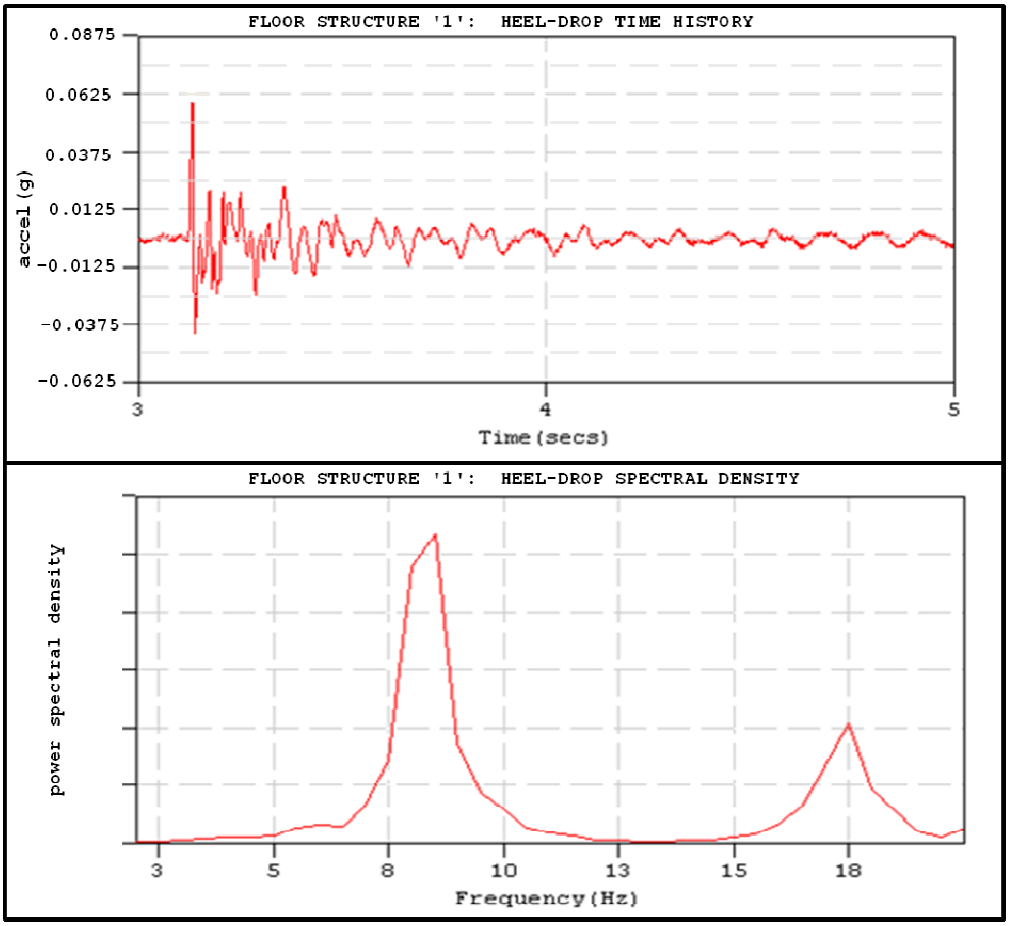

Figure 5.4: Field Instrumentation – Floor Structure '2' HEEL-DROP Time History and Spectral Density Results

data acquisition system was used to obtain the acceleration time-history record and power-spectrum on site. Several Heel-Drop tests were conducted to ensure that the data acquisition equipment was working properly and that the response measurements were consistent. The typical power-spectrum and acceleration time-history acceleration records for Heel-Drop tests conducted on this panel are given in Figure 5.4. It can be seen from the time-history acceleration record that there is an initial peak response of approximately 588mm/s^2 (0.06$gravty$) and the measured response frequency for Floor Structure '1' was approximately 8.6Hz

5.3.2. ***RCRF Correlation***

The geometric and material properties of Floor Structure '1' are as follows:

- L_x (mm) = 8200; $L_{x,drop}$ (mm) = 1800
- L_y (mm) = 8200; $L_{y,drop}$ (mm) = 1800
- d (mm)= 170; d_{drop} (mm)= 325
- $d_{adjusted}$ (mm) = 204
- I (mm^3) = $d^3/12$ = 707.7$x10^3$
- m ($tonne/mm^2$) = 490$x10^{-9}$
- f'_c = 32MPa
- $E_{c,dyn}$ = 1.04(5055.75)(f'_c)$^{.5}$ = 29.74GPa

These properties correspond to the RCRF method parameters:

- α = 1.0
- λ = 9.51

By substituting the values of 'α' and 'λ' into Equation 6, the RCRF predicted response of Floor Structure '1' would be calculated as follows:

Frequency (FCRF) –

$$f_1(\alpha,\lambda) = \left(1.925(1.0)^2 - 6.9629(1.0) + 8.6583\right)\left[\left(0.7273(1.0)^2 - 2.0478(1.0) + 3.9542\right)\sqrt{9.51}\right] = \underline{\mathbf{8.5}\boldsymbol{Hz}}$$

Acceleration (ACRF) –

$$a_1(\alpha,\lambda) = \left(37.152(1.18)^2 - 67.251(1.18) + 33.858\right)x10^3\left[\left(-0.0374(1.18)^2 + 0.1886(1.18) - 1.3575\right)\sqrt{12.45}\right] = \underline{\mathbf{581}\boldsymbol{mm/s^2}}$$

In this case, RCRF predicted acceleration very accurately correlates with the measured peak acceleration by 1%, and the RCF predicted frequency is within 1% of measurements. It can be concluded that in the case of Floor Structure '2' that the RCRF calculated response shows excellent agreement with the measured response.

5.4. **Floor Structure '3'**

The third floor structure to be instrumented was the post-tensioned, floor of a commercial building in use. Because this floor structure was an active workplace, careful coordination and planning was necessary to gain access to conduct tests without disrupting office personnel. At the time of testing, the floor panel was in full operation, loaded with people, office furniture, bookshelves and filing cabinets. A photo of the office taken at the time of testing is shown in Figure 5.6. Because the floor was occupied, an unfactored superimposed load of 1.0 kPa was used as a reasonable estimated of the actual the mass component in the calculation of 'λ' (e.g., SIL= 1.0 kPa = 1x10^{-7} $tonne/mm^2$).

Figure 5.6: Field Instrumentation – Floor Structure '3' Office in Operation

This floor structure and its RCRF parameters are shown in Figure 5.3, which is a sketch replicated from the as-constructed structural drawings for the project. The supporting columns are all the same size and shape on a rectangular grid of L_x = 6.2m and L_y = 8.4m. The slab is 170mm thick and the drop panels over the

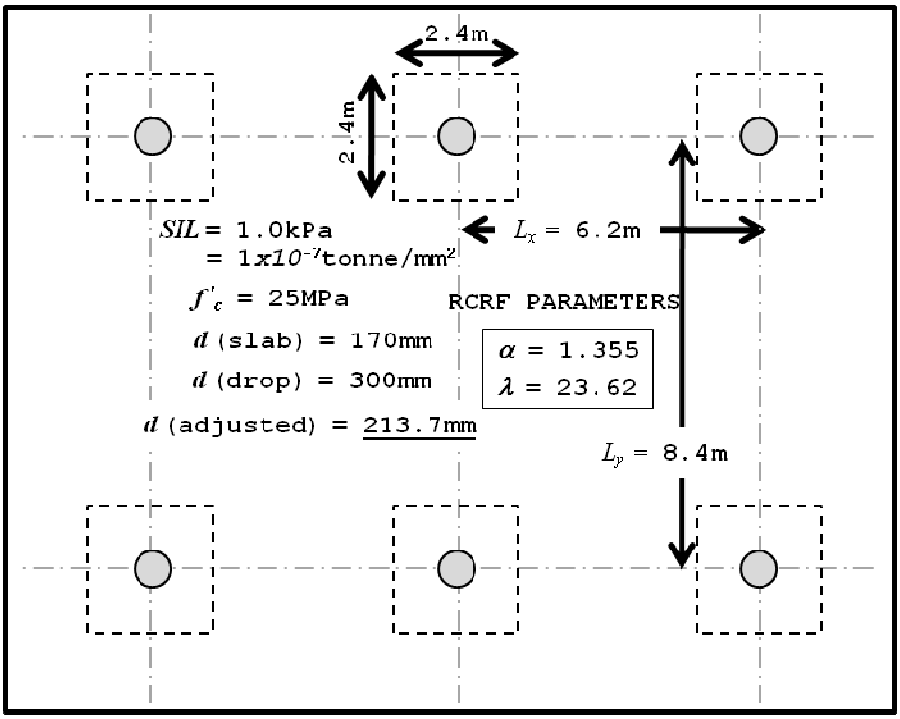

Figure 5.5: Field Instrumentation – Floor Structure '3' RCRF Parameters

columns can also be observed in as 2.4m square thickenings each with a depth of 300mm. Because the RCRF method was derived using finite- element analysis with models having uniform slab depths and no drop-panels, an 'adjusted' slab depth must be considered. The adjusted slab depth for Floor Structure '3' is 213.7mm as calculated by Equation 1.13. Because this floor structure is continuous on all sides, it may be categorized as Panel type '1' according to Figure 4.9 for RCRF calculation purposes. Figure 4.9

5.4.1. ***Measured Response***

Because the top surface of Floor Structure '3' was finished with carpet, a SVAN956 AcuVibe data acquisition system with soffit-mounted magnetic base accelerometer fixed to a steel washer which was epoxied to the underside of the concrete slab. A photo of the data acquisition set-up for Floor Structure '3' is shown in Figure 5.7. A researcher would prepared the data acquisition system

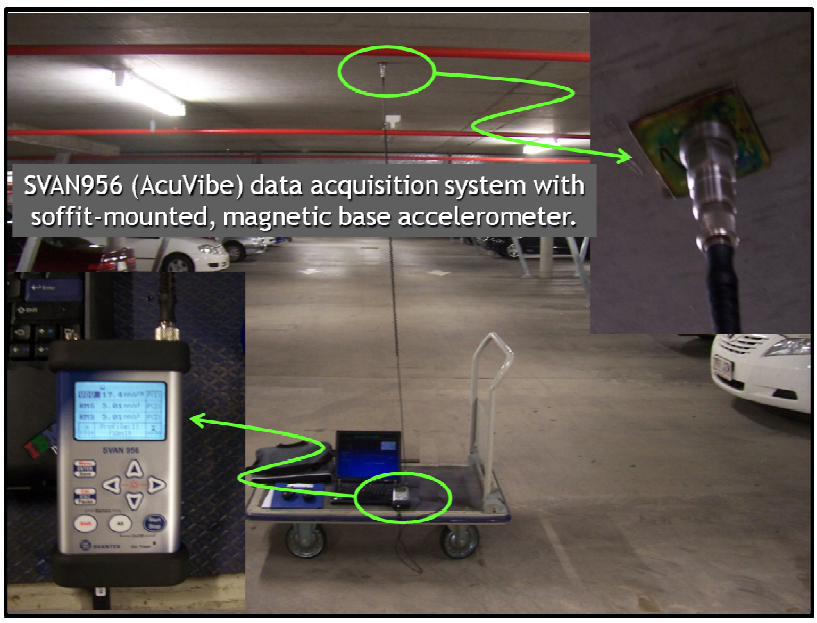

Figure 5.7**:** Field Instrumentation – Floor Structure '3' Data Acquisition System

below the floor, while a research assistant located the centre of the panel on the top of the floor. When both researchers were in position and ready, hand-held radios were used to coordinate heel-drop tests. Several heel-drop tests were conducted to ensure that the data acquisition equipment was working properly and that the response measurements were consistent. The typical power-spectrum and acceleration time-history acceleration records for Heel-Drop tests conducted on this panel are given in Figure 5.8. It can be seen from the time-history acceleration record that there is an initial peak response of approximately 315mm/s^2 (RMS) and the measured response frequency for Floor Structure '3' was approximately 9.7Hz.

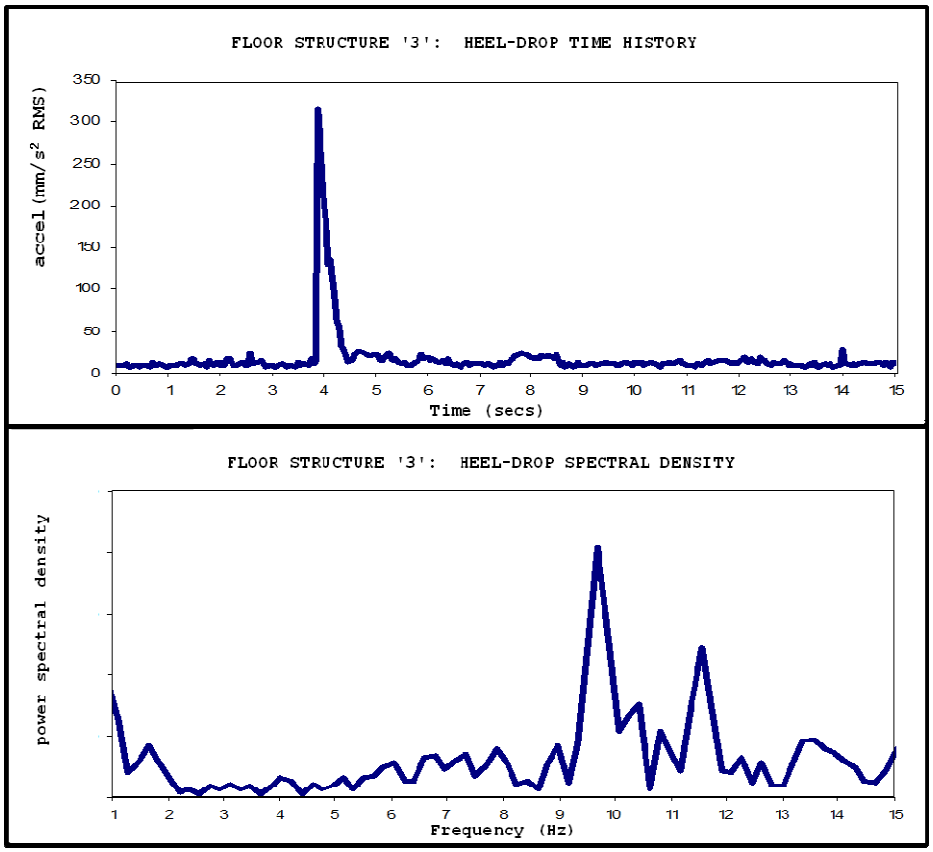

Figure 5.8: Field Instrumentation – Floor Structure '3' HEEL-DROP Time History and Spectral Density Results

5.4.2. ***RCRF Correlation***

The geometric and material properties of Floor Structure '1' are as follows:

- L_x (*mm*) = 6200; $L_{x,drop}$ (*mm*) = 2400
- L_y (*mm*) = 8400; $L_{y,drop}$ (*mm*) = 2400
- d (*mm*)= 170; d_{drop} (*mm*)= 300
- $d_{adjusted}$ (*mm*) = 213.7
- I (mm^3) = $d^3/12$ = $813.6x10^3$
- SIL = . $1.0x10^{-7}$ (*tonne*/mm^2); m (*tonne*/mm^2) = $613x10^{-9}$
- f'_c = $25MPa$
- $E_{c,dyn}$ = 1.04(5055.75)(f'_c)$^{.5}$ = $26.29GPa$

These properties correspond to the RCRF method parameters:

- α = 1.355
- λ = 23.62

By substituting the values of 'α' and 'λ' into Equation 6, the RCRF predicted response of Floor Structure '3' would be calculated as follows:

Frequency (FCRF) –

$$f_1(\alpha,\lambda) = \left(1.925(1.355)^2 - 6.9629(1.355) + 8.6583\right)\left[\left(0.7273(1.355)^2 - 2.0478(1.355) + 3.9542\right)\sqrt{23.62}\right] = \underline{\mathbf{9.7Hz}}$$

Acceleration (ACRF) –

$$a_1(\alpha,\lambda) = \left(37.152(1.355)^2 - 67.251(1.355) + 33.858\right)x10^3\left[\left(-0.0374(1.355)^2 + 0.1886(1.355) - 1.3575\right)\sqrt{23.62}\right] = \underline{\mathbf{734mm/s^2}}$$

In this case, the RCRF predicted frequency agrees exactly with measurements; however, the RCRF predicted acceleration overestimates the measured peak acceleration by nearly 60%. A plausible explanation for the RCRF overestimation of acceleration response in the case of Floor Structure '3' may be

attributed to a considerable reduction of the heel-drop impulse because the impact of the heel-drop was cushioned by a layer of carpet and underlay. Furthermore, Floor Structure '3' was fully fitted-out with furniture and occupied by people. Although the actual damping ratio of Floor Structure '3' was not directly measured, the carpet finish and office fit-out would easily result in a damping ratio greater that 1.2%, which is the magnitude of damping used in the development of the RCRF method. Office floors with fit-out may have damping ratios that range from as low as 2% to a high as 7% (C. Hewitt, 2004) It has been well established that significantly less energy is required to excite a floor structure with low damping that would be required for one with high damping. Therefore, the overestimation acceleration response for Floor Structure '3' predicted by the RCRF method would be expected. This warrants the need for further refinement of the proposed RCRF method through future research to account for the influence of various levels of damping on the acceleration response.

5.5. **Summary of Field Instrumentation**

The aim of this phase of research was to measure the response frequencies of two-way, flat slab concrete floor structures in real buildings, and to compare the measured response frequencies and accelerations with those predicted by the RCRF method. The results in this chapter confirm that the proposed RCRF method is sufficiently accurate for its intended purpose.

CHAPTER 6

CONCLUSIONS

6.1. General Summary

Floor structures will vibrate in response to dynamic loads. Vibration is a serviceability limit state for the design of suspended floor systems in buildings that is not well understood by many structural engineers. Dynamic behaviour is an important design consideration for suspended floors, particularly of slender, two-way, suspended concrete construction. Although the field of floor vibration has been extensively developed theoretically, at present, there are no convenient design guidelines that deal with this problem. Results from this research have enabled the development of a new approach for assessing the vibration serviceability of flat, suspended concrete floors in buildings.

The acceptability criterion for human exposure to vibration in buildings is function of frequency of vibration and the acceleration response. Predictive determination of the frequency of vibration and the acceleration response of a floor structure is crucial for assessing its dynamic serviceability during the design phase of a project. Without the ability to predict the dynamic performance of a floor, vibration assessment becomes retrospective. If vibration is determined to be a serviceability problem after the floor has been constructed, costly structural retrofit could be required that may disrupt or alter the originally intended function of the tenancy.

This thesis describes a comprehensive research program designed to develop an empirical method for assessing the vibration serviceability of flat, suspended concrete floors in buildings. Full-scale, laboratory tests have been conducted on a post-tensioned floor specimen in the university's structural laboratory. Special support brackets were fabricated to perform as frictionless pins at the corners to isolate the specimen, which allowed an accurate material model to be established. A series of static and dynamic tests were performed in the laboratory to obtain basic material and dynamic properties of the specimen. Finite-element-models have been calibrated against data collected from laboratory experiments to simulate the static and dynamic behaviour of the floor specimen. Computational finite-element-analysis has been extended to investigate a variety of floor configurations. Field instrumentation and testing of floors in existing buildings has also been carried out. Measurements from field tests are in good agreement with computational studies. Results from this parametric investigation have led to the development of new approach for predicting the natural frequency of flat, two-way concrete floor structures. This new method has been named, the Response Coefficient-Root Function (RCRF) method. The RCRF method is convenient tool that structural engineers can use to assist them in the design for the vibration serviceability limit-state of in-situ concrete floor systems.

6.2. **Significance and Contribution to Industry**

The main achievement of this research is the development of two empirical expressions for predicting the frequency and acceleration response of flat-slab floor structures subjected to transient dynamic, human-induced loads. These proposed expressions and the manner in which they are intended to be applied in practice have been referred to as the Response Coefficient-Root Function (RCRF) method, given by Equations 1.9 and 1.11. These proposed expressions are similar to that proposed by Wyatt in Equation 1.7. The difference between Wyatt's method and the proposed RCRF method is that the coefficient and root of the stiffness-to-mass ratio 'λ' are not constant, instead they are functions of the panel aspect ratio, '$\alpha = L_y/L_x$' where L_y is the long span, and L_x is the short span dimension of the panel. This new approach to assessing dynamic performance will assist engineers in the design of suspended floors for vibration serviceability, particularly those of slender, post-tensioned concrete construction.

6.3. **Future Research**

6.3.1. ***Expanded Floor Configurations***

The RCRF method calculations described in this dissertation apply to flat slab floor structures supported by external and internal columns as shown in Figure 4.9. Future work on further the development of the RCRF method should include analyses for two-way floor panel configurations having external and internal wall supports and those with external wall and interior columns as illustrated in Figure 6.1 as well as one-way band beam floor systems.

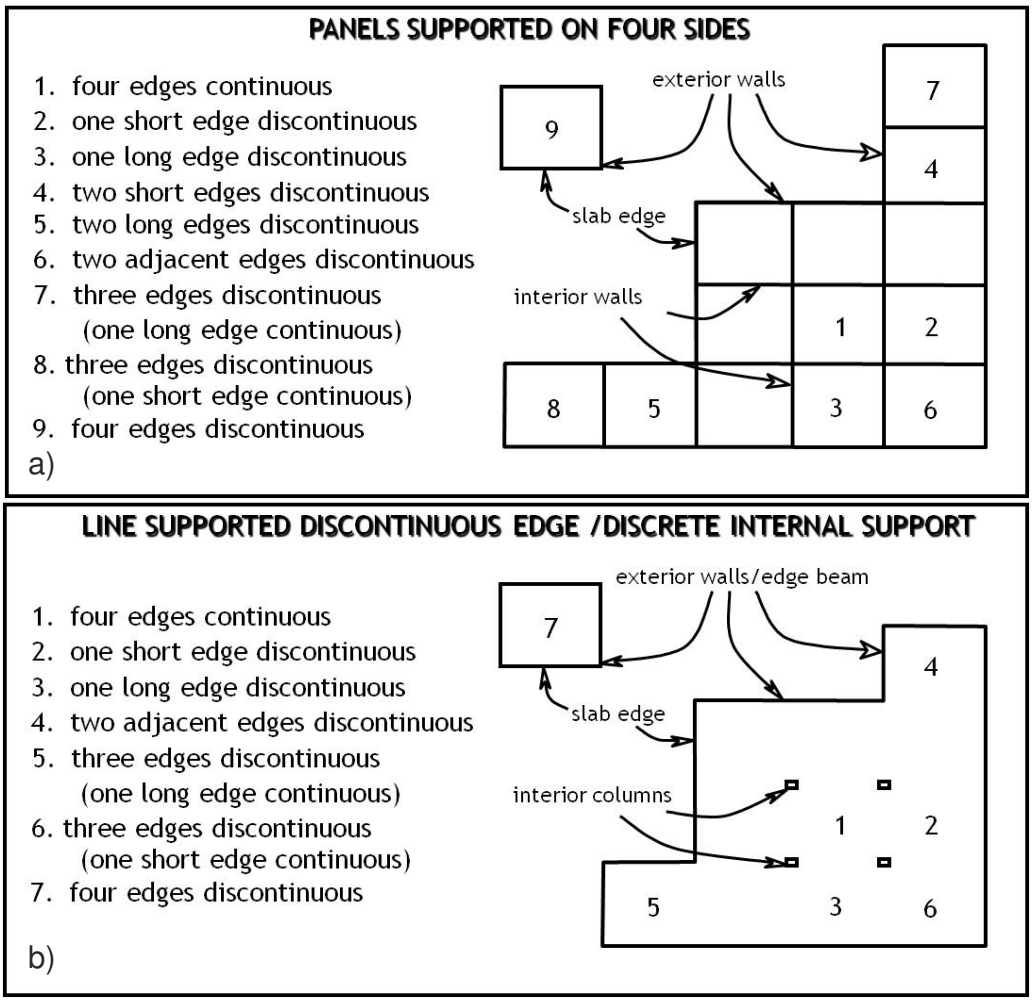

Figure 6.1: Proposed two-way floor configurations for future research

6.3.2. ***Velocity Response and Excitation Location***

The RCRF method expressions described in this dissertation were derived by studying the response of floors subjected to Murray's heel-drop excitation at the centre of a floor panel. This approach provides an accurate estimation of the lowest frequency response of a floor panel for which acceleration acceptability limits are most stringent, so the scope of this research was limited to the acceleration response. The acceptability criteria of high frequency floors, e.g., floors with frequency responses greater than 10Hz, are typically governed by

velocity limits rather than acceleration. Although the frequency response of a floor at the centre of a panel may greater than 10Hz depending on the span-to-depth ratio or stiffness-to-mass ratio 'λ', future work on further developing the RCRF method should include analyses of two-way systems subjected to excitation along the column lines where the floor plate is stiffest and thus where the frequency response would be higher than at the centre of the panel. For this reason RCRF expressions for velocity response should also be developed. In doing so a comprehensive and convenient set of empirical equations would be available to assist engineers in the design of both acceleration and velocity acceptability criteria of floors subjected to transient, human-induced loads.

6.3.3. ***Damping and Continuous Vibration***

The RCRF method expressions described in this dissertation were derived by finite-element analysis (FEA) using a material model developed from the calibration of results of laboratory tests conducted on an isolated, pin-supported, bare floor specimen. The viscous damping behaviour of the FEA material model was relatively low, e.g., damping ratio, ζ ~ 1.2%. Measurements of the acceleration response from field tests conducted on Floor Structures '1' and '2', which were also bare floors, showed very good correlation with the acceleration response predicted by the RCRF method as described in Chapter 5. The measured acceleration response of Floor Structure '3'; however, was overestimated by approximately 60%. Although the RCRF frequency response was well predicted, the discrepancy in acceleration is likely due Floor Structure '3' having a damping ratio higher than 1.2% due to it being an occupied floor with

full fit-out. For this reason, further development of the proposed RCRF method should consider the influence of various values of damping on estimating both acceleration and vibration response.

Despite the need for further research, this dissertation demonstrates that there is a promising potential for the RCRF method to become a valuable tool in for engineers to use for the design of human-induced transient vibration serviceability of suspended concrete floors in buildings.

ACKNOWLEDGEMENTS

The author is especially grateful to the local industry leaders who generously donated resources, material and time to this project. The laboratory phase of this research would not have been possible without their assistance. All of the necessary materials, equipment and trained personnel for post-tensioning were donated by TEAM POST TENSIONING. For formwork, BORAL Formwork and Scaffolding donated shores, jackscrews, bearers, joists and formply. HANSON Concrete and Quarry Products have donated 6 cubic meters of 40MPa concrete. For support brackets, SMORGON Steel donated 1000kg of Gr250 steel plate. YERONGA Institute of TAFE incorporated fabrication of the four steel support brackets into their curriculum. ULTIMATE Concrete Cutting dismantled the laboratory floor specimen by sawing it into six pieces, which have been used for a much needed extension to the boat launch at the Lake Sampsonvale Sailing Club during a time of low water levels due to drought. It is comforting to know that the specimen found a good home and final resting place.

Very special thanks and credit is extended to the university's technical staff for their effort and cooperation with laboratory testing. In particular, thanks to Arthur Powell for sharing his experience with instrumentation and data acquisition. Thanks to Brian Pelin, James Grandy and Jim Hazelman for their enthusiasm and practical minds. The university's structural laboratory has since been demolished. It was a building that produced years of quality research and good memories with you both. It will be missed.

This research project also served to facilitate the honours thesis requirements for undergraduate students, Leah McKenzie and Truong Nguyen as well as graduate thesis requirements for Trond Skogdal and Vegard Andersen. Leah and Truong were of valuable assistance in the experimental laboratory phase of this program. They conducted concrete cylinder tests as well as calibrated the data acquisition system testing of the post-tensioned floor specimen in addition to assistance with the literature review for this dissertation. Field instrumentation and data acquisition for the testing of Floor Structure '1' and Floor Structure '2' is entirely to the credit of Trond and Vegard. Over several months, their coordination with the contractors and construction managers to gain access on site was critical in maintaining the forward progress of this research on program.

The voluntary research assistance of Andrew Grice, and a group of year-three and year-four undergraduate engineering students, too many to name, is also acknowledged. Andrew's involvement was an essential contribution to the smooth instrumentation and data acquisition of Floor Structure '3'. The voluntary help of our undergraduate students in the laboratory was very much appreciated for the concrete pour of the floor specimen. Thank you all for getting your hands dirty.

Thanks are extended to my fellow postgraduate students Sandun De Silva Mostafa Darestani, Julius Marko, Rahila Hareer and Huang Ming-Hui who shared their knowledge and experience with me to help me develop my own.

Lastly, but not at all in the least, my thanks goes to Professors David Thambiratnam and Stephen Kajewski for their supervision. I am proud to have been guided by you both. To David especially, I am grateful for the day we met.

REFERENCES

ACI318-05. (2005). Building Code Requirements for Structural Concrete and Commentary.

Allen, D. E. (1990). "Building Vibrations from Human Activities". *Concrete International Vol 4(No 6)* , 66-73.

Allen, D. E. (1990). "Floor Vibration from Aerobics" . *Canadian Journal of Civil Engineering 17* , 771-119.

ANSI-S2.71. (2006). Guide to the Evaluation of Human Exposure to Vibration in Buildings. In A. N. Standards. Acoustical Society of America.

AS1012.17. (1997). *Methods of Testing Concrete: Determinaiton of the Static Modulus of Elasticity.* Standards Australia.

AS2670. (1990). *"Evaluation of Human Exposure to Whole-body Vibration - Continuous and Shock Induced Vibrations in Buildings (1-80Hz)".* Standards Australia.

AS3600. (2009). *Australian Standard - Concrete Structures.* Standards Australia.

Bachman, H. (1995). *Vibration Problems in Structures.* Germany: Birkhauser Verlag Basel.

Bachmann, H. (1987). *Vibrations in Structures Incuuced by Man and Machines.* Switzerland: IABSE-AIPC-IVBH.

Bendickson, Y. V. (1993). *Dealing with Excessive Floor Vibrations.* Canada.: Institute for Research in Construction.

Brownjohn, J. M. (2004). "A Spectral Density Approach for Modelling Continuous Vertical Forces on Pedestrian Structures Due to Walking.". *Canadian Journal of Civil Engineering Vol. 31* , 65-71.

BS6472. (2008). *Guide to evaluation of human exposure to vibration in buildings. Vibration sources other than blasting .* British Standards.

BS8110-1. (1997). BS 8110-1:1997. In *Structural use of concrete. Code of practice for design and construction.* British Standards Institution.

C. Hewitt, T. M. (2004, April). Office Fit-Out and Floor Vibrations. *Modern Steel Construction* , pp. 34-38.

C. Jetann, D. T. (2007). *"Frequency Response of Flat Post-tensioned Floor Plates: Frequency Coefficient-Root Funciton Method.* Cairns, Australia: 14th International Congress on Sound and Vibration.

C. Jetann, D. T. (2006). *"Vibration of Flat Post-tensioned Floor Plates".* Vienna, Austria: 13th International Congress on Sound and Vibration.

Caverson, R. W. (1994). "Review of vibration guidelines for suspended Concrete Slabs.". *Canadian Journal of Engineering* .

Coermann, R. R. (1962). "The Mechanical Impedance of the Human Body in Sitting and Standing Positions at low Frequencies." Human Factors(No. 4): 227-253. *Human Factors (No. 4)* , 227-253.

CSTR43. (1994). *Post-Tensioned Concrete Floors - Design Handbook.* Slough, UK: Concrete Society.

CSTR43. (2005). *Post-Tensioned Concrete Floors - Design Handbook 2nd Ed.* Slough, UK: Concrete Society .

Ebrahimpour, A. H. (1996). "Measuring and Modelling Dynamic Loads Imposed by Moving Crowds." . *Journal of Structural Engineering* , 122(12): 1468-1474.

Errikson, P. E. (1994). *Vibration of Low-Frequency Floors - Dynamic Forces and Response Prediction.* Gothenburg, Sweden : Chalmers University of Technology.

Farah, A. (1986). *"Structural Servicability Under Dynamic Loading"; SP-86-19 (Deflections of Concrete Structures.* Detroit: A.C. Institute.

Galambos, T. V. (1988). Vibration of Steel Joist Concrete Slab Floor Systems. . *Technical Digest. 5.*

Griffin, M. M. (1990). *Handbook of Human Vibration.* London, UK.: Academic Press.

ISO10137. (2007). *Bases for design of structures - Serviceability of buildings and walkways against vibrations.* Geneva: International Standards Organisation.

ISO2631.1. (1997). *"Evaluation of Human Exposure to Whole-body Vibration: General Requirements".* Geneva: International Standards Organization.

ISO2631.2. (2003). *ISO 2631.2 "Evaluation of Human Exposure to Whole-body Vibration - Continuous and Shock Induced Vibrations in Buildings (1-80Hz)".* Geneva: International Standards Organization.

Ji, T. A. (1994). "Floor Vibration Induced by Dance -Type Loads: Theory.". *The Structural Engineer 72(3)* , pp. 37-44.

M. Willford, P. Y. (2006). *A Design Guide for Footfall Induced Vibration of Structures .* UK: The Concrete Society.

MatLab. (2003). *R5.3.* The Math Works Inc.

Murray T. M., A. D. (1993). *Floor Vibrations: A New Design Approach.* Gothenburg, Sweden: International Colloquium on Structural Serviceability of Buildings.

Murray, T. (1975). "Design to Prevent Floor Vibrations'". *Engineering Journal, AISC, Vol. 12, No. 3.,* .

Murray, T. M. (1997). *"Floor Vibrations Due to Human Activity".* Chicago, Ill.: AISC.

Naeim, F. (1991). *Design Practice to Prevent Floor Vibrations.* Structural Steel Education Council, September.

Pavic A., R. P. (2001). *Critical Review of Guidelines for Checking Vibration Serviceability of Post-tensioned Concrete Floors.* Cement and Concrete Composites., Vol. 23(No. 1): p. pp. 21-31.

Pavic, A. (2003). Modal Testing and FE Model Correlation and Updating of a Prototype High-Strength Concrete Floor. *Cement and Concrete Composites Vol. 25, No. 7* , 787-799.

Pavic, A. R. (2001). Dynamic Modeling of Post-Tensioned Concrete Floors Using Finite Element Analysis. *Finite Elements in Analysis and Design, 2001. Vol. 37, No. 4.* , 305-323.

Pavic, A. R. (2002). Vibration Serviceability of Long-Span Concrete Building Floors. Part1: Review of Background Information. *The Shock and Vibration Digest, Sage Publications. 34* , pp. 191-211.

Pavic, A. (1998). *Vibration Serviceability of Suspended Cast In-situ Concrete Floors.* University of Sheffield: Department of Civil and Structural Engineering .

Paz, M. (1997)). *Structural Dynamics - Theory and Computation.* USA: Chapman and Hal.

Pernica, G. (1990). "Dynamic Load Factors for Pedestrian Movements and Rythmic Exercises". *Canadian Acoustics 18(2)* , 467-467.

Rainer, J. H. (1988). "Dynamic Loading and Response of Footbridges" . *Canadian Journal of Civil Engineering 15* , 66-71.

Reynolds P., P. A. (1998). *FE Analysis and FE Correlation of 600 tonne Post-tensioned concrete Floor.* p. p. 1129.: ISMA Vol. 3.

Smith, J. W. (2002). *Dynamic Loading and Design of Structures. Human-induced Vibrations.* New York, NY: Spon Press .

Strand7. (2003). *R2.2.3.* G+D Computing.

Ungar, E. E. (1979). "Footfall-Induced Vibrations of Floors Supporting Sensitive Equipment". *Sound and Vibration* , 10-13.

Warner R., R. B. (1998). *"Concrete Structures".* Addison Wesley.

Williams, M. S. (1994). "Evaluation of Methods for Predicting Occupant-induced Vibrations in Concrete Floors" . *The Structural Engineer 72(20)* , 334-340.

Wyatt, T. (1989). *Design Guide on the Vibration of Floors.* London, UK; Berkshire UK: Construction Industry Research and Information Association, ed. S.C. Institute.

NOTES